GENETIC SCREENING IN MYCOBACTERIUM TUBERCULOSIS UTILIZING TRANSPOSON INSERTION SEQUENCING

A Dissertation

Presented to the Faculty of the Weill Cornell Graduate School

of Medical Sciences

In Partial Fulfillment of the Requirements for the Degree of

Doctor of Philosophy

by

Weizhen Xu

January 2017

GENETIC SCREENING IN MYCOBACTERIUM TUBERCULOSIS UTILIZING TRANSPOSON INSERTION SEQUENCING

Weizhen Xu, Ph. D.

Cornell University 2017

The treatment of tuberculosis (TB) is challenging – its etiological agent, *Mycobacterium tuberculosis* (Mtb), is intrinsically resistant to the majority of antibiotics normally effective against other bacterial pathogens, and the ones that demonstrate efficacy against Mtb require prolonged treatment durations to eliminate the pathogen from the host. Current treatment regimens result in toxic side-effects for many patients and often lead to patient non-compliance, which contributes to treatment failure and the development of drug-resistant TB. Consequently, there is a pressing need for the development of a shorter therapeutic regimen, as well as a better understanding of the factors limiting the effectiveness of current drugs. Transposon insertion sequencing (TnSeq) is a high-throughput methodology using next-generation-sequencing to quantify bacterial mutant phenotypes *en masse*. In this dissertation, we describe the use of TnSeq to address two different questions related to the problem of stress resistance in Mtb, in particular antibiotic resistance.

The first problem was determining the functional role of mycobacterial acid resistance protease (MarP), a protein necessary for tolerance of not just acidic environments but also oxidative, detergent and antimicrobial stresses. Using a TnSeq-based genetic interaction screen, we identified genes that could be functionally related to *marP*. Our screen indicated that MarP had parallel functionality to multiple proteins involved in cell envelope biosynthesis and remodeling, suggesting a role for MarP in these processes. We also identified a few genes that could be functionally antagonistic to *marP*, possibly by promoting

increased cell envelope permeability to substrates. The loss of *marP* also alleviated fitness defects resulting from mutations in the ESX-5 secretion system, the mycobactin biosynthesis pathway and *rv0812,* a previously uncharacterized gene. Characterization of *rv0812* indicated that its main function was in para-aminobenzoic acid (PABA) biosynthesis, and that the loss of *marP* might promote activity of a bypass pathway to *rv0812*.

In a second study, we screened for mutants with altered susceptibility to rifampicin, ethambutol, isoniazid, vancomycin and meropenem. Through TnSeq, we were able to identify and rank genes mediating antibiotic susceptibility in Mtb. Multiple cell envelope mutants were predicted to be strongly sensitive to the drugs tested, whereas inactivation of individual efflux pumps did not appear to contribute majorly to drug sensitivity. We also identified *fecB* as a gene contributing to cross-sensitivity toward all five antibiotics – characterization of the Δ*fecB* mutant indicated that it had a more permeable cell envelope and was attenuated for growth *in vivo* and on solid media.

Together, the data from the two screens implicate the cell envelope to be a major determinant of Mtb resistance toward antibiotic and *in vivo* stresses, and suggest the existence of a functionally-linked cluster of cell envelope genes that could be synergistic targets supplementing current antibiotic regimens.

BIOGRAPHICAL SKETCH

Weizhen Xu was born on July 3, 1985 in Singapore, an island city-state famous for its good food, oppressive humidity and rather severe criminal justice system. He attended Raffles Institution in his secondary school days, and was first exposed to scientific research then, working on an odd mix of projects including the cryopreservation of orchid pollen, computer-aided drug design, and screening for possible ligands of the protein CD157. On graduating Raffles Junior College in 2013, he did a brief stint as a substitute biology teacher before being conscripted into the Singapore Army, where he was a military clerk for two-and-half-years; while largely a waste of his much-squandered youth, it imbued him with a healthy respect of Microsoft Excel. He later studied at the National University of Singapore (NUS) from 2006-2010, where he graduated with a BSc. in Life Sciences. In NUS, he was a member of the student-run Special Programme for Science, where he spent a summer in a marine biology lab studying the colonization of substrates by coral larvae; he later became a student mentor and subsequently the head Biology mentor in 2010. From 2009-2010, he joined the lab of Dr. Sylvie Alonso and studied the infection of dendritic cells by *Mycobacterium bovis* BCG, developing an interest in mycobacterial pathogenesis. In the fall of 2010, he flew diametrically across the world to New York and attended the Weill Cornell Graduate School of Medical Sciences. He joined the laboratory of Dr. Sabine Ehrt in 2011, pursuing his Ph.D. on genetic screening in *Mycobacterium tuberculosis*.

To the happy few

ACKNOWLEDGMENTS

It is oddly poetic that I should be writing this section on Thanksgiving. I have much to be grateful for, and getting to this stage of my long Ph.D. journey would not have been possible without the support of all the people in my life; it is my hope that this little Thanksgiving essay conveys a special sense of gratitude to everyone here who deserves it.

A large share of the thanks goes to my mentor, Sabine Ehrt. Sabine was recommended to me by my former mentor Sylvie Alonso at NUS to be "the best Ph.D. mentor in the TB field", and I am happy to say that she has lived up to that qualifier. Sabine is an inspiring teacher and leader, and through her example of her highly intellectual, ethical and practical conduct, I have learnt what it means to be a true scientist. I am particularly grateful for her encouragement and enthusiasm in the face of my boundless pessimism, which has been instrumental in challenging me to be the best I can be. I thank her for giving me the opportunity to learn from her, and her patience in doing so. I would also like to acknowledge my committee members for their feedback and fresh perspectives toward my research – special thanks goes to Dirk Schnappinger for his precise and insightful critiques.

Excellence in scientific leadership begets an excellent research team, and it has been my honour to work in the combined Ehrt/Schnappinger lab over these years. Thank you for creating and being part of a fantastic research environment – your support and friendship has helped me get where I am today. In particular, I would like to thank my fellow Ehrt Lab students Uday Ganapathy, Susan Puckett, Kan Lin, Ruojun Wang and Meredith Wright for their companionship in our shared journey through graduate school and for being there in the best and worst of times. Thanks goes to the postdocs for their experience and wisdom – in particular, Carolina Trujillo, Divya Tiwari and Ritu Sharma for the long extended conversations about life and such. A special mention goes to all who have contributed to this dissertation – Jennifer Small, Xiaoxiao Pan and Hélène Botella for laying the groundwork for the *marP* project, Sae Woong Park for learning and establishing TnSeq techniques for the lab,

Nadine Rücker for her assistance and tutelage in performing the mouse experiments, Curtis Engelhart for his expertise on cutting edge MIC assay technology, Meredith for her help with some of the meropenem experiments, and Claire Healy, Kan Lin, and Ruojun Wang for their generous donation of strains for MIC validation. I am also grateful to be part of the wider BRB-11 community – thanks goes to the members of the Nathan and Rhee labs for their expertise and perspectives on all things antibiotic-related, and for the many brief but friendly encounters along the hallways of the 11th floor.

The grand enterprise of scientific research is built upon collaboration, and the contributions of our multiple collaborators (many of whom are faceless names behind long threads of email correspondence) has been instrumental in this research. Thanks goes to Ed Long and Christopher Sassetti of UMass Medical School, and Jun-Rong Wei, Marte Dragset and Eric Rubin for their advice and guidance on the conduct of TnSeq experiments. A special mention goes to Michael DeJesus and Thomas Ioerger of Texas A&M for their technical support with the TRANSIT analysis tool as well as their much-needed statistical advice, which has helped greatly in cutting through the Gordian knots of TnSeq data.

My journey through the world of science would not have been possible without the many teachers and mentors in life. In particular, I would like to thank Mr. Ting Huat Seng of Nanyang Primary School, Mr. Mark Wee of Raffles Institution and Sylvie Alonso at NUS for showing me the beauty and joy of doing Science. It is my hope that I will be able to do the same as an educator for the students of tomorrow.

Finally, I would like to thank my friends and family, especially my parents, in Singapore for their constant love and support, even in my prolonged absence. Thank you supporting my dreams and guiding me to becoming who I am today.

TABLE OF CONTENTS

LIST OF FIGURES

LIST OF TABLES

CHAPTER 1: INTRODUCTION

1.1 Tuberculosis – global and historical perspectives

Tuberculosis (TB) is an infectious disease caused by *Mycobacterium tuberculosis* (Mtb), a slow-growing facultative intracellular bacterium. TB is a major global health problem today, being the leading cause of mortality due to infectious disease alongside HIV/AIDS – in 2014, the death tolls of TB and HIV/AIDS were estimated to be 1.5 million and 1.2 million respectively, with 0.4 million deaths resulting from co-morbidity from both diseases. There were approximately 9.6 million new TB cases in 2014, contributing to a global total of 13 million cases (WHO, 2015). The problem has been further compounded by the emergence of multidrug-resistant (MDR) strains, which are resistant to the two frontline drugs isoniazid and rifampicin, and require regimens with more expensive and toxic antibiotics, but with prolonged treatment times and increased treatment failure rates.

1.1.1 From pre-history to the age of microbiology

Mtb is an obligate pathogen with *Homo sapiens* being its exclusive host, which reflects the long history of co-evolution of both species since the dawn of humanity. Phylogenetic analyses suggest the Mtb emerged around 70,000 years ago and began its global spread with the migration of hunter-gatherer populations out of Africa, and flourished as a consequence of increased human population densities during the Neolithic period (Comas et al., 2013). While it was originally believed that Mtb may have originated from zoonotic transmission, recent phylogenetic analyses suggest that mycobacterial strains causing non-human mammalian TB have in fact diverged from the major human strains. Mtb has branched into seven lineages, with the East-Asian Lineage 2 and the Euro-American Lineage 4 accounting for the large majority of TB cases in the world (Brites and Gagneux, 2015). These lineages have been demonstrated to be more virulent in animal models and are implicated in faster progression to active disease relative to the other lineages (Coscolla and

Gagneux, 2014); of particular, the Beijing family of strains within lineage 2 exhibit hypermutability (Ford et al., 2013) and a greater tendency to acquire mutations conferring drug resistance and also compensatory mutations mitigating the fitness costs associated with drug resistance (Casali et al., 2012; Merker et al., 2015).

Mtb has thrived in the midst of human civilization and left its mark on human history – TB has been well-documented since antiquity, going by multiple names including consumption, the ancient Hebrew *schachepheth,* the Greco-Roman *pthisis*, the Classical Chinese 癆， the Medieval Anglo-French scrofula/king's evil, and the Great White Plague of 17th century Europe (Daniel, 2006; Daniel and Daniel, 1999). Befitting of the moniker "the Great White Plague", TB was responsible for 20% of the adult deaths in Europe and North America between the 17th and 19th centuries (Wilson, 2005). A major turning point in humanity's struggle with TB was the discovery of its causative agent *Mycobacterium tuberculosis* in 1882 by Robert Koch(Koch, 1952), paving the way for directed therapies against the pathogen. Following Koch's discovery were advances such as the diagnostic Mantoux test and the partly efficacious Bacille Calmette Guérin (BCG) vaccine; however, TB therapy was largely limited to surgical intervention and the improved nutrition and bed rest afforded by the prolific TB sanatoria of the time(Riva, 2014). It was only with the advent of anti-TB antibiotics that humanity could finally push back against the TB epidemic.

1.1.2 The rise and decline of TB chemotherapy

The early 20th marked the start of the age of antimicrobial chemotherapy, beginning with Paul Ehrlich's "magic bullet" of the anti-syphilitic arsphenamine and followed by the discovery and eventual mass production of sulfonamides and penicillin between 1930 and the 1940s. The realization of TB chemotherapy lagged behind slightly - after an initial misstep in 1925 with the non-effective and toxic gold-based compound sanocrysin, the first two drugs effective in controlling TB were discovered almost simultaneously in 1944 (Riva, 2014); streptomycin was isolated from *Streptomycin griseus* by Selman Waksman and Albert

Schatz(Schatz et al., 1944), whereas para-aminosalicylic acid (PAS) was synthesized by Jörgen Lehmann in collaboration with the Swedish pharmaceutical Ferosan (Lehmann, 1964). They were subsequently followed by the discoveries of the current front-line TB drugs isoniazid(McDermott, 1969), rifampicin(Sensi, 1983), ethambutol (Doster et al., 1973) and pyrazinamide (HKCS, 1981) between 1950 to the 1970s, which reduced treatment duration from 24 to 6 months, and multiple other compounds currently employed as second-line TB drugs. This golden age of TB drug discovery led Waksman, who had won the Nobel Prize in 1952 for his discovery of streptomycin, to optimistically declare that "the complete eradication of the disease is in sight"(Waksman, 1964).

Progress in anti-TB chemotherapy has however been closely shadowed by the development of drug resistance. The initial clinical trial of streptomycin was promptly followed by a report of streptomycin resistance developing in 12 out of 13 individuals within a treatment group (Crofton and Mitchison, 1948). It was subsequently shown that co-administration of streptomycin with PAS improved cure rates and reduced the development of antibiotic resistance(Jamieson, 1950), setting the standard of multi-drug regimens in the treatment of TB. The implementation of combination drug therapy could however only delay the inevitability of drug resistance – isoniazid resistance increased from 6.3% to 9.7% in newly reported cases of TB in the US between 1961 and 1968 (Steiner et al., 1970), and multiple outbreaks of multidrug-resistant (MDR) TB made their appearance in the 1970s (Keshavjee and Farmer, 2012). Despite this trend, development and innovation of novel anti-TB drugs and drug regimens had already begun to taper off (the next novel anti-TB drug TMC207/bedaquiline would only be approved 40 years later (Diacon et al., 2012)). The rise of MDR-TB, the growing HIV epidemic and also the increasing prevalence of diabetes (Restrepo and Schlesinger, 2014) led to a resurgence in TB cases in the 1980s, leading the World Health Organization to declare TB to be a global health emergency in 1993. The return of TB was only held in check with the aggressive implementation of the directly observed treatment,

short-course (DOTS) strategy combining an easily accessible, standardized treatment regimen with a comprehensive system of monitoring encompassing case detection, diagnosis and the evaluation of treatment outcomes, improving patient compliance and treatment success rates (WHO, 2010).

TB mortality has fallen 47% since the 1990s; however, the threat of MDR-TB is still ever-present, accounting for an estimated 480,000 cases worldwide, of which only 50% were successfully treated globally (WHO, 2015). The last decade has also seen the emergence of extensive drug-resistant (XDR) TB, defined as MDR TB with additional resistance to at least one fluoroquinolone and a second-line injectable (amikacin, capreomycin or kanamycin) – an estimated 9.7% of MDR-TB cases are also XDR. The prognosis for XDR-TB is even poorer than that of MDR-TB – a global study of a cohort of 2,685 XDR-TB patients between 2012 to 2015 saw only 2.6% completing treatment successfully (WHO, 2015). The poor treatment outcomes of MDR and XDR TB are a major hurdle in the complete eradication of the disease, and necessitate the development of novel, efficacious anti-TB antibiotics.

1.2 The challenges of TB treatment

TB is a particularly challenging bacterial disease to treat – Mtb is intrinsically resistant to the majority of antibiotics normally effective against other bacterial pathogens (Morris et al., 2005; Nguyen and Pieters, 2009), and the ones that demonstrate efficacy against Mtb require prolonged treatment durations to eliminate the pathogen from the host. The so-called “short-course” HRZE (isoniazid, rifampicin, pyrazinamide and ethambutol) regimen for drug-sensitive TB needs at least 6 months, whereas more complicated cases of multidrug-resistant (MDR) and extensively-drug-resistant (XDR) TB require the additional use of second-line drugs for an extended duration of 18 months and beyond (WHO, 2010). Consequently, there is a pressing need for the development of novel, more effective anti-TB drugs, and also shorter therapeutic regimens.

The list of ideal characteristics for novel anti-TB drugs is extensive – these include potent bacteriocidality against both replicating and non-replicating bacteria, extended pharmacokinetic duration, synergistic effects with other anti-tubercular drugs, low toxicity, oral activity and novel mechanisms of action refractory to the development of resistance (Protopopova et al., 2007). While a large extent of anti-tubercular drug design is a problem of medicinal chemistry, rational prioritization of effective drug targets within the physiology of Mtb and a clear understanding of the processes limiting the effectiveness of current antibiotics would definitely accelerate the development of novel antibiotics and antibiotic regimens. The recalcitrance of Mtb in the face of chemotherapy results from the complex interplay of its privileged niche within the host environment and its unique bacterial physiology, which will be discussed in detail in this section.

1.2.1 Mtb and the host

Mtb is transmitted via aerosol infection, with an infectious dose as small as a single infectious droplet (estimated to contain between 1-10 bacilli) capable of causing disease (Riley, 1957; Russell et al., 2010); the lung being the primary site of infection, pulmonary TB represents 70-90% of TB cases, with possible extrapulmonary manifestations resulting from dissemination of Mtb to other organ systems including the lymph nodes, bones/joints and central nervous system. Upon inhalation, Mtb is taken up by professional phagocytes in the airways – in addition to its primary host cell, the alveolar macrophage, Mtb can also reside in neutrophils, monocytes and dendritic cells (Ernst, 2012; Kang et al., 2011; Wolf et al., 2007). As an intracellular pathogen, Mtb is able to survive and replicate in phagosomal compartments within the resting macrophage by inhibiting phagolysosomal fusion and phagosomal acidification (Armstrong and Hart, 1971; Goren et al., 1976). The onset of adaptive immunity occurs 4-6 weeks post-infection in humans (Wolf et al., 2007), leading to macrophage activation and promoting phagolysosomal fusion and acidification (MacMicking et al., 2003). While replication is inhibited, Mtb is nonetheless able to survive the multitude

of stresses within the phagolysosome, including acidification, the production of reactive oxygen/nitrogen species, hypoxia, and nutrient limitation (Ehrt and Schnappinger, 2009; Vandal et al., 2008).

Granuloma formation is a defining feature of Mtb infection. In basic pathology, a granuloma is simply defined as an organized aggregation of macrophages, however, this definition fails to capture the cellular and structural complexity as well as the dynamic nature underlying the TB granuloma. The TB granuloma is an evolving structure built by successive waves of immune cell migration – phagocytosis of Mtb by alveolar macrophages triggers chemokine production, attracting a variety of innate immune cells including neutrophils, monocyte derived macrophages, NK cells and γδ T-cells. With the induction of adaptive immunity, the granuloma becomes more well-defined, consisting of a central core of infected macrophages surrounded by a peripheral cuff of lymphocytes. The later stages of granuloma development may be accompanied by macrophage differentiation into multinucleated Langhans giant cells, epitheloid cells or foamy cells, cellular necrosis in the center of the granuloma and the formation of a capsule of fibroblasts around the granuloma, which contributes to the containment of the infection (Ehlers and Schaible, 2012). There is a large degree of granuloma heterogeneity even within a single host (in humans and also the complex granuloma-forming animal models such as the rabbit, guinea pig and non-human primates), ranging from fully cellular granulomas composed of macrophages, neutrophils and lymphocytes to “caseous” granulomas with a necrotic center(Lenaerts et al., 2015), with great variability in microenvironmental conditions such as oxygen tension, nutrient availability, pH and oxidative/nitrosative stress, and also in the ability to contain and sterilize Mtb infection (Lin et al., 2014). While Mtb is commonly thought to be an intracellular pathogen, large numbers of extracellular Mtb have been observed to reside in the necrotic foci of caseous granulomas (Hoff et al., 2011; Orme, 2014); the microenvironmental variability between the intracellular and extracellular compartments within a granuloma

further adds to the environmental heterogeneity that the Mtb population faces within the host.

The immune response of the host to Mtb is a double-edged sword – while generally able to contain Mtb infection, it can also inadvertently create an environment that nurtures and shields the pathogen. Containment of Mtb infection is generally quite effective – it is estimated primary infection with Mtb results in latent TB 90% of the time without therapeutic intervention, with active TB developing in only the minority of the cases. Most cases of adult TB result from reactivation a long time after the primary infection, representing a loss in ability of the immune response to contain the latent infection; this is exemplified by the increased risk of TB reactivation in HIV/AIDS patients due to depletion of CD4+ T cells, and also in patients undergoing therapeutic neutralization of TNF (Ernst, 2012).

Conversely, the host immune response complicates TB chemotherapy; as mentioned previously, the large degree of heterogeneity between environmental niches occupied by Mtb in the host may impose differential adaptive pressures on the pathogen, resulting in physiologically distinct subpopulations varying in susceptibility to antibiotic stress (Dartois and Barry, 2013; Lenaerts et al., 2015). The fact that Mtb resides in the granuloma and the macrophage led to early speculation that these structures may be a major physical barrier to antibiotic penetration, facilitating chemotherapeutic evasion and the development of drug resistance (Crofton and Mitchison, 1948). On a cellular level, the macrophage can act as a permeability barrier – higher concentrations of rifampicin (but not isoniazid and ethambutol) were required to kill Mtb within macrophages as opposed to extracellular Mtb(Hartkoorn et al., 2007). Early clinical studies also indicated that rifampicin and isoniazid concentrations were lower in tuberculous lung lesions relative to the levels in blood plasma (Canetti et al., 1969; Kislitsyna and Kotova, 1980). Recent mass-spectrometry (MS)-based studies of drug distribution in the rabbit model of Mtb infection have shed further light on this issue – distribution varies between drugs, with moxifloxacin showing favorable partitioning into lung

tissue and granulomas, while levels of isoniazid, rifampicin and pyrazinamide were substantially lower in tuberculous lesions relative to blood plasma (Kjellsson et al., 2012); drug distribution was particularly poor in the center of necrotic granulomas, reflective of the absence of vascularization and active transport in this acellular zone, and of the TB drugs tested, only pyrazinamide was able to diffuse effectively through the caseum(Dartois, 2014). This observation could partially account for the observation of "persister" Mtb populations in caseous granulomas that are recalcitrant to chemotherapy (Lenaerts et al., 2007; Lin et al., 2013). In summary, TB chemotherapy is hindered by the inaccessibility of its resident niches to antibiotics; however, this it but the first of the hurdles preventing antibiotic access to its targets in Mtb.

1.2.2 The physiology of Mtb and antibiotic resistance

Antibiotic resistance can be classified into two categories – acquired resistance, in which the bacterium gains resistance by the acquisition of genes via horizontal transfer or spontaneous mutation within its genome that can transmitted vertically to subsequent generations, and intrinsic resistance, in which the bacterial species in general already possesses insensitivity to certain antibiotics prior to encounters with the relevant antibiotic selection pressures (Cox and Wright, 2013). Both classes of resistance are important in the context of TB chemotherapy. Mtb is exceptional amongst bacterial pathogens in terms of intrinsic resistance, with many common classes of antibiotics being ineffective against the pathogen, limiting the chemotherapeutic arsenal against Mtb to a few specialized anti-tubercular drugs. This problem of intrinsic resistance is further compounded by that of acquired resistance; while Mtb has not been reported to acquire resistance via horizontal transmission in a clinical setting, the aforementioned problems of extended chemotherapeutic duration and patient non-compliance have created an environment conducive to the selection of antibiotic resistant clinical strains just from spontaneous

mutation alone. This subsection examines the various aspects of the physiology of Mtb contributing to both intrinsic and acquired resistance.

1.2.2.1 The mycobacterial cell envelope

The mycobacterial cell envelope is a central player in determining antibiotic susceptibility in Mtb, being a target for multiple first and second-line anti-tubercular drugs, and also acting as the major barrier limiting accessibility of antimicrobial compounds to their targets within the mycobacterium. The uniquely-structured cell envelope is a hallmark feature of mycobacteria as well as other members of the bacterial suborder Corynebacterineae - while phylogenetically classified as gram-positive bacteria, the Corynebacterineae possess a complex multi-layered cell envelope that distinguishes it from both Gram-positive and gram-negative bacteria. This cell envelope can be subdivided into three main layers: the plasma membrane, an inner mycolic acid-arabinogalactan-peptidoglycan (mAGP) core, and an outer capsular layer (Brennan, 2003; Kaur et al., 2009). The plasma membrane is a phospholipid bilayer similar to that of other bacteria, and is surrounded by the core mAGP complex – closest to the plasma membrane is the surrounding peptidoglycan layer, which is covalently linked to an arabinogalactan layer, which forms multiple ester linkages with α-alkyl, β-hydroxy (C_{60}-C_{90}) mycolic acids, resulting in a covalently-attached mycolic acid layer. This mycolic acid layer intercalates with non-covalently attached lipids and lipoglycans to form a lipid bilayer commonly referred to as the mycobacterial outer membrane – these include the phthiocerol dimycoserates (PDIMS), phosphatidylinositol mannosides (PIMs), phenolic glycolipids (PGLs), mannosylated-lipoarabinomannan (ManLAM) and acyltrehaloses. The outer membrane and plasma membrane thusly encompass the periplasmic space (Bansal-Mutalik and Nikaido, 2014; Brennan, 2003; Hoffmann et al., 2008; Jackson, 2014; Kaur et al., 2009). Exterior to the outer membrane is the mycobacterial capsule, a detergent-soluble layer primarily comprised of

polysaccharides and proteins with low amounts of lipids (Daffe and Etienne, 1999; Jackson, 2014; Sani et al., 2010)

The mycobacterial cell envelope is a thick and highly hydrophobic structure, and is exceptional amongst the various bacterial cell envelopes in their impermeability to exogenous substrates and antibiotics. Early work in *Mycobacterium chelonei* established that the permeability coefficients for hydrophilic substrates including glucose, glycine, leucine and glycerol were approximately 10 and 1000-fold lower than *Pseudomonas aeruginosa* (*P. aeruginosa)* and *Escherichia coli* (*E. coli*) respectively (Jarlier and Nikaido, 1990). Permeability coefficients for β-lactam drugs were 100-fold lower in Mtb relative to *E. coli*, demonstrating the importance of cell envelope impermeability in intrinsic antibiotic resistance (Chambers et al., 1995). The relation between cell envelope integrity and intrinsic antibiotic resistance has been further highlighted by studies in mycobacterial cell wall mutants. Mycobacterial mutants deficient in mycolate biosynthesis (e.g. *kasB* and *virS-mymA* operon mutants) exhibit increased permeability and sensitivity to antibiotics including rifampicin, chloramphenicol, isoniazid, pyrazinamide and ciprofloxacin (Gao et al., 2003; Liu and Nikaido, 1999; Singh et al., 2003), whereas a *Mycobacterium smegmatis* mutant in *fbpA*, which catalyzes the biosynthesis of trehalose dimycolates, was observed to be hypersensitive to multiple broad-spectrum antibiotics and anti-tubercular drugs (Nguyen et al., 2005).

It has been noted that lipophilic antibiotic classes such as the macrolides, fluoroquinolones and rifamycins are more likely to effectively penetrate the highly hydrophobic mycobacterial cell wall to reach their targets; comparisons between compounds of the same antibiotic class indicate that the more lipophilic derivatives demonstrate a higher inhibitory activity against mycobacteria (Brennan and Nikaido, 1995; Danilchanka et al., 2008; Sarathy et al., 2012). This passive transport of hydrophobic substrates across the cell envelope is limited by cell envelope thickness and fluidity of the mycobacterial outer membrane – increased levels of the *trans*- isomeric form of mycolic acids resulting from

increased incubation temperatures was associated with lower outer membrane fluidity and permeability to the lipophilic agents norfloxacin and chenodeoxycholate(Liu et al., 1996a).

Recent work in the last decade have shed light on the mechanisms facilitating the diffusion of hydrophilic substrates (including antibiotics) across the mycobacterial outer membrane. In gram-negative bacteria, influx of hydrophilic substrates across the outer membrane is largely facilitated by porins, which are transmembrane proteins forming a beta-barrel structure around an open water-filled channel; while substrate specificity can be partially governed by pore and channel size and charge, porins represent a major route by which antibiotics can cross the gram-negative outer membrane (Nikaido, 2003; Pages et al., 2008). Mycobacterial porins were first identified in *M. smegmatis* – the protein MspA was shown to form stable oligomers with high channel-forming activity (Niederweis et al., 1999), and homology searches within the *M. smegmatis* genome led to the further discovery of three more *mspA* –like porin genes, accordingly named *mspB, mspC* and *mspD* . Studies of *mspA* and *mspC* deletion mutants as well as *Mtb* and *M. bovis* BCG strains heterologously expressing *mspA* further confirmed the role of the MspA-like porins in the transport of hydrophilic solutes; with *mspA/mspC* deletion linked to increased antibiotic MICs, and *mspA* expression resulting in accelerated growth and increased antibiotic susceptibility in Mtb and *M. bovis* BCG (Danilchanka et al., 2008; Stahl et al., 2001; Stephan et al., 2004).

MspA-like porins are absent from the genomes of Mtb and other slow-growing pathogenic bacteria, and the identity of Mtb porins and hydrophilic substrate transportation mechanisms is less certain. The Mtb protein OmpATb/Rv0899 was previously postulated to be a porin based on its homology to the *E. coli* porin OmpA (Senaratne et al., 1998), however, structural studies indicated that it does not form the typical transmembrane β-barrel structure typical of porins, but rather a mixed α/β structure with a hydrophobic core and polar/acidic exterior, making it unlikely to be a transmembrane channel (Teriete et al., 2010). Functional characterization of OmpATb identified a functional role in surviving under acid

stress by rapid extrusion of ammonia to neutralize environmental pH levels; OmpATb expression was however unable to complement a permeability defect to the hydrophilic substrates serine, glycerol and glucose when expressed in an *M. smegmatis mspA* mutant, indicating that OmpATb is not likely to be a general porin. (Song et al., 2011). Recent efforts have focused on the identification of outer membrane proteins that could possibly serve as channels for hydrophilic solutes (Rana et al., 2014; Song et al., 2008) – MctB/Rv1698 was shown to localize to the outer membrane and could complement the deletion of *mspA* in *M. smegmatis*, restoring sensitivity to ampicillin and chloramphenicol and increasing permeability to glucose (Siroy et al., 2008); later work demonstrated increased accumulation of copper as well as increased susceptibility to copper toxicity in an Mtb mutant lacking MctB, suggesting a role in copper efflux (Wolschendorf et al., 2011).

Another outer membrane channel protein CpnT was shown to be involved in uptake of glycerol and glucose, as well as a variety of both hydrophilic and hydrophobic antibiotics in *M. bovis* BCG (Danilchanka et al., 2015; Danilchanka et al., 2014); the Mtb ΔcpnT mutant however exhibited a phenotypically-weaker defect in the uptake and utilization of glucose/glycerol, and no significant changes in antibiotic susceptibility. In addition to its functionality as a channel, CpnT possesses a secreted C-terminal domain that functions as a necrosis-inducing exotoxin by hydrolyzing NAD (Danilchanka et al., 2014; Sun et al., 2015). While the hunt for possible porins or porin-like proteins is still ongoing, it is plausible that the uptake of hydrophilic substrates may be facilitated not by dedicated porins/porin-like channels, but rather an extensive, highly redundant network of multifunctional proteins similar to the ones discussed here.

1.2.2.2 Efflux pumps

The permeability barrier of the mycobacterial cell envelope only provides partial protection against the influx of antibiotics; in the absence of a mechanism eliminating intracellular antibiotics, equilibration of drug concentrations across the cell envelope would

eventually be achieved despite the reduced influx rate. This elimination of intracellular antibiotics may occur via drug metabolism and degradation, or by the active efflux of antibiotics back into the extracellular domain (Jarlier and Nikaido, 1994). Bacterial efflux pumps can be categorized into five main superfamilies distinguished by their structures, substrates and energy sources – the ATP-binding cassette (ABC) transporter superfamily, the major facilitator superfamily (MFS), the small multidrug resistance (SMR) superfamily, the resistance-nodulation-cell division (RND) superfamily and the multidrug and toxic compounds extrusion (MATE) superfamily. Efflux is an active process requiring an energy source, with the ABC superfamily utilizing ATP hydrolysis and the other classes relying on the transmembrane proton-motive force (PMF) or Na^+/H^+ electrochemical gradient. (Pule et al., 2016; Viveiros et al., 2012).

The Mtb genome encodes multiple putative efflux pumps, representing most of the efflux superfamilies apart from the MATE superfamily (Black et al., 2014; Viveiros et al., 2012). The role of efflux pumps in intrinsic antibiotic resistance in mycobacteria was first demonstrated by the *M. smegmatis* efflux pump LfrA (Liu et al., 1996b) – LfrA overexpression resulted in reduced intracellular accumulation of norfloxacin and increased norfloxacin resistance, while disruption of the *lfrA* genes reduced the MIC of ethidium bromide and acriflavine by 8-fold, and the MIC of ciprofloxacin, doxorubicin and rhodamine by two-fold (Li et al., 2004; Sander et al., 2000). The Mtb genome lacks an *lfrA* homolog, and fluoroquinolone resistance in Mtb may be mediated by other efflux pumps such as Rv1634 and Rv2686c-2688c (De Rossi et al., 2002; Pasca et al., 2004). Since LfrA, multiple studies have shown an association between efflux pump overexpression/disruption on antibiotic susceptibility, upregulation of putative efflux pumps in Mtb under antibiotic stress as well as an effect of efflux pump inhibitors on antibiotic sensitivity; these studies are exhaustively discussed in recent comprehensive reviews (da Silva et al., 2011; Pule et al., 2016; Viveiros et al., 2012).

The role of efflux pumps in intrinsic antibiotic resistance in Mtb has however not been conclusively established, and a few questions remain. Given the broad specificity of efflux pumps, it is difficult to determine whether the observed antibiotic sensitivity or reduced accumulation is due to drug efflux or the defective secretion of another physiologically important substrate. Multiple putative pumps such as the P55 MFS transporter (Rv1410c), Rv1747 and MmpL7/MmpL8 have been implicated in the export of cell envelope components such as mycolic acids, triacylglycerides, and phthiocerol dimycocerosate (pdim) (De Rossi et al., 2002; Domenech et al., 2005; Martinot et al., 2016; Spivey et al., 2013) , and the essentiality of certain efflux pumps in the absence of antibiotic selection such as EfpA, MmpL3 and Rv2477c (Griffin et al., 2011) suggest key physiological roles independent of antibiotic efflux. The extent of efflux-mediated antibiotic resistance also shows variability across mycobacteria species and strains – while there was evidence suggesting resistance resulting from fluoroquinolone efflux in drug resistant Mtb strains (Escribano et al., 2007; Louw et al., 2011), intracellular concentrations of fluoroquinolones, rifamycins and linelozid were unaffected in the drug-sensitive H37Rv laboratory strain upon treatment with the efflux inhibitors verapamil and reserpine in a separate study (Sarathy et al., 2013). In addition to basic gene overexpression/deletion studies and antibiotic susceptibility testing, quantitative methods measuring antibiotic accumulation and uptake, as well as comprehensive multi-strain studies are needed to conclusively establish the importance of efflux in antibiotic resistance.

1.2.2.3 Metabolism of antibiotics

The chemical deactivation of antibiotics is a principal strategy in bacterial antimicrobial resistance. In addition to the previously-mentioned cell envelope impermeability, Mtb is able to further blunt the effect of β-lactam antibiotics via the action of β-lactamases (Chambers et al., 1995; Flores et al., 2005). The main β-lactamase of Mtb is BlaC, which possesses strong broad-spectrum activity and is able to hydrolyze even

carbapenems (Voladri et al., 1998). The importance of this mechanism of intrinsic resistance to β-lactamase antibiotics has been demonstrated by the potentiating activity of β-lactamase inhibitors such as clavulanic acid under *in vitro, in vivo* and clinical settings (Flores et al., 2005; Kumar et al., 2012; Segura et al., 1998; Tiberi et al., 2016). Mycobacteria may also neutralize antibiotics by chemical modification – *M. fortuitum* and *M. smegmatis* have been shown to encode an aminoglycoside 2'N-acetyltransferase (AAC), conferring resistance to the aminoglycoside antibiotics dibekacin, gentamicin, netilmicin and tobramycin (Ainsa et al., 1996). Mtb and *M. leprae* possess AAC homologs, and structural comparisons indicate the the Mtb AAC may have a secondary role in mycothiol biosynthesis(Vetting et al., 2003).

A few key anti-tuberculars are prodrugs requiring enzymatic activation by Mtb, and mutations resulting in a loss of this activation are highly represented in drug-resistant clinical strains. These include mutations in *katG* and its negative regulator *furA* in the case of isoniazid resistance (Hazbon et al., 2006; Ramaswamy et al., 2003; Vilcheze and Jacobs, 2007), the activator *ethA* and its regulator *ethR* for ethionamide resistance(Brossier et al., 2011; Morlock et al., 2003), *pncA,* which activates pyrazinamide (Konno et al., 1967; Scorpio and Zhang, 1996) and the dihydrofolate synthase *folC*, which activates PAS (Chakraborty et al., 2013; Zheng et al., 2013)

1.2.2.4 Target modification

Apart from chemical neutralization, another central theme of bacterial antibiotic resistance is the mutation of antibiotic targets rendering them less susceptible to antibiotic binding and action. Mutations in drug target genes are common in drug-resistant clinical strains of Mtb, and have been extensively documented and reviewed (Da Silva and Palomino, 2011; Nguyen, 2016). As antibiotic targets generally represent essential processes in bacterial physiology, mutations in these genes are commonly associated with a fitness cost manifesting as a reduction in growth, virulence or transmission (Andersson, 2006). A case in point is rifampicin resistance resulting from missense mutations in *rpoB*, the gene encoding

the β-subunit of RNA polymerase. Given the central role of RNA polymerase on transcription, rifampicin-resistant clinical strains with mutations in *rpoB* exhibit extensive transcriptional changes (Bisson et al., 2012; de Knegt et al., 2013) and an altered metabolic profile characterized by a reduction in mycobactin siderophore and sulfolipid biosynthesis (Lahiri et al., 2016), which may account for observed fitness costs *in vitro* (Billington et al., 1999; O'Sullivan et al., 2005). The fitness costs of *rpoB* mutation can be mitigated by the acquisition of secondary compensatory mutations, as demonstrated by secondarily-mutated clinical strains with a restored competitive fitness *in vitro* and a higher prevalence globally (Comas et al., 2011); fitness costs are also determined by strain genetic background and may account for increased rates of drug resistance in certain strains such as the Lineage 2 Beijing strain (Gagneux et al., 2006). Drug target mutations do not always come with a fitness cost – the K42R mutation in the ribosomal protein RpsL that confers streptomycin resistance is not attenuated *in vitro*, and its high prevalence clinically suggests a minimal impact on *in vitro* fitness (Bottger et al., 1998; Sander et al., 2002). Drug targets that have a higher fitness cost associated with mutation to resistance may thus prove to be more attractive for antibiotic lead development.

While target modification is commonly associated with acquired resistance, constitutive modification of target proteins may function as a mechanism for intrinsic drug resistance. While the pathogenic species *Mtb* and *M. bovis* are intrinsically resistant to the macrolide and lincosamide classes of antibiotics, which bind reversibly to ribosomal RNA and inhibit ribosomal function, the Pasteur vaccine strain of *M. bovis* BCG is notably susceptible to these antibiotics. BCG possesses chromosomal deletions from extensive passaging of *M. bovis* under laboratory conditions, and its unique susceptibility to these ribosomal agents was traced to the loss of the *erm37* (*rv1988)* gene (Buriankova et al., 2004). Erm37 methylates 23S ribosomal RNA and reduces the affinity of the ribosomes to these antibiotics,

and expression of *erm37* from Mtb restored macrolide and lincosamide resistance in BCG (Buriankova et al., 2004; Madsen et al., 2005).

1.2.2.5 Phenotypic drug tolerance

In addition to the intrinsic and acquired genetic factors already described, a large part of Mtb's recalcitrance to chemotherapy lies in the phenomenon of phenotypic drug tolerance. Phenotypic drug tolerance refers to a physiological state by which the bacterium is able to survive exposure, but can be restored to a state of antibiotic sensitivity after in vitro outgrowth; in short, a state of non-heritable antibiotic resistance (Levin and Rozen, 2006). Phenotypic drug tolerance can be divided into two classes – class I phenotypic tolerance occurs in a small subset of individuals within a bacterial population before antibiotic exposure, whereas class II tolerance refers to a state of physiological tolerance present in the majority of the population, imposed by environmental conditions (Girgis et al., 2012; Nathan, 2012; Nathan and Barry, 2015).

Class I phenotypic tolerance (or persistence) was first described in *Staphylococcus pyogenes* – a sensitive population was subjected to penicillin treatment, and approximately 1 in 10^6 bacteria survived the treatment; expansion of these survivors resulted in bacterial populations with the same sensitivity and proportion of survivor cells as the original parental population, leading to the conclusion that the resistant state was not heritable (Bigger, 1944). This class of persistence has since been described in multiple bacterial species and attributed to a vast variety of mechanisms, the unifying theme being the stochastic regulation of gene expression. Analysis of individual Mtb cells within a replicating population revealed that stochastic reduction of KatG expression occurring prior to isoniazid exposure could account for phenotypic tolerance to isoniazid (Wakamoto et al., 2013). Mtb cells have also been shown to undergo asymmetric division, resulting in daughter cells with differential growth rates, protein distributions and antibiotic susceptibility (Aldridge et al., 2012; Vaubourgeix et al., 2015). Genetic screening for Mtb mutants with a higher persister

subpopulation identified carbon metabolism, toxin-antitoxin systems, lipid biosynthesis and transcriptional regulators as possible functional pathways contributing to the state of antibiotic persistence (Torrey et al., 2016)

Class II phenotypic tolerance is distinguished from class I tolerance in that it occurs in the majority of bacteria in the population, and is induced by environmental conditions that limit replication (Nathan, 2012; Nathan and Barry, 2015). Class II tolerance was also first described in the previously mentioned Bigger study, in which the induction of bacteriostasis in *S. pyogenes* by incubation in distilled water, boric acid or lower temperatures increased the population of persisters toward penicillin (Bigger, 1944). Pioneering work by Wayne et al. showed that a gradual depletion of available O_2 in liquid culture led to reduced growth and eventual bacteriostasis, and increased Mtb tolerance of anaerobiosis. This state was associated with negligible Mtb sensitivity to ciprofloxacin and isoniazid, reduced effectiveness of rifampicin, but also sensitization to metronidazole, which is not effective under replicating conditions (Wayne and Hayes, 1996; Wayne and Sramek, 1994). Since the Wayne model, other non-replicating (NR) Mtb models have been developed for the screening of anti-TB antibiotics, including the use of Mtb strain 18b, a streptomycin-dependent mutant that undergoes replication arrest but not killing when streptomycin is withdrawn (Sala et al., 2010), and a multiple stress NR model combining low pH, mild hypoxia, nitrosative stress and low amounts of the fatty acid butyrate as a carbon source (Darby and Nathan, 2010; Gold et al., 2015).

The exact mechanisms contributing to the development of class II tolerance have yet to be comprehensively characterized. While it is commonly held that non-replicating bacteria may be more resistant to antibiotic action due to reduced activity in cell envelope, nucleic acid and protein biosynthesis pathways, which are major processes targeted by antibiotics (Keren et al., 2011), other transcriptomic studies indicate a stress-dependent robust transcriptomic response associated with an upregulation of iron scavenging and lipid

biosynthesis pathways, indicating continued metabolic activity in spite of arrested growth that may be important in dormancy/persistence (Schnappinger et al., 2003; Voskuil et al., 2004). As the state of class II phenotypic tolerance confers cross-resistance to multiple antibiotics within an anti-TB drug regimen, understanding and developing ways to circumvent this phenomenon will be important in the realization of rapid, effective TB chemotherapy.

1.3 Genetic screening in Mtb

The field of mycobacterial genetics was opened up by the sequencing and annotation of the complete *Mtb* genome, which spans 4.4 megabases and is comprised of approximately 4000 genes (Cole et al., 1998). Faced with this vast catalogue of genetic information, the main challenge for the mycobacterial geneticist is to sift out the most interesting candidates for study. While the rational prioritization of study candidates is a universal problem common to all branches of genetics, it is one of paramount importance for a geneticist studying Mtb. Mtb is exceptional amongst bacteria for its intractability as a research subject – it has a doubling time of 18-24h and it takes 2-3 weeks for colonies to form on solid culture media; and its capacity for causing chronic life-threatening disease necessitates specialized biosafety level 3 procedures and facilities that are costly to maintain and limit the speed at which research can be performed. The high cost of Mtb research coupled with the inexorable march of time demands an efficient and accurate system for the triage of the most worthwhile and important genes for further study.

A major breakthrough with regard to this problem was achieved with the creation of an efficient transposon mutagenesis method using a temperature-sensitive mycobacteriophage to deliver a highly-active *Himar1*- mariner transposon system (Sassetti et al., 2001). The high efficiency of the transposon mutagenesis system in tandem with the relatively unbiased nature of *Himar1* transposon insertion (the *Himar1* transposon inserts specifically into TA dinucleotide sites, of which there are ~ 75,000 in the Mtb genome)

permitted the creation of diverse transposon libraries approaching saturating levels of coverage of the Mtb genome. Additionally, the transposon insertion sites could be easily mapped via genetic footprinting with the appropriate PCR primers, providing a major advantage over other random mutagenesis methods.

While these factors made *Himar1* transposon libraries the ideal starting material for classical genetic screens selecting for specific Mtb mutants, the main utility of the *Himar1* system was in the genome-wide determination of gene essentiality in Mtb. In his seminal work, Sassetti et al. combined the transposon mutagenesis system and microarray hybridization to develop a methodology to identify conditionally essential genes in *M. bovis* BCG, which was accordingly dubbed transposon site hybridization (TraSH) – transposon mutants essential for survival under a specific condition (minimal media) were lost from the library, and these mutants could be determined by measuring mutant frequency in the library relative to a control library (rich media) via microarray hybridization (Sassetti et al., 2001). Optimization of the technique further led to the determination of genes essential for *in vitro* growth from highly saturated Mtb transposon libraries (Sassetti et al., 2003) – the absence/paucity of transposon insertions in a genetic locus in a saturated library could be interpreted as an indication that the gene function was necessary for Mtb viability. TraSH was subsequently employed in the identification of genes involved in Mtb survival and persistence during infection (Dutta et al., 2014; Sassetti et al., 2003), adaptation and survival in macrophages (Dutta et al., 2014; Sassetti et al., 2003) and genes differentially required under conditions of fast and slow growth (Beste et al., 2009).

The TraSH approach was expanded upon and refined with the application of next-generation-sequencing (NGS) methods in the highly-parallel deep sequencing of transposon mutant libraries, yielding a series of similar experimental methodologies collectively referred to as transposon insertion sequencing (TnSeq) (Chao et al., 2016; Griffin et al., 2011; van Opijnen et al., 2009). Prior to TnSeq, analyses of essentiality by TraSH were limited by the

small dynamic range of microarray signals (less than 10-fold), the inability to map insertions to their precise locations and the need for a prefabricated microarray; these problems were overcome by the use of NGS, which permitted the mapping of transposon insertion sites to a single-base pair resolution and improved precision in the quantification of insertions in both coding and non-coding regions (Chao et al., 2013b; Griffin et al., 2011). Subsequent improvements to TnSeq methodology include a system for identifying genes possessing both essential and non-essential domains (Zhang et al., 2012), random barcoding of PCR amplicons to correct for possible amplification biases during sample preparation (Long et al., 2015), and an array of methods for making robust statistical calls of essentiality from TnSeq data (Chao et al., 2013b; DeJesus et al., 2015; DeJesus and Ioerger, 2013, 2015; DeJesus et al., 2013; Pritchard et al., 2014). The benefits from TnSeq screening in Mtb have yielded more definitive lists of genes essential for *in vitro* and *in vivo* survival (Zhang et al., 2012; Zhang et al., 2013). Recent efforts have focused on the use of TnSeq in genetic interaction screening - the identification of secondary mutations significantly modulating the phenotype of a primary mutant, which would imply a functional relation between the mutated genes; this approach has led to the discovery of the components of a membrane associated oxidoreductase complex involved in reactive oxidative species detoxification (Nambi et al., 2015) and genetic factors differentially required for growth in mutants of the penicillin binding proteins (PBPs) *ponA1* and *ponA2* (Kieser et al., 2015).

1.4 Thesis research aims

This dissertation describes the use of TnSeq screening to answer two disparate problems related to the tolerance of exogenous stresses by *Mycobacterium tuberculosis*, with a particular focus on antibiotic stress. In chapter 2, we sought to identify genetic interaction partners of mycobacterial acid resistance protease (MarP), a protein necessary for the tolerance of not just acidic environments but also oxidative, detergent and antimicrobial stresses. Through a TnSeq-based genetic interaction screen, our goal was to

identify novel genes functionally related to *marP* in order to understand the mechanisms behind its role in pleiotropic stress resistance. Chapter 3 presents a series of chemical genomic screens aimed at finding genetic factors modulating antibiotic susceptibility in Mtb, with the goals of better understanding the mechanisms of intrinsic antibiotic resistance in the pathogen, and the possible discovery of synergistic targets potentiating antibiotic treatment. The study culminates in the construction and characterization of a *fecB* knockout mutant, notable for its cross-sensitivity to multiple antibiotics and attenuation *in vivo*. In addition to contributing to our understanding of mycobacterial stress resistance, this work attempts to lay out guidelines for the proper implementation and interpretation of TnSeq screens.

CHAPTER 2: SCREENING FOR GENETIC INTERACTION PARTNERS OF MARP

2.1 Background

Mtb mainly resides in the phagosomal compartment the of host macrophage, a hostile microenvironment that imposes a multitude of environmental stresses upon the pathogen. Among these stresses is phagosomal acidification – before the onset of adaptive immunity, phagosome-lysosome fusion of the Mtb-containing phagosome is arrested, resulting in a mildly acidic intraphagosomal environment of ~pH 6.2; subsequent macrophage activation by interferon gamma (IFN-γ) is able to overcome to overcome the blockade of phagolysosomal fusion, permitting the further acidification of the phagolysosome to ~pH 4.5 (Armstrong and Hart, 1971; Huynh and Grinstein, 2007; Ohkuma and Poole, 1978). In spite of macrophage activation and phagosomal acidification, Mtb is able to maintain its intrabacterial pH at ~ 6.76-7.5 (Vandal et al., 2008). A genetic screen of 10,100 Mtb transposon mutants was performed to identify mutants defective in recovery after exposure to acidified 7H9-Tween 80 media at a pH of 4.5; 34 mutants representing 21 different Mtb genes, of which two (*rv2136c* and *marP*) were found to be consistently defective in recovery from the three different types of acidified media tested (7H9-Tween, 7H9-tyloxapol and phosphocitrate buffer at pH 4.5). The *marP* mutant also failed to maintain intrabacterial pH in activated macrophages, and was attenuated for growth in the mouse aerosol infection model, failing to persist during the chronic phase of infection (Vandal et al., 2008). In addition to acidification, the *marP* transposon mutant was also hypersensitive to other stresses such as oxidative stress (Biswas et al., 2010) and multiple antimicrobial compounds including erythromycin, rifampicin (Vandal et al., 2008), malachite green, nigericin and vancomycin (Pan, unpublished). It was also recently shown that an *M. marinum* ΔmarP mutant is similarly unable to survive phagosomal acidification and fails to establish infection in a zebrafish infection model (Levitte et al., 2016)

marP is conserved across multiple mycobacteria species including *M. leprae, M. bovis, M. avium paratuberculosis*, *M. bovis* and *M. smegmatis* (Ribeiro-Guimaraes and Pessolani, 2007) and was predicted to encode a membrane associated serine protease with four transmembrane helices (Cole et al., 1998; Sonnhammer et al., 1998). Structural studies confirmed that the periplasmic domain of *marP* is a functional serine protease of the chymotrypsin family, and that the periplasmic localization of a catalytically active protease domain was essential for its protective function against oxidative and acid stress (Biswas et al., 2010; Small et al., 2013). The protease substrate/s for MarP *in vivo* eluded research efforts at identification for some time; however, recent work in our lab has identified the peptidoglycan hydrolase RipA as a proteolytic target of MarP. MarP was observed to cleave RipA *in vitro* and coimmunoprecipitate to a greater extent under acidic pH relative to neutral conditions in a *M. smegmatis* system expressing tagged versions of $MarP_{TB}$ and $RipA_{TB}$. Expression of RipA-LG (a mutant form of RipA with amino acid substitutions in its predicted MarP cleavage site, and was confirmed to be less efficiently processed by MarP) was unable to complement growth and morphological defects in a RipAB knockdown *M. smegmatis* strain, indicating that cleavage by MarP may be required to activate RipA *in vivo* (Botella, 2016, study under review).

This chapter describes a concurrent attempt to identify genetic interaction partners of *marP* by TnSeq-screening, with the aim of discovering other functionally related proteins.

2.2 Defining genetic interaction under TnSeq

Genetic interaction/epistasis is the phenomenon by which the effects of one gene are able to modulate the phenotypes arising from a second gene; more succinctly put, genetic interaction refers to an unexpected phenotype resulting from the combination of two or more mutations (Baryshnikova et al., 2013; Dixon et al., 2009). The effective measurement of genetic interaction requires both a quantitative indicator of phenotypic strength, and a neutrality function, which basically defines the “expected” baseline

phenotype arising from two functionally independent mutations (Mani et al., 2008). Genetic interactions can thus be quantified and classified into two main classes according to how the double mutant deviates phenotypically from the neutral baseline – negative/aggravating interaction refers to a case where the double mutant exhibits a more severe phenotype than expected, whereas positive/alleviating interactions reflect the opposite situation where the double mutant phenotype is less severe than the expected baseline.

The functional relationship of a secondary unknown mutation to a primary "bait" mutant of interest may be inferred from genetic interaction, though accurate interpretation may be complicated by the pleiotropic and highly-interconnected nature of genetic interaction networks. Negative interactions mainly indicate a functional relationship by which the function of one gene buffers against the loss of the other; the most extreme case of negative interaction, synthetic lethality, arises when two mutations with little or no growth defect individually result in the unviability of the double mutant, indicative of the total loss of buffering capacity. Negative interaction commonly results from individual genes acting in parallel, redundant biological pathways fulfilling a common function; it may also arise in a situation referred to as a defect-damage-repair cycle, in which the loss of one gene leads to secondary damages which are repaired by a second gene functionally different from the first (Ting et al., 2008) (Fig. 2.1a).

Positive interaction can be slightly more difficult to interpret due to the multiple possibilities resulting in the double mutant having a less severe phenotype than expected. One of the more basic subclasses of positive interaction is coequal interaction, in which the phenotypes of the single mutants and the double mutant are quantitatively similar (Baryshnikova et al., 2013); this is suggestive of the mutants being in the same biological pathway - when one mutation deactivates the entire pathway, additional lesions within the pathway will have no additional impact on the organism. Positive interaction may also be indicative of suppression, by which one mutation is able to rescue the fitness defect caused

by another; mechanisms for suppression include the restoration of homeostatic equilibrium by the antagonistic effect of the secondary mutation, relief of a toxic effect caused by a primary mutation, or induction of a compensatory pathway (Fig. 2.1B).

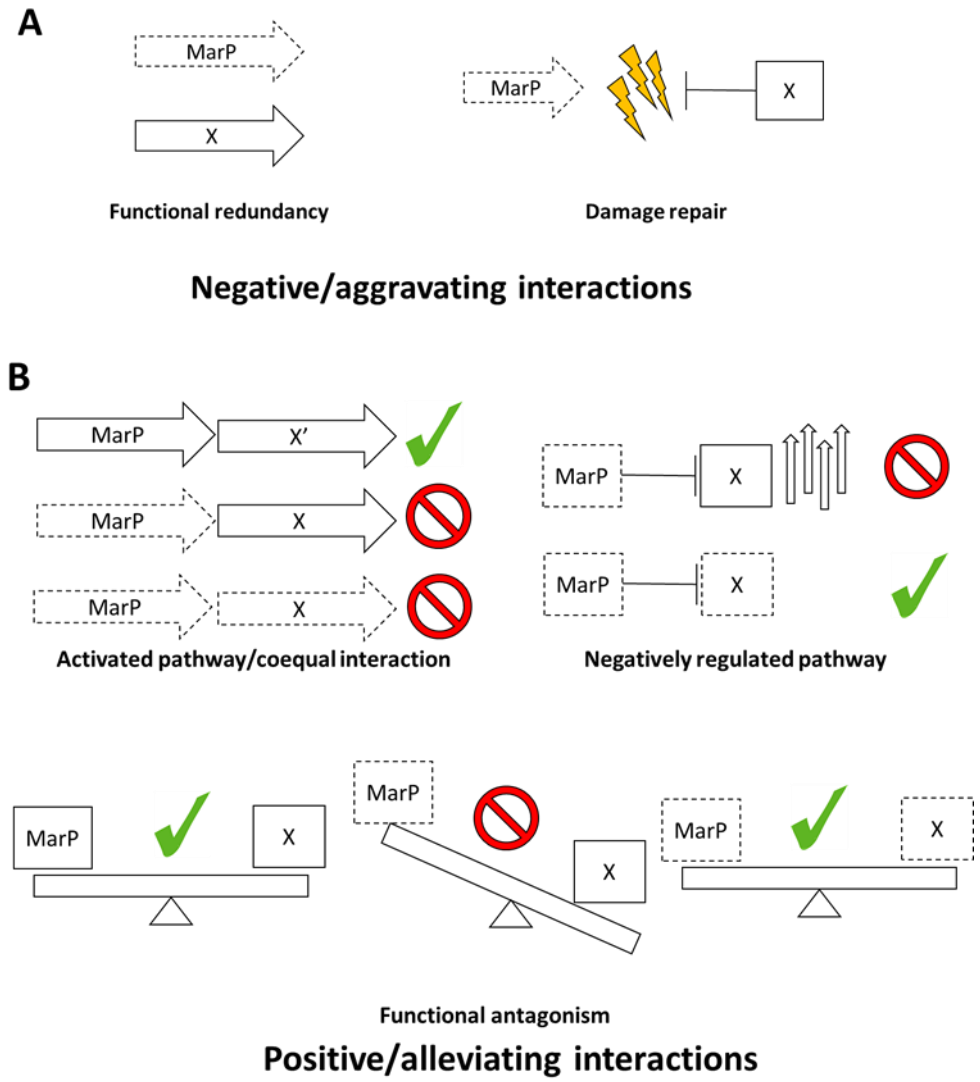

Figure 2.1 – Interpretation of genetic interaction within the context of the *marP* TnSeq genetic screen. Schematic diagrams of possible functional interactions between MarP and unknown interactor protein X. Shapes outlined by dashed lines denote loss-of-function mutation of the protein indicated. **A -** Negative interaction may indicate the presence of parallel pathways with similar functions redundant to MarP, or damage repair pathways compensating for deleterious secondary effects from MarP deletion. **B –** Positive interactions may identify pathways regulated by MarP – MarP may activate functional proteins, and loss-of-function mutations in MarP, the activated protein or both proteins

should result in similar phenotypes as both proteins are in the same functional pathway. MarP may also negatively regulate the function of another protein, and the resultant gain of function from the loss of regulation may result in deleterious effects. Toxicity from the loss of function may be suppressed by the loss of the protein. Suppression mutations by which loss of function of protein X rescues the loss of MarP (or vice versa, as the relationship can be asymmetric or symmetric) may also indicate an antagonistic functional relationship between the two; loss of either protein results in homeostatic disequilibrium, which may be restored when both proteins are lost.

TnSeq allows for the highly-parallel quantitative fitness analysis of mutants within a transposon library, and is well-suited for the purposes of genetic interaction screening by the comparison of transposon insertion libraries constructed in the wildtype and bait mutant (in this case a gene-deletion mutant of *marP*) backgrounds (van Opijnen et al., 2009; van Opijnen et al., 2014). The readout of a TnSeq analysis reports the proportional frequencies at each transposon mutant within the output library – mutant frequency at the end of a TnSeq experiment is a function of three factors - 1. the initial mutant frequency, 2. the degree of outgrowth of the entire population over the course of the experiment , and 3. the exponential growth rate of the mutant relative to the overall exponential growth rate of the library (W_{mt}) (van Opijnen and Camilli, 2013). Assuming that the majority of mutations have a minimal impact on fitness, and that the selection conditions of the experiment only perturb the fitnesses of a minority of the mutants in the library, the overall growth rate of the library approximates that of the parental wild-type strain it was constructed form (van Opijnen et al., 2009) . If factors 1 and 2 are held constant for all transposon mutants within the analysis, mutant frequency is correlated with the W_{mt}, and can be used as an index of mutant fitness – transposon mutants with a higher fitness and growth relative to the overall library will have higher frequency within the library, and conversely, low frequency or absence of the mutant in a library indicates reduced fitness.

The multiplicative/product function is the most widely-accepted neutrality function in genetic interaction studies, and it predicts that the fitness of a double mutant to be the product of the fitnesses of each of the single mutants, fitness in this case being the

exponential growth rate of the mutant relative to the wild type (Mani et al., 2008), or approximately the W_{mt} observed from the TnSeq experiment. Under this definition of neutrality, a non-interacting mutant would have the same W_{mt}, and consequently output mutant frequency in both the WT and ΔmarP backgrounds, supposing initial mutant frequencies and the degree of outgrowth of the WT/ΔmarP libraries are equivalent. An index of genetic interaction for each gene can thus be derived from the log-transformed ratio of the transposon insertion frequencies for the gene between the ΔmarP and WT library background, otherwise referred to as the log_2Fc:

$$log_2 Fc = log_2\left(\frac{Mutant\ frequency\ in\ \Delta marP\ background}{Mutant\ frequency\ in\ WT\ background}\right)$$

A negative log_2-Fc indicates reduced mutant frequency in the knockout background relative to the WT, and hence lower-than-expected double mutant fitness/negative interaction, whereas a positive TnSeq-Fc indicates positive interaction.

Possible functional interpretations of genetic interactions from the screen are summarized in Fig. 2-1. As the bait *marP* mutation is a gene deletion, and transposon insertions in general completely disrupt gene function (though this is not always the case); mutations in the context of this experiment are generally assumed to be complete loss-of-function mutations, constraining and simplifying the possible interpretations. Negative interactions may indicate functional pathways redundant to MarP, or damage-repair pathways repairing secondary damages resulting from the loss of MarP. Of greater mechanistic interest are the positive interactions – as the function of MarP has been shown to be dependent on serine protease activity in the periplasm (Biswas et al., 2010; Small et al., 2013), the implication is that MarP acts by regulating the activity of other proteins via proteolysis, and positive interactions may indicate proteolytic substrates that may be activated or degraded by MarP. Suppression mutations by which transposon mutation rescues growth defects caused by *marP* deletion, or vice versa, may suggest functionally antagonistic pathways to MarP.

2.3 Genetic interaction analysis using TnSeq

In order to identify potential genetic interaction partners of MarP, we constructed quadruplicate Mtb transposon mutant libraries using the aforementioned *Himar1* transposon mutagenesis system (Sassetti et al., 2001) in both the WT H37Rv and Δ*marP* backgrounds. After phage transduction, transposon mutants were selected for on rich Middlebrook 7H9 solid media. 7H9 was used instead of the commonly used 7H10/11 media to avoid selective pressure from malachite green. It was assumed that at the point of mutagenesis, each possible transposon insertion site had an equal probability of transposon insertion in both the WT and Δ*marP* backgrounds, fulfilling one of the premises necessary for the direct comparison of mutant frequencies between the two strains. The Δ*marP* strain has a slight growth defect on 7H9 plates relative to the WT background; to standardize the degree of outgrowth between the two experimental groups, the WT and Δ*marP* libraries were incubated for 19 and 21 days post-mutagenesis respectively before analysis/storage. The constructed libraries consisted of ~10^5 unique mutants each, suggestive of high library diversity.

Libraries were sequenced via the Illumina® HiSeq platform, and transposon-chromosome junctions were mapped to TA-dinucleotide insertion sites as previously described, in order to determine the respective frequencies of each transposon mutant (Long et al., 2015). 500,000 to 3,200,000 unique transposon insertions were mapped to the genome for each library, with coverage of the possible TA insertion sites ranging from 50-70% each; after aggregation of the quadruplicates, both the WT and the Δ*marP* backgrounds had a TA site coverage of ~78-79%, indicative of a highly-saturating coverage of non-essential TA sites (Table 2.1).

Table 2.1 - Sequencing statistics of TnSeq libraries

Library	Unique insertions mapped	#TA sites hit	% TA coverage
WT1	995,189	47,768	64.0
WT2	888,503	49,309	66.1
WT3	3,195,442	39,441	52.9
WT4	3,042,234	46,408	62.2
WT total	**8,121,368**	**58,212**	**78.0**
KO1	757,952	41,442	55.6
KO2	500,802	42,315	56.7
KO3	3,069,648	48,589	65.1
KO4	2,455,883	52,107	69.7
KO total	**6,784,285**	**58,638**	**78.6**

Downstream TnSeq library analysis was performed using the TRANSIT analysis tool (DeJesus et al., 2015). Insertion counts across libraries were normalized by the trimmed-total-reads (TTR) procedure to adjust for differences in sequencing depth and saturation between library samples. Insertions were then totaled for each gene, and gene-level $\log_2$Fcs were computed from the ratio of normalized insertion counts between the Δ*marP* and WT backgrounds; the statistical significance of each gene-level WT/KO comparison was assessed by resampling under a variation of the classical permutation test , and false discovery rate was controlled via the Benjamini Hochberg procedure (DeJesus et al., 2015). Under a statistical cutoff of $q<0.05$, there were 194 significant negative interactors and 83 significant positive interactors with *marP* (Table 2.2, Figure 2.3A). In addition to genetic interaction analysis, gene essentiality was assigned using a 4-state Hidden Markov Model (HMM) (DeJesus and Ioerger, 2013) under each of the library backgrounds; the mean number of insertions per TA site per gene was also computed as a continuous quantifier of mutant fitness/gene essentiality in each set of libraries (Table 2.2, Figure 2.2). Genome-wide mutant fitness in both libraries was distributed on a long-tailed, heavy-peaked bimodal distribution with peaks centered at the limit of detection (representing essential genes) and the library mean of insertions per site; excluding essential genes, the majority of mutants displayed fitnesses close to the library mean (~70% of genes had mean insertion counts per TA site within ±2-fold of the library mean) (Figure 2.2), indicating that the mean library fitness was

likely to be approximately similar to the fitness of the parental strain. Approximately 12% of the genes in each library set were marked as essential by the HMM; the fitness distribution of the ΔmarP libraries was slightly longer-tailed, with 17.1% of genes classified as either essential/growth-defect causing and 8.4% conferring a growth advantage versus 15.1% and 5.4% in the WT background, indicating genetic interaction between the *marP* deletion and transposon insertions (Table 2.2, Figure 2.2).

Table 2.2 - Essentiality statistics of WT/ΔmarP libraries. Gene essentiality calls from 4-state HMM and conditional essentiality calls from the resampling test. Gene essentiality could not be determined for 17 genes due to the low number of TA insertion sites in these genes.

Gene essentiality (HMM)				
	WT		**Δ*marP***	
	# genes	**% genes**	**# genes**	**% genes**
Non-essential	3188	79.0	2989	74.1
Essential	478	11.8	493	12.2
Growth-defect	135	3.3	197	4.9
Growth advantage	218	5.4	340	8.4
Undetermined	17	0.4	17	0.4
Conditional essentiality (ΔmarP vs WT)				
	# genes		**% genes**	
Negative interactors	194		4.8	
Positive interactors	83		2.1	

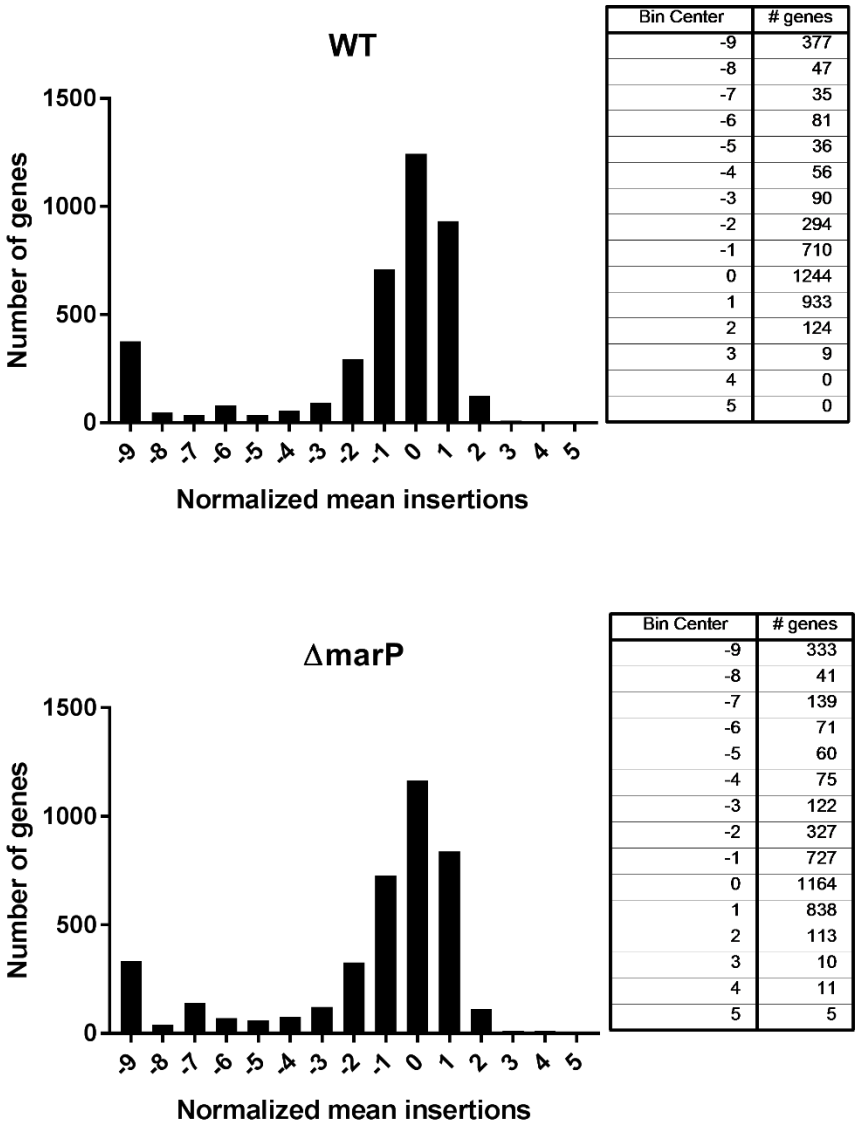

Bin Center	# genes
-9	377
-8	47
-7	35
-6	81
-5	36
-4	56
-3	90
-2	294
-1	710
0	1244
1	933
2	124
3	9
4	0
5	0

Bin Center	# genes
-9	333
-8	41
-7	139
-6	71
-5	60
-4	75
-3	122
-2	327
-1	727
0	1164
1	838
2	113
3	10
4	11
5	5

Figure 2.2 - Transposon mutant fitness distribution in WT/Δ*marP* library backgrounds. Histograms of distributions of mutant fitness for each gene based on the mean insertions per TA site per gene metric; to accommodate the long-tailed distributions, fitness is expressed as a $\log_2$ transformed ratio of the mean insertion count per TA site for each gene relative to the mean insertion count per TA site over the entire genome (~40 insertions per site after read normalization over all libraries). Distributions are representative of quadruplicated transposon libraries in the WT/Δ*marP* library backgrounds,

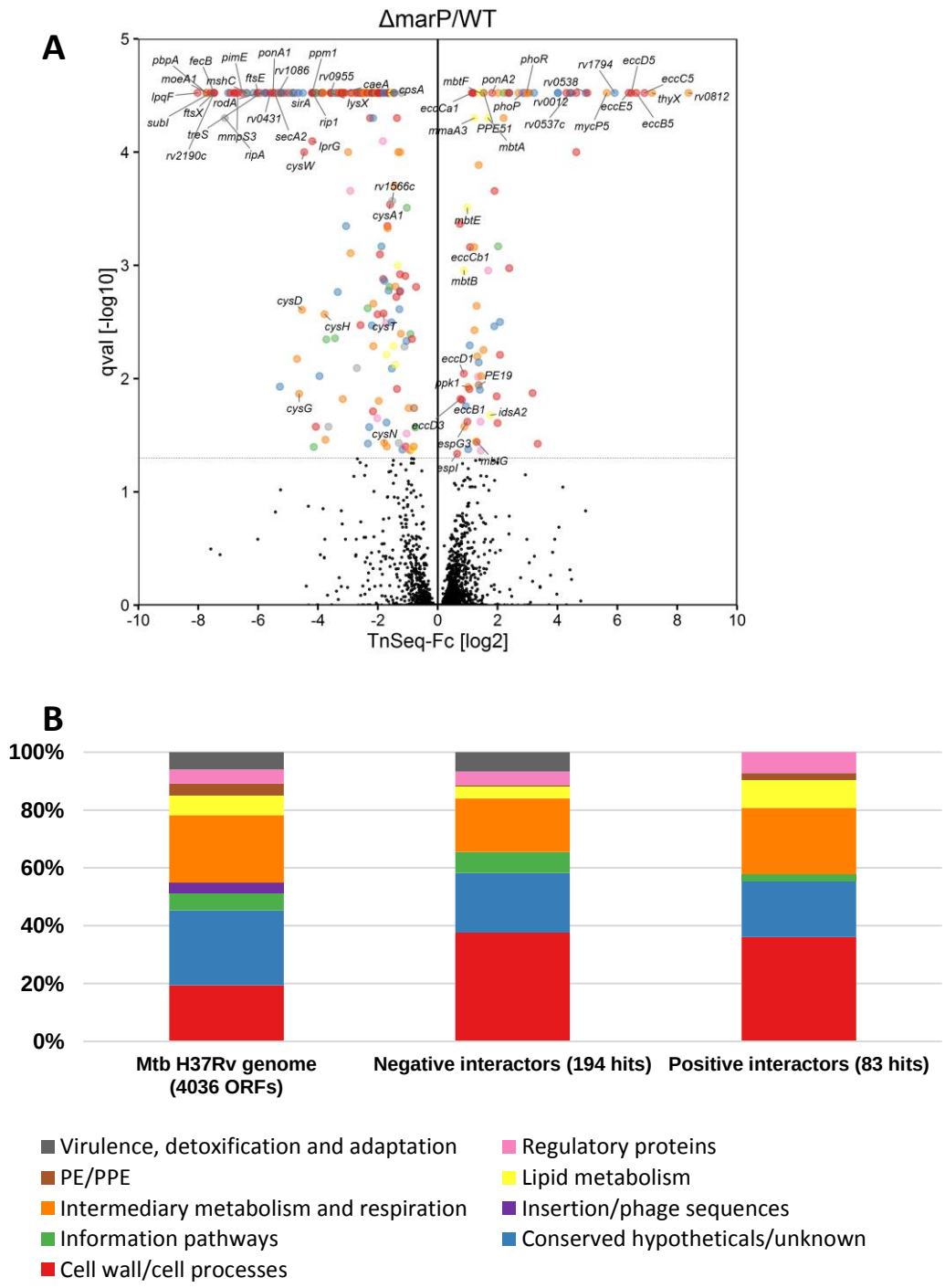

Figure 2.3 – Functional categorization of genetic interaction partners of *marP.* A – Volcano plot of q-values obtained from resampling testing against TnSeq-Fc for each gene locus. Genes passing the significance threshold (q<0.05) are coloured based on their functional categories in Tuberculist, and notable genes have been labeled with their gene names. **B-** Categorical breakdown of negative and positive interactors of *marP* based on Tuberculist functional categories. Proportions of each functional category in the H37Rv Mtb genome are displayed alongside as a point of reference.

2.3.1 Negative interactors

We identified 194 significant ($q < 0.05$) negative interactors of *marP* (Fig. 2.3A, Appendix A1). Based on the functional categories defined by Tuberculist, there was a notably higher representation of cell wall/cell process genes in the set of negative interactors (73/194, or 37.6%) relative to the overall proportion of cell wall/process genes in the Mtb genome (779/4036, or 19.3%) (Fig. 2.3B). Negative interactors within this category were functionally diverse, including genes involved in peptidoglycan biosynthesis/remodeling (*pbpA*, *ponA1* and the short-chain Z-isoprenyl diphosphate synthase *rv1086*), cell division (*ftsE*, *ftsX, ftsI/rv2864c,* r*odA*), inorganic ion transport (the phosphate transport operon *rv0928-rv0930* and sulfate transport operon *rv2400c-rv2397c*), substrate exporters (*mmpS3, mmpL7, secA2, rv1410c* and the putative efflux pump operon *drrABC*), various lipoproteins, and membrane-associated proteins of unknown function. In addition to genes formally classified as cell wall/cell process genes, the NlpC/P60 family peptidoglycan hydrolases *ripA*, *ripC(rv2190c)* and *ripD(rv1566c)* were identified as negative interactors of *marP* in the virulence, detoxification and adaptation functional category.

As negative interaction implies parallel functionality and redundancy, we were interested in seeing which of the other 20 genes identified in the acid sensitivity screen alongside *marP* were also negative interactors (Vandal et al., 2008). 8 out of the 20 genes were significant negative interactors (*pbpA, ponA1, ppm1, lysX, rv0955, caeA, mpa* and *rv2136c*) (Table 2.3), suggesting that in addition to resistance to acidic conditions, these genes may also mediate parallel functions that become more essential in the absence of *marP*, resulting in synthetic sickness/lethality in the double mutant. Most of these genes fall under the cell wall/cell processes Tuberculist functional category with the exception of lysyl-tRNA synthetase *lysX*, which may contribute to peptidoglycan peptide bridge formation, which has been observed in tRNA synthetases in other bacteria (Neihardt et al., 1975; Vandal et al., 2008; Villet et al., 2007). Among the other genes with established functions, *pbpA* and

ponA1 encodes penicillin-binding proteins involved in peptidoglycan biosynthesis and remodeling, whereas *ppm1* encodes a polyprenol-monophosphomannose synthase involved in the biosynthesis of lipomannan and lipoarabinomannan. Given the predominance of known and putative genes involved in cell envelope biosynthesis amongst the negative interactors, it is likely that *marP* plays a role in cell envelope integrity, which could possibly account for its pleiotropic stress-sensitive phenotype.

In addition to genes annotated as contributing to cell wall structure, we also noticed that *marP* was synthetically sick/lethal with multiple genes involved in sulfur utilization (Table 2.4). These include the primary sulfate transport complex operon (*subI-cysTWA1*/rv2400c-2397c) and the sulfur metabolism genes *sirA, cysD, cysH, sseA, cysG, cysN* and the thiosulfate sulfurtransferase gene *sseA*. Loss of these genes (with the exception of *sseA*) results in profound growth attenuation in the WT background, as indicated by the HMM essentiality calls and the low mean insertions per TA site (<7 vs the library mean of 43); these genes became fully essential under the Δ*marP* background. This may be interpreted as *marP* activating secondary sulfur transport pathways, however, it is more likely that intact sulfur utilization pathways are necessary for cell envelope integrity and function.

Table 2.3 - List of mutants hypersensitive to 7H9-Tw at pH4.5 from a prior acid sensitivity screen Mutant fitness is expressed in terms of mean insertions per TA site in the gene (the mean across the entire genome is ~43 in the WT background and ~48 in the ΔmarP background, post-normalization for library size). Significant q-values (q<0.05) are highlighted in green, while insignificant results are highlighted in yellow. Essentiality calls under the WT/KO library backgrounds are labeled as NE- non-essential, ES – essential, GD – growth defective, GA – growth advantageous.

		Mean insertions per TA site							
Rv #	Gene	WT	ΔmarP	log2FC	q-val	Tuberculist category	Function	WT Call	KO call
Rv0016c	pbpA	13.9	0.1	-7.73	0	Cell wall/cell processes	penicillin-binding protein PbpA	NE	ES
Rv0050	ponA1	21.9	0.5	-5.50	0	Cell wall/cell processes	bifunctional penicillin-binding protein 1A/1B PonA1	NE	GD
Rv2051c	ppm1	126.7	7	-4.19	0	Cell wall/cell processes	polyprenol-monophosphomannose synthase Ppm1	ES	ES
Rv1640c	lysX	69.7	5.8	-3.58	0	Information pathways	lysyl-tRNA synthetase 2 LysX	NE	GD
Rv0955	rv0955	58.9	5	-3.57	0	Cell wall/cell processes	integral membrane protein	NE	GD
Rv2224c	caeA	276.4	29.9	-3.21	0	Cell wall/cell processes	carboxylesterase CaeA	GA	NE
Rv2115c	mpa	32	7.3	-2.13	0	Cell wall/cell processes	mycobacterial proteasome ATPase Mpa	NE	GD
Rv2136c	rv2136c	125.9	33	-1.93	0.0008	Cell wall/cell processes	undecaprenyl-diphosphatase	NE	NE
Rv2206	rv2206	19.4	7.9	-1.30	0.1263	Cell wall/cell processes	transmembrane protein	NE	NE
Rv3679	rv3679	18.8	10.3	-0.87	0.5009	Cell wall/cell processes	anion transporter ATPase	NE	NE
Rv3680	rv3680	16.1	10	-0.69	0.3206	Cell wall/cell processes	anion transporter ATPase	NE	NE
Rv2052c	rv2052c	58.6	42.7	-0.46	0.7532	Conserved hypotheticals	hypothetical protein	GA	NE
Rv1272c	rv1272c	33.5	31	-0.11	1	Cell wall/cell processes	ABC transporter membrane protein	NE	NE
Rv1781c	malQ	78.1	79.9	0.03	1	Intermediary metabolism and respiration	4-alpha-glucanotransferase MalQ	NE	NE
Rv1273c	rv1273c	28.8	39.9	0.47	0.5197	Cell wall/cell processes	ABC transporter membrane protein	NE	NE
Rv0007	rv0007	183.6	335.1	0.87	0.08	Cell wall/cell processes	membrane protein	GA	GA
Rv2222c	glnA2	32.5	76.5	1.23	0.0037	Intermediary metabolism and respiration	glutamine synthetase GlnA2	NE	NE
Rv2379c	mbtF	7.4	19.6	1.41	0	Lipid metabolism	peptide synthetase MbtF	NE	NE
Rv3682	ponA2	262	925.2	1.82	0	Cell wall/cell processes	bifunctional membrane-associated penicillin-binding protein 1A/1B PonA2	GA	GA

Table 2.4 – Negative interactors involved in sulfur utilization

		Mean insertions per TA site							
Rv #	Gene	WT	ΔmarP	log2FC	q-val	Tuberculist category	Function	WT Call	KO call
Rv2400c	subI	4	0	-7.58	0	Cell wall/cell processes	sulfate-binding lipoprotein SubI	GD	ES
Rv2391	sirA	3.1	0.1	-4.86	0	Intermediary metabolism and respiration	ferredoxin-dependent sulfite reductase SirA	GD	GD
Rv1285	cysD	3.2	0.1	-4.53	0.0025	Intermediary metabolism and respiration	sulfate adenylyltransferase subunit 2 CysD	GD	ES
Rv2398c	cysW	3.5	0.2	-4.46	0.0001	Cell wall/cell processes	sulfate-transport ABC transporter integral membrane protein CysW	GD	ES
Rv2392	cysH	3.8	0.3	-3.78	0.0027	Intermediary metabolism and respiration	3'-phosphoadenosine 5'-phosphosulfate reductase CysH	GD	GD
Rv2399c	cysT	2.5	0	-1.81	0.0027	Cell wall/cell processes	sulfate-transport ABC transporter integral membrane protein CysT	GD	ES
Rv2397c	cysA1	2	0	-1.59	0.0003	Cell wall/cell processes	sulfate-transport ABC transporter ATP-binding protein CysA1	GD	GD
Rv3283	sseA	55.7	23.4	-1.25	0.0001	Intermediary metabolism and respiration	thiosulfate sulfurtransferase SseA	NE	NE
Rv3778c	rv3778c	0.9	0	-0.92	0.043	Intermediary metabolism and respiration	cysteine desulfurase	GD	ES
Rv2847c	cysG	2.2	0.1	-4.63	0.0136	Intermediary metabolism and respiration	uroporphyrin-III C-methyltransferase	GD	ES
Rv1286	cysN	6.5	1.9	-1.79	0.0368	Intermediary metabolism and respiration	bifunctional enzyme CysN/CysC	GD	ES

Proteases that negatively interact with *marP* may indicate redundant regulatory roles, and common proteolytic substrates. We identified 5 proteases that were negative interactors of *marP* (Table 2.5). Rip1/Rv2869c is a site-2-protease (S2P) that controls multiple transcriptional pathways, including the regulation of lipid biosynthesis and cell envelope composition (Makinoshima and Glickman, 2005; Schneider et al., 2014). However, since Rip1 acts via intramembrane proteolysis of transmembrane segments, and the protease domain of *marP* is localized to the periplasm, it is unlikely that they independently regulate a common substrate; sequential processing of the same protein substrate at starting with periplasmic cleavage followed by transmembrane proteolysis, as in the case of a site-1-protease/S2P system, would instead be implied by positive genetic interaction. It is thus likely that the negative interaction from *rip1* is not dependent on a shared substrate, but independent regulation of cell envelope integrity.

The remaining four proteases are all membrane-associated proteins. HtpX is a putative heat shock protein while PepD is a HtrA-like serine protease, suggesting a possible role for *marP* in processing misfolded proteins. Rv2224c/CaeA is a membrane-associated

protease shown to be important for virulence in the mouse model of Mtb infection (Lun and Bishai, 2007; Rengarajan et al., 2008) and was also identified as a factor involved in acid resistance (Vandal et al., 2008), whereas Rv3194c is a PDZ-domain containing Lon-like protease. Known proteolytic substrates of these proteases include GroEL2, which is processed by CaeA (Rengarajan et al., 2008), and Rv2744c, which is processed by PepD and is classified as a member of the PspA-family of proteins involved in the phage-shock process in Gram-negative bacteria (White et al., 2011). These known substrates, alongside those that have not been identified yet, may be shared proteolytic targets of *marP*.

Table 2.5 – Negatively-interacting proteases

		Mean insertions per TA site						
Rv #	**Gene**	**WT**	**ΔmarP**	**log2FC**	**q-val**	**Tuberculist category**	**Function**	**WT Call**	**KO call**
Rv0563	htpX	29.8	2.9	-3.35	0	Virulence, detoxification and adaptation	protease transmembrane protein heat shock protein HtpX	NE	NE
Rv0983	pepD	21.1	2.2	-3.26	0	Intermediary metabolism and respiration	serine protease PepD	NE	GD
Rv2224c	caeA	276.4	29.9	-3.21	0	Cell wall/cell processes	carboxylesterase CaeA	GA	NE
Rv2869c	rip1	36.3	2	-4.18	0	Cell wall/cell processes	metalloprotease RseP	NE	GD
Rv3194c	rv3194c	74.6	35.2	-1.08	0.0012	Cell wall/cell processes	PDZ domain-containing protease	NE	NE

As RipA was identified by our lab to be a proteolytic substrate activated by MarP (Botella, study under review), it was unexpected that *ripA* was classified as a negative interactor (Fig. 2.4A), which would imply that it lies on a parallel functional pathway to *marP* as opposed to being on the same pathway. The analysis of *ripA* is complicated by the fact that RipA possesses both essential and non-essential domains as indicated by a prior TnSeq study (Zhang et al., 2012), and the transposon mutants detectable in the output TnSeq library are not complete loss of function mutants, but plausibly neutral/partial loss of function mutants. Mapping of the transposon insertions in *ripA* in the WT and Δ*marP* library backgrounds revealed that *ripA* could sustain transposon insertions in its C-terminal non-essential domain in the WT background, in agreement with the prior TnSeq study, but not in the Δ*marP* background, indicating the domain becomes synthetically essential in the absence of *marP.* Under these special circumstances, the synthetic lethal interaction observed could

be interpreted as the combined effect of two partial loss-of-function mutations producing a complete loss-of-function of an essential pathway. The further implications of this *ripA-marP* genetic interaction will be discussed in detail in section 2.x

A

Rv #	Gene	Mean insertions per TA site: WT	Mean insertions per TA site: ΔmarP	log2FC	q-val	Tuberculist category	Function	WT Call	KO call
Rv1477	ripA	26.9	0.2	-7.11	5E-05	Virulence, detoxification and adaptation	Peptidoglycan hydrolase	ES	ES

B

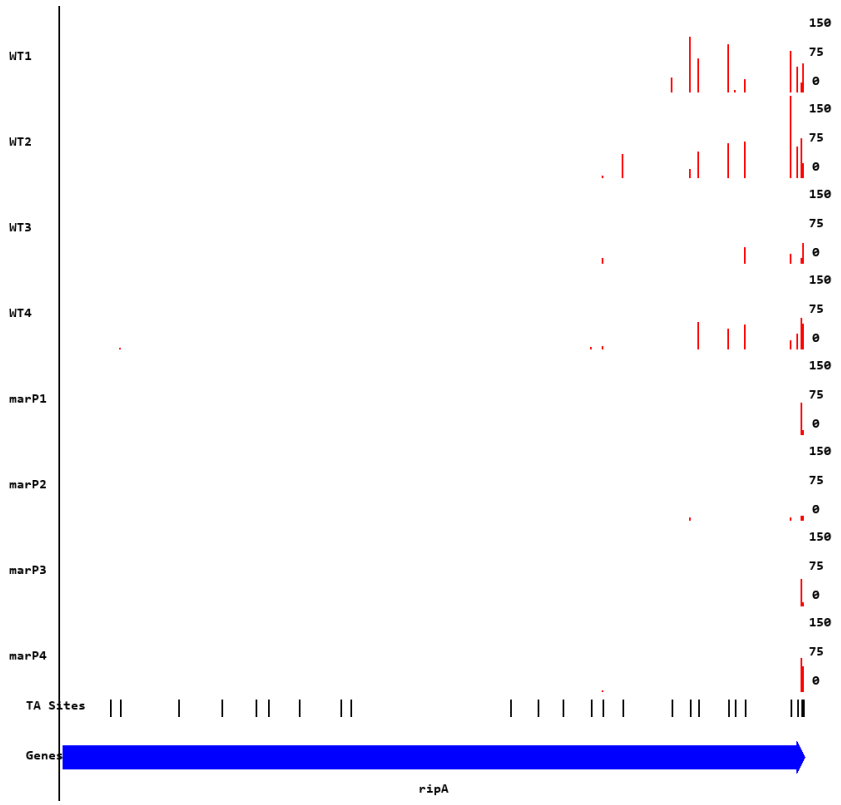

Figure 2.4 – Negative interaction of *ripA* with *marP*. **A –** TnSeq statistics for *ripA*. **B –** Transposon insertion map for *ripA* in quadruplicated WT/Δ*marP* libraries. Histogram bars indicate the number of unique transposon insertions sequenced at each TA site in each library

2.3.2 Positive interactors

We also identified 83 significant positive interacting partners of *marP* (Fig. 2.3A) – as positive interaction may be the result of *marP* deletion alleviating the fitness defects of the transposon mutant, or conversely, that of the transposon mutant alleviating the *marP* phenotype, we sub-classified positive interactors based on the degree of fitness defect of the transposon mutant in the WT background: group 1 positive interactors had less than half of the library mean of insertions per TA site (<21 insertions per TA site), and were interpreted to be growth defective or essential in the WT background, and the positive interaction likely represents alleviation of the transposon mutant fitness defect; whereas group 2 positive interactors (>21 insertions per TA site) had minimal/no growth defects in the WT background, indicating that positive interaction was likely due to increased fitness of the double mutant relative to the parental Δ*marP* strain. These groups are only approximate classifiers of the type of positive interaction; for example, some mutants (e.g. *rv1178*) have a low transposon count in the WT background and a higher than average insertion count in the Δ*marP* background, suggesting that the double mutant alleviates fitness defects observed in both single mutants in a two-way antagonistic relationship.

Similar to the case of negative interactors, there was an overrepresentation of cell wall/cell process genes amongst the positive interactors (30/83 genes, or 36.1%, relative to 19.3% in the whole genome). Notably, genes from the type VII secretion systems ESX-1, ESX-3 and ESX-5 were represented amongst the positive interactors (Table 2.6). Of these three systems, the ESX-5 genes *(eccBCDE5, mycP5, rv1794)* exhibited the strongest group 1 positive interactions (log2Fc > 5.5) – mutants exhibited strong attenuation in the WT background (mean insertions per TA site <= 1) but not in the Δ*marP* background, with mutation of *eccB5, eccC5* and *eccE5* conferring a slight fitness advantage (mean insertions per TA site >60, relative to the library mean of ~48 insertions per site). The ESX-1 genes *eccB1, eccCa1, eccCb1, espI* and *eccD1* exhibited weaker group 2 positive interactions – mutations in these

genes conferred a slight fitness advantage in the WT background (>60 insertions per TA site, relative to the WT library mean of 43 insertions per site), and a larger fitness advantage in the Δ*marP* background (>100 insertions per TA site). Finally, the ESX-3 genes *espG3, eccD3* and *mycP5* exhibited weak group 1 positive interaction with *marP* – insertions in these genes were not detectable in the WT background, leading to these genes being labelled as essential in the WT background by the HMM, but could be detected (~1 insertion per TA site) in the Δ*marP* background, suggesting weak alleviation of the ESX-3 essentiality phenotype.

Table 2.6 – Positively-interacting type VII secretion system genes Rv numbers of ESX-1 genes are highlighted in yellow, ESX-3 genes in red and ESX-5 genes in blue.

		Mean insertions per TA site								Positive interaction group
Rv #	Gene	WT	ΔmarP	log2FC	q-val	Tuberculist category	Function	WT Call	KO call	
Rv0289	espG3	0	1	0.99	0.024	Cell wall/cell processes	ESX-3 secretion-associated protein EspG3	ES	GD	1
Rv0290	eccD3	0	0.7	0.76	0.0151	Cell wall/cell processes	ESX-3 secretion system protein EccD3	ES	GD	1
Rv0291	mycP3	0	1.5	1.32	0.0064	Intermediary metabolism and respiration	membrane-anchored mycosin MycP3	ES	GD	1
Rv1782	eccB5	0.7	66.6	6.63	0	Cell wall/cell processes	ESX-5 secretion system protein EccB5	GD	NE	1
Rv1783	eccC5	0.5	60.3	6.91	0	Cell wall/cell processes	ESX-5 secretion system protein EccC5	GD	NE	1
Rv1794	rv1794	0.5	27.2	5.91	0	Conserved hypotheticals	hypothetical protein	GD	NE	1
Rv1795	eccD5	0.4	39.3	6.47	0	Cell wall/cell processes	ESX-5 secretion system protein EccD5	GD	NE	1
Rv1796	mycP5	0.6	27.6	5.65	0	Intermediary metabolism and respiration	proline rich membrane-anchored mycosin MycP5	GD	NE	1
Rv1797	eccE5	1	86.9	6.38	0	Cell wall/cell processes	ESX-5 secretion system protein EccE5	GD	NE	1
Rv3869	eccB1	79.3	139.2	0.81	0.0155	Cell wall/cell processes	ESX-1 secretion system protein EccB1	NE	GA	2
Rv3870	eccCa1	64.7	142.8	1.14	3E-05	Cell wall/cell processes	ESX-1 secretion system protein EccCa1	NE	GA	2
Rv3871	eccCb1	61.6	130.5	1.08	0.00069	Cell wall/cell processes	ESX-1 secretion system protein EccCb1	NE	GA	2
Rv3876	espI	65.8	103.4	0.65	0.04602	Cell wall/cell processes	ESX-1 secretion-associated protein EspI	NE	GA	2
Rv3877	eccD1	63.2	115.4	0.87	0.00903	Cell wall/cell processes	ESX-1 secretion system protein EccD1	NE	GA	2

As the main substrates of type VII secretion systems are PE/PPE proteins, we were interested in whether any of the PE/PPE genes could contribute to the positive interaction observed. *pe19*, which is associated with the ESX-5 operon, and *ppe51*, which is not directly adjacent to any of the type VII secretion operons, conferred a minor growth advantage when disrupted in the *ΔmarP* background (Table 2.7). The magnitude of this positive interaction

effect was far lower than that observed in the ESX-5 system, suggesting that the collective effect of defective secretion of multiple substrate by ESX-5 may account for the strong positive interaction observed.

Table 2.7 – Positively interacting PE/PPE proteins

		Mean insertions per TA site							Positive interaction group
Rv #	Gene	WT	ΔmarP	log2FC	q-val	Tuberculist category	Function	WT Call	KO call	
Rv1791	PE19	36.2	93.6	1.37	0.0114	PE/PPE	PE family protein PE19	NE	NE	2
Rv3136	PPE51	29	84.5	1.54	0	PE/PPE	PPE family protein PPE51	NE	NE	2

marP deletion was also able to alleviate fitness defects caused by disruption of genes in mycobactin biosynthesis (Table 2.8). There were a lower than average number of TA insertions (<22) in *mbtA, mbtB, mbtE, mbtF* and *mbtG* in the WT background, and an approximate 2-fold increase in transposon insertions in these genes in the ΔmarP background.

Table 2.8 – Positively-interacting mycobactin biosynthesis genes

		Mean insertions per TA site							Positive interaction group
Rv #	Gene	WT	ΔmarP	log2FC	q-val	Tuberculist category	Function	WT Call	KO call	
Rv2378c	mbtG	21.7	52.4	1.27	0.0353	Lipid metabolism	lysine-N-oxygenase MbtG	NE	NE	2
Rv2379c	mbtF	7.4	19.6	1.41	0	Lipid metabolism	peptide synthetase MbtF	NE	NE	1
Rv2380c	mbtE	8.1	16.1	0.99	0.0003	Lipid metabolism	peptide synthetase MbtE	NE	NE	1
Rv2383c	mbtB	13	23.9	0.88	0.0011	Lipid metabolism	phenyloxazoline synthase MbtB	NE	NE	1
Rv2384	mbtA	7.2	23	1.68	5E-05	Lipid metabolism	salicyl-AMP ligase MbtA	NE	NE	1

Of the 20 other acid-sensitive mutants identified in the Vandal acid-sensitivity screen, three (*mbtF*, *glnA2* and *ponA2*) were positive interactors (Table 2.4). Apart from the previously discussed mycobactin biosynthesis gene *mbtF*, *glnA2* and *ponA2* were group 2 positive interactors conferring a fitness advantage to the Δ*marP* mutant. Disruption of *ponA2* conferred a significant growth advantage in the WT background (262 insertions per TA site

versus the WT library mean of 43), and an even larger increase in fitness in the Δ*marP* background (925 insertions per TA site versus the Δ*marP* library mean of 48).

Group 2 positive interactors indicate an alleviation of the *marP* fitness defect on plates, and may represent functional processes directly antagonistic to the mode of action of *marP*. To identify these processes, we focused on a list of mutants specifically conferring a fitness advantage in the Δ*marP* background (Table 2.9). Regulatory processes possibly involved in the control of MarP functional antagonism include the PhoPR two-component system, which regulates multiple functions including respiratory metabolism, response to hypoxia, stress responses and the secretion of pathogenic lipids (Gonzalo-Asensio et al., 2008), DisA/DacA, a protein with diadenylate cyclase activity (Bai et al., 2012) and MprA, a regulatory protein required for persistent infection in the mouse model (Zahrt and Deretic, 2001). Many of the strongest group 2 positive interactors are membrane proteins of unknown function (*rv0537c, rv0538*, *rv0012, rv1823-1825* and *rv2091c*) and may possibly be proteolytic substrates negatively regulated by MarP. We tested if Rv0537c, Rv0538 and Rv0012 were possible proteolytic substrates of MarP by expressing FLAG-tagged versions of these proteins in WT and Δ*marP* and performing a Western blot using an anti-FLAG antibody to check for possible differences in cleavage products; however, we were unable to determine if there was any differential cleavage between the two strains due to non-specific staining and low protein expression in the case of Rv0537c and Rv0538 (Fig. 2.5).

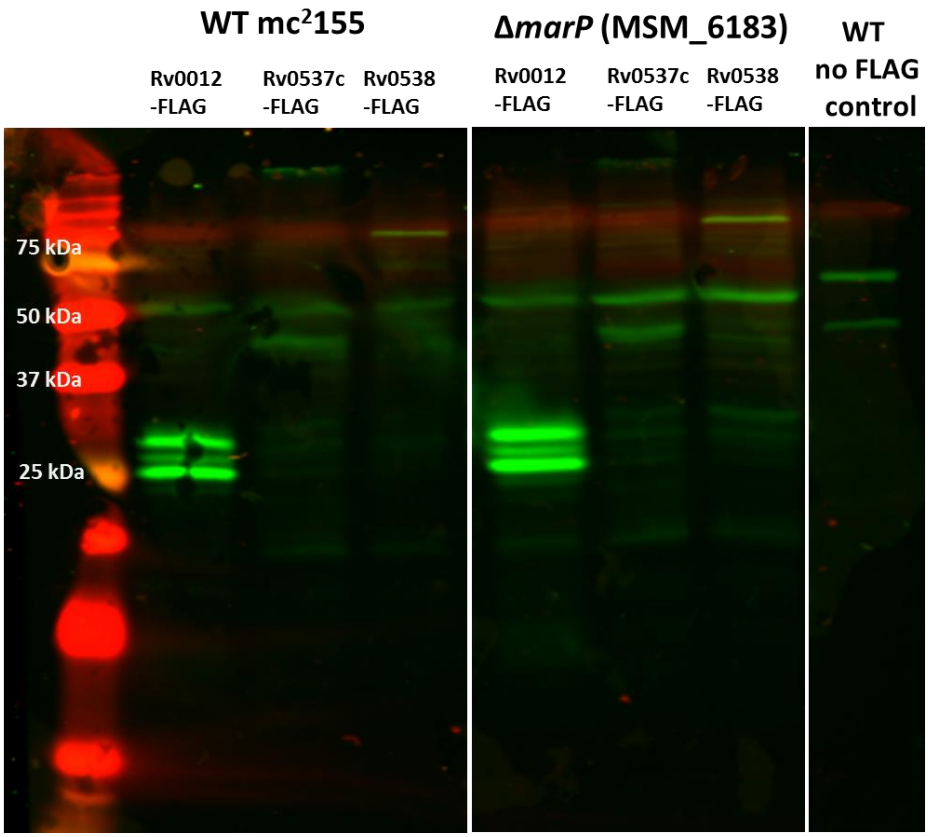

Figure 2.5 – Proteolysis assay of possible protein substrates negatively regulated by MarP. FLAG-tagged versions of Rv0012 (29.5kDa), Rv0537c (51.3kDa) and Rv0538 (56.1kDa) were expressed in WT and Δ*marP* strains of *M. smegmatis* mc^{2}155, and proteins from the cell wall fraction were extracted and resolved using 15% SDS-PAGE gel electrophoresis. Western blots were probed with fluorescent-tagged anti-FLAG antibody (green) and anti-Dlat antibody (red band at ~80kDa) as a loading control.

Coequal interactors could indicate genes in the same functional pathway – such mutants would recapitulate the slight growth defect of the *marP* mutant in the WT background (27 insertions per TA site versus the library mean of 43) while not having any growth defect in the Δ*marP* background. However, due to the subtle nature of this class of positive interaction, we were unable to identify any positive interactors that fulfilled that description and passed the significance cutoffs ($q<0.05$) under the parameters of our screen.

Table 2.9 - Specific group 2 positive interactors of *marP.* This list of group 2 interactors was filtered based on essentiality calls from the HMM, including only genes that were classified as non-essential (NE) in the WT background, and growth-advantageous (GA) in the ΔmarP background

		Mean insertions per TA site							
Rv #	Gene	WT	ΔmarP	log2FC	q-val	Tuberculist category	Function	WT Call	KO call
Rv0538	rv0538	44.2	1416	5.00	0	Cell wall/cell processes	membrane protein	NE	GA
Rv3586	rv3586	22.4	686.9	4.94	0	Conserved hypotheticals	DNA integrity scanning protein disA	NE	GA
Rv0012	rv0012	45.3	1119	4.63	0	Cell wall/cell processes	membrane protein	NE	GA
Rv1824	rv1824	44.6	1106	4.63	0.0001	Cell wall/cell processes	hypothetical protein	NE	GA
Rv0537c	rv0537c	73.1	1568	4.42	0	Cell wall/cell processes	membrane protein	NE	GA
Rv2091c	rv2091c	40.8	807	4.30	0	Cell wall/cell processes	membrane protein	NE	GA
Rv1825	rv1825	68.4	1106	4.02	0	Conserved hypotheticals	hypothetical protein	NE	GA
Rv1823	rv1823	47.6	767.5	4.01	0	Conserved hypotheticals	hypothetical protein	NE	GA
Rv2376c	cfp2	71.8	727.1	3.34	0.0376	Cell wall/cell processes	antigen CFP2	NE	GA
Rv3067	rv3067	79.2	738	3.22	0	Conserved hypotheticals	hypothetical protein	NE	GA
Rv0758	phoR	56.9	446.8	2.97	0	Regulatory proteins	OmpR family two-component system sensor histidine kinase	NE	GA
Rv0062	celA1	42.1	328.9	2.97	0	Intermediary metabolism	cellulase CelA1	NE	GA
Rv2375	rv2375	137.6	1024	2.90	0	Conserved hypotheticals	hypothetical protein	NE	GA
Rv0757	phoP	78.7	572	2.86	3E-05	Regulatory proteins	OmpR family two-component system response regulator	NE	GA
Rv0995	rimJ	33.7	136.4	2.02	0.0007	Information pathways	ribosomal-protein-alanine acetyltransferase RimJ	NE	GA
Rv2203	rv2203	78.5	292.9	1.90	0.0002	Cell wall/cell processes	membrane protein	NE	GA
Rv3683	rv3683	69.5	184.1	1.41	0.0125	Conserved hypotheticals	hypothetical protein	NE	GA
Rv0981	mprA	77.8	197.8	1.35	0.0096	Regulatory proteins	mycobacterial persistence regulator MPRA	NE	GA
Rv3870	eccCa1	64.7	142.8	1.14	3E-05	Cell wall/cell processes	ESX-1 secretion system protein EccCa1	NE	GA
Rv3871	eccCb1	61.6	130.5	1.08	0.0007	Cell wall/cell processes	ESX-1 secretion system protein EccCb1	NE	GA
Rv3877	eccD1	63.2	115.4	0.87	0.009	Cell wall/cell processes	ESX-1 secretion system protein EccD1	NE	GA
Rv3869	eccB1	79.3	139.2	0.81	0.0155	Cell wall/cell processes	ESX-1 secretion system protein EccB1	NE	GA
Rv3876	espI	65.8	103.4	0.65	0.046	Cell wall/cell processes	ESX-1 secretion-associated protein EspI	NE	GA

2.4 Characterization of Rv0812

Based on log2Fc magnitude, *rv0812* was the highest ranked positive interactor of *marP* (log2Fc = 8.38) - it was strongly attenuated and possibly essential in the WT background (0.2 insertions per TA site) but did not a fitness defect in the Δ*marP* background (57.7 insertions per TA site), indicating that the deletion of *marP* was able to completely rescue the growth defect phenotype of *rv0812:tn* mutants (Fig. 2.5A). Rv0812 has been largely uncharacterized – it is annotated as a probable amino acid aminotransferase in Tuberculist (Cole et al., 1998) and alternatively annotated as a 4-amino-4-deoxychorismate lyase (ADCL) in the NCBI RefSeq database (Tatusova et al., 2016). Comparative analysis with blastp indicates that Rv0812 is a class IV pyridoxal phosphate dependent enzyme (PLPDE) superfamily member. PLPDEs are a ubiquitous class of enzymes catalyzing a large variety of chemical reactions, and frequently demonstrate catalytic promiscuity, with a single enzyme catalyzing multiple reactions; it is plausible that Rv0812 may act through multiple pathways as well (Percudani and Peracchi, 2003). Rv0812 expression was also upregulated during Mtb infection in the mouse lung, suggesting a possible role in virulence.

A

	Mean insertions per TA site							Positive interaction group
Gene	WT	ΔmarP	log2FC	q-val	Tuberculist category	Function	WT Call	KO call	
rv0812	0.2	57.7	8.38	0	Intermediary metabolism and respiration	amino acid aminotransferase	GD	NE	1

B

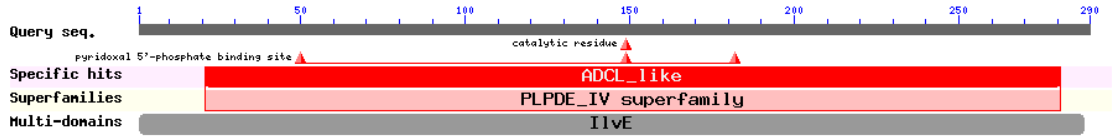

Figure 2.6 – *rv0812* is a top positive interactor of *marP* **A** – TnSeq statistics for *rv0812* **B** – Protein domain identification using NCBI blastp

ADCL (otherwise known as the para-aminobenzoate biosynthesis enzyme PabC) is part of the folate biosynthesis pathway in bacteria, protists, plants and fungi - the chemical

precursor chorismate is converted to aminodeoxychorismate (ADC) by the enzymes PabA and PabB, and is cleaved by ADCL/PabC into para-aminobenzoate (PABA) and pyruvate; PABA is subsequently converted into folate by the later steps of the biosynthetic pathway (Basset et al., 2004; Magnani et al., 2013; Stolz et al., 2007). Rv0812 was previously expressed in a partially soluble form in *E. coli*, and demonstrated *in vitro* ADCL activity (Chim et al., 2011)

The class IV PLPDE superfamily also contains the enzyme D-amino acid transaminase (Dat), which was first identified in *Lysinibacillus sphaericus* (Jones et al., 1985; Soper et al., 1977) . Dat catalyzes the interconversion of D-amino acids by a transamination reaction:

D-alanine + 2-oxoglutarate ↔ pyruvate + D-glutamate

Both D-alanine (D-Ala) and D-glutamate (D-Glu) are components of the peptide stem of peptidoglycan, and are thus essential for bacterial viability (Radkov and Moe, 2014). As comparative protein sequence analysis indicated a high degree of similarity between Rv0812 and the Dat of *Lysinibacillus sphaericus* (Table 2.10), and experimental/genetic interaction screen data suggested that MarP was likely to be involved in cell envelope integrity and function, this raised the attractive hypothesis that Rv0812 was an uncharacterized Dat functionally antagonistic to MarP due to its role in D-amino acid biosynthesis, and that the loss of *marP* was able to rescue the growth defect of the *rv0812:tn* mutant by restoring physiological equilibrium.

Table 2.10 – Similarity of Rv0812 and *Bacillus sphaericus* Dat. NCBI blastp analysis using Rv0812 as the query protein sequence and *Bacillus sphaericus* genomes (taxid:1421) as the search set, using the PSI-BLAST algorithm Hits passing the E-value threshold are displayed.

Description	Max score	Total score	Query cover	E value	Ident	Accession
D-amino-acid transaminase [Lysinibacillus sphaericus]	56.6	56.6	91%	3.00E-09	23%	AOV07189.1
4-amino-4-deoxychorismate lyase [Lysinibacillus sphaericus]	46.2	46.2	86%	9.00E-06	24%	AOV09010.1
MULTISPECIES: D-amino-acid transaminase [Lysinibacillus]	44.7	44.7	90%	3.00E-05	22%	WP_036118799.1
D-amino-acid transaminase [Lysinibacillus sphaericus]	41.6	41.6	90%	2.00E-04	22%	WP_054549929.1
D-amino-acid transaminase [Lysinibacillus sphaericus]	40.4	40.4	90%	6.00E-04	21%	WP_036220927.1
D-amino-acid transaminase [Lysinibacillus sphaericus]	40	40	90%	7.00E-04	21%	WP_012295709.1
D-amino-acid transaminase [Lysinibacillus sphaericus]	37.7	37.7	90%	0.005	21%	WP_069513841.1
4-amino-4-deoxychorismate lyase [Lysinibacillus sphaericus]	37.7	37.7	73%	0.005	25%	WP_069510861.1
D-alanine aminotransferase [Lysinibacillus sphaericus]	37.7	37.7	90%	0.005	20%	WP_024363741.1

2.4.1 Construction of Δ*rv0812* mutants

To investigate if the main functional role of Rv0812 was as an ADCL or a Dat, we attempted to construct *rv0812* knockout Mtb strains in both the WT and KO backgrounds. Based on the low transposon insertion count in *rv0812* in the WT background and essentiality predictions from previous studies (Griffin et al., 2011; Sassetti et al., 2003), it seemed likely that *rv0812* could be essential either due to its role in the biosynthesis of PABA, D-Glu or D-alanine. In order to culture and isolate these potentially auxotrophic mutants, we replaced the chromosomal copy of *rv0812* in both the WT and Δ*marP* strain with a zeocin-resistance cassette by allelic exchange/recombineering as previously described (Murphy et al., 2015), and plated equal volumes of each transformation onto 7H10 plates without or with supplementation with either PABA or a mix of D-Glu/D-Ala. The number of colonies isolated on each plate provided a semi-quantitative indication of the putative function of Rv0812 – a higher number of colonies on a supplemented plate could indicate metabolic rescue, but colony counts could include false positives/cointegrants from off-target recombineering. There were slightly more candidate *rv0812*-deletion colonies on plates supplemented with PABA relative to the unsupplemented/D-amino acid supplemented plates (Table 2.11A) in both the WT/KO backgrounds; to confirm that this increase in colony counts was due to a higher number of true *rv0812* knockouts being recovered, we screened 10 colonies from each plate for the loss of *rv0812* using PCR – we could only isolate mutants lacking *rv0812* under PABA supplementation (Table 2.11B), providing an early indication that the main role of Rv0812 was as an ADCL necessary in both genetic backgrounds. It should be noted that colony counting/isolation was performed after 20 days of incubation post-transformation, and slow growing mutant colonies might not have been detected at this timepoint. Deletion of *rv0812* was further confirmed in a Δ*rv0812* single-knockout mutant and a *Δrv0812 ΔmarP* double knockout mutant via Southern blot analysis (Figure 2.6), and these mutants were used in downstream analysis.

Table 2.11 Supplementation with PABA improves *rv0812* mutant isolation on 7H10 media
A- Colony counts from transformation reactions (including a no-DNA sham transformation control) plated on 7H10 unsupplemented /supplemented with 1µg/ml PABA or 1 µg/ml D-Ala/D-Glu. **B –** Proportion of isolated colonies lacking *rv0812*. 10 colonies from each plate were screened via PCR for the absence of *rv0812* gene copies

A

Strain	**no DNA control**	**7H10 only**	**7H10 + PABA**	**7H10 + D-Ala/D-Glu**
WT	0	27	124	40
ΔmarP	0	31	57	39

B

Strain	**7H10 only**	**7H10 + PABA**	**7H10 + D-Ala/D-Glu**
WT	0/10	5/10	0/10
ΔmarP	0/10	6/10	0/10

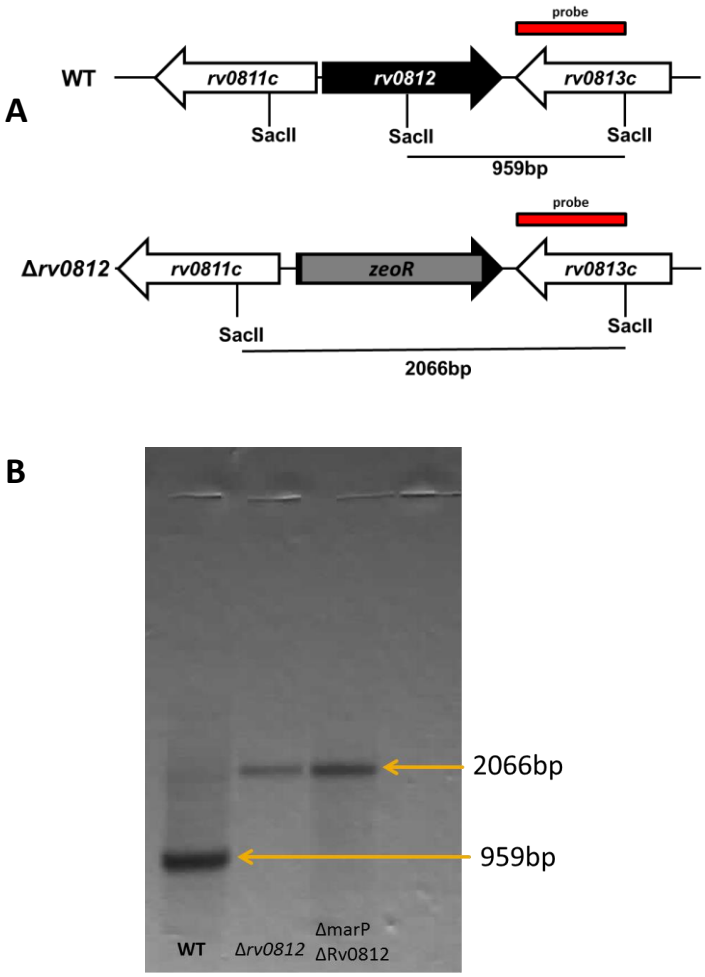

Figure 2.7 – Confirmation of *rv0812* deletion via Southern blot. A - Southern blot strategy showing organization of the *rv0812* genomic region and probe-binding /SacII digestion sites B – Southern blot analysis of WT, *Δrv0812* and *ΔmarP Δrv0812* strains. Genomic DNA was digested with SacII.

2.4.2 Rv0812 is involved in PABA biosynthesis but is not essential for *in vitro* viability

To confirm that the main role of Rv0812 was as an ADCL involved in PABA biosynthesis, we performed growth assays of the WT, Δ*marP*, Δ*rv0812* and Δ*marP* Δ*rv0812* strains in unsupplemented 7H9 liquid media and 7H9 supplemented with PABA or D-Ala/D-Glu. In spite of the implied essentiality of Rv0812 in the earlier mutant construction phase, both the Δ*rv0812* and Δ*marP* Δ*rv0812* mutant strains were able to grow in the absence of PABA supplementation. However, the Δ*rv0812* single mutant exhibited a partial growth

defect in the absence of PABA supplementation relative to the other strains, suggesting a requirement for Rv0812-dependent PABA biosynthesis for optimal growth; this growth defect was not apparent in the Δ*marP* Δ*rv0812* strain, which was agreement with the prediction from the TnSeq screen that *marP* is a positive interactor of *rv0812*, and that the loss of *marP* was able to rescue growth defects associated with the deletion of *rv0812* (Fig. 2.7A). In order to account for the possibility that Rv0812 non-essentiality was due to PABA/folate precursor carryover from the preculture, we passaged the Δ*rv0812* and Δ*marP* Δ*rv0812* strains twice to allow for the depletion of these metabolites. While the growth defect became slightly more pronounced after subsequent passages, both strains were able to grow after two passages, with the Δ*rv0812* mutant exhibiting slower growth (Fig. 2.7B). The growth defect of the Δ*rv0812* mutant could be complemented by the expression of *rv0812* under the control of the *hsp60* promoter from an integrative plasmid (Fig. 2.7C)

As 7H9 media contains bovine serum albumin, which may contain trace amounts folate precursors, we next investigated the growth of the Mtb strains under the metabolite-defined Sauton's medium. Similarly, *rv0812* was not essential for growth in Sauton's media, and the Δ*rv0812* but not the Δ*marP* Δ*rv0812* strain exhibited a growth defect in the absence of PABA supplementation; this suggested that *rv0812* was not essential for *in vitro* growth in liquid media (Fig. 2.8)

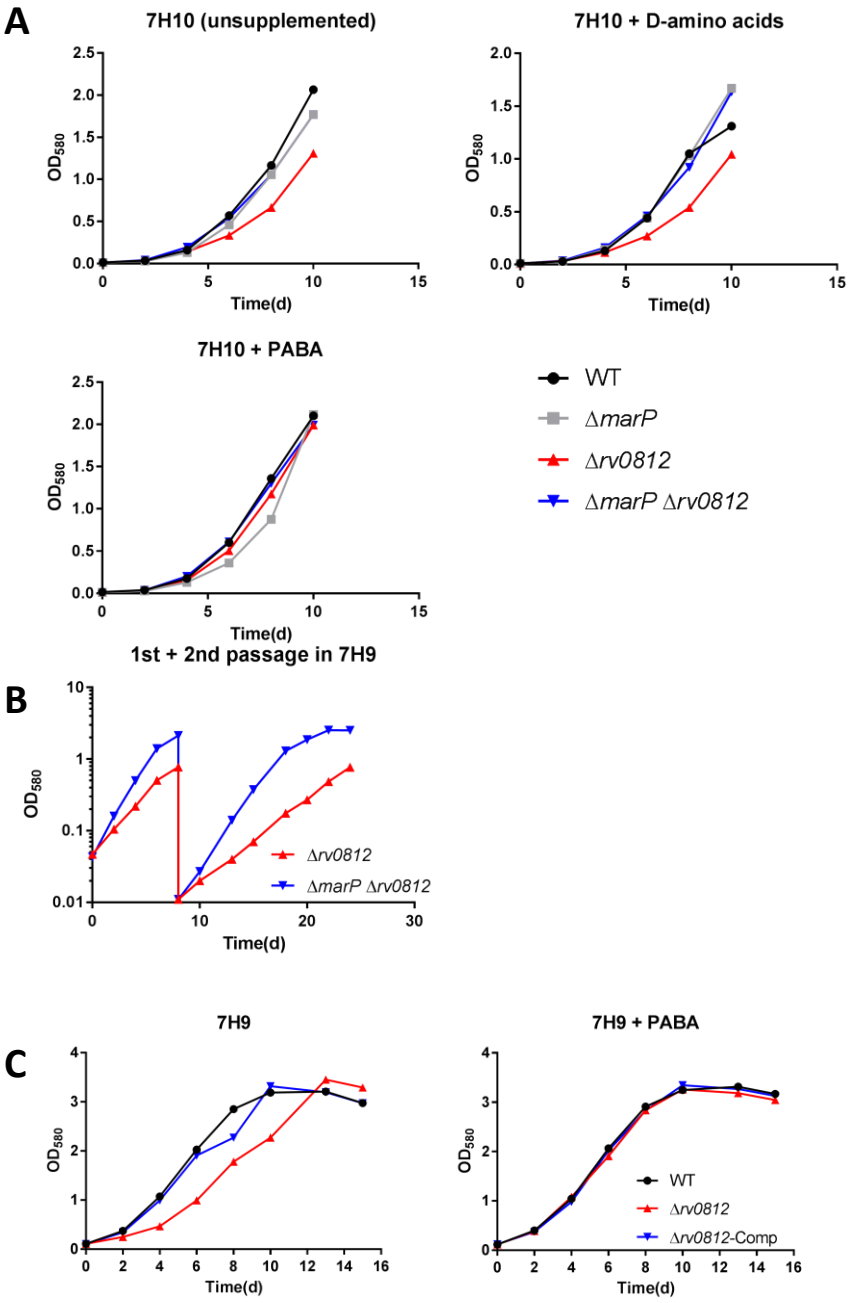

Figure 2.8 – *rv0812* is required for optimal growth but is not essential in 7H9 media. A – Growth of WT and deletion mutant strains in 7H9 without or with supplementation with PABA or D-Glu/D-Ala. OD_{580} values are plotted on a linear scale to emphasize the mild growth defect **B –** Growth of Δ*rv0812* and Δ*marP* Δ*rv0812* after repeat passaging in unsupplemented 7H9. The first passage culture was started at an OD of 0.05 from a mid-log phase unsupplemented 7H9 culture, and subsequently passaged again at D8 to an OD of 0.01. **C –** Growth of WT, Δ*rv0812* and complementation strain in 7H9 with or without PABA supplementation. Cultures were started from mid-log phase precultures grown in the absence of PABA supplementation.

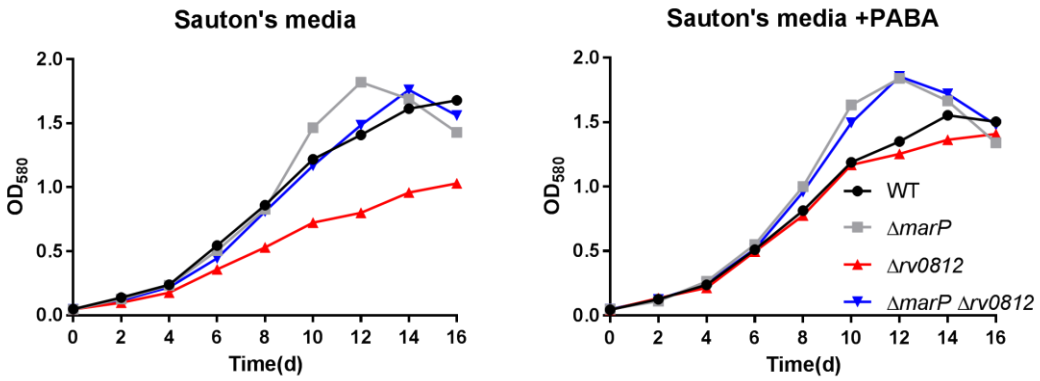

Figure 2.9 – *rv0812* is not essential for growth in defined Sauton's media. Growth curves of WT, Δ*rv0812* and complementation strains in Sauton's media with or without PABA supplementation. Cultures were started from mid-log phase precultures grown in Sauton's media without PABA supplementation

In light of the observed non-essentiality of *rv0812* in liquid media, we plated out 200 cfu each of the Δ*rv0812* and Δ*marP* Δ*rv0812* cultures on 7H9 agar to determine if *rv0812* was essential on solid media, as implied by the difficulty in isolating *rv0812* knockouts in the earlier mutant construction step. Both mutants exhibited a growth defect in the absence of PABA supplementation, however, small colonies could be visualized by D30 post-plating, with the Δ*marP* Δ*rv0812* double mutant showing better growth than the Δ*rv0812* mutant. (Fig. 2.9)

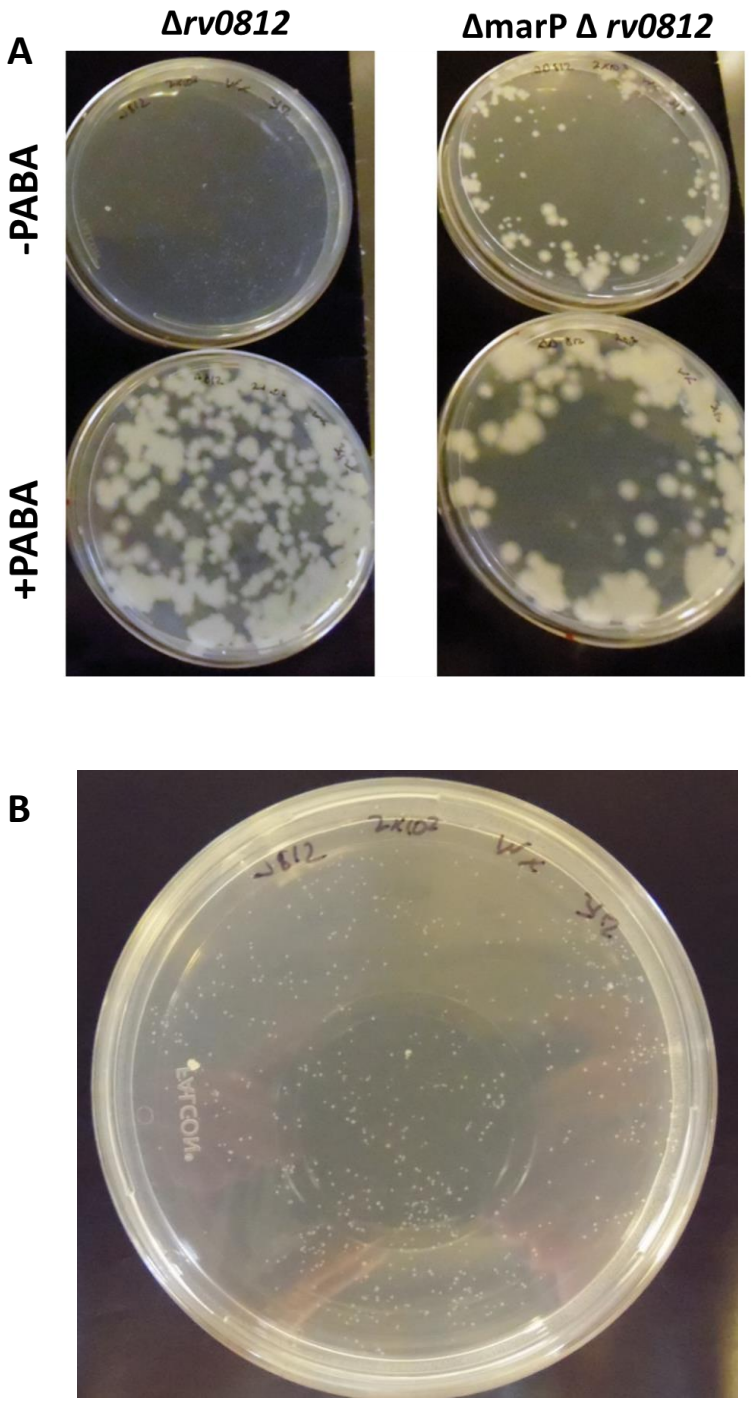

Figure 2.10 – *rv0812* is required for optimal growth on solid media, but is not essential. A – Growth of Δ*rv0812* and Δ*marP* Δ*rv0812* colonies. ~200 cfu of each strain was plated on 7H9 agar plates with or without agar supplementation. Colonies shown are from D30 post-plating. B – Close-up of unsupplemented 7H9 plate showing small Δ*rv0812* Mtb colonies D30 post-plating

2.5 Discussion

2.5.1 The functional role of Rv0812

The *marP* genetic interaction screen identified a total of more than 200 negative and positive interacting partners – from this extensive list of candidates, *rv0812* was chosen for follow-up study as 1. it was the highest ranking positive interactor, implying a strong functional relationship with *marP*, 2. it was predicted to be an essential gene, suggesting high physiological importance and relevance as a drug target, and 3. it seemed to have a plausible direct mechanistic link to *marP* and cell envelope function, based on the possibility that it was a D-amino acid aminotransferase. Characterization of the Δ*rv0812* mutant however indicated that *rv0812* was not an essential gene under multiple *in vitro* conditions and that its main physiological role was as an ADCL, and was thus unlikely to contribute directly to D-amino acid biosynthesis and peptidoglycan structure. In agreement with the predictions of the genetic interaction screen, *marP* deletion was able to alleviate the growth defect resulting from the loss of *rv0812*.

One would expect Rv0812/ADCL to be essential given the importance of folate biosynthesis for Mtb viability. Previous studies in the related Actinobacteria species *Corynebacterium glutamicum* and *Streptomyces* sp. FR-008 have however shown that deletion of *pabC*/ADCL does not result in loss of viability but rather a growth defect, similar to what we have observed in Mtb (Stolz et al., 2007; Zhang et al., 2009). A possible explanation for this non-essentiality may lie in the highly labile nature of ADC, which undergoes spontaneous decomposition to PABA even in the absence of an enzyme (Tewari et al., 2002), providing sufficient PABA to support slower bacterial growth. Alternatively, ADCL activity could be facilitated by secondary promiscuous activities of other enzymes, possibly other PLPDEs. At this point, it is unknown how *marP* deletion can alter the requirement for Rv0812 for optimal growth – the loss of *marP* may affect cell envelope structure and alter physiological conditions within the cytoplasm (e.g. pH, ionic concentration) that may further

destabilize ADC, generating a higher PABA concentration; alternatively, the gene expression profile may be altered in the Δ*marP* mutant, and enzymes fulfilling secondary bypass pathways to Rv0812 may be upregulated. Further metabolomic, transcriptomic and TnSeq interaction studies with *rv0812* may reveal the nature of this bypass pathway.

While our characterization of Rv0812 does not necessarily disprove the possibility that it may have secondary D-amino acid aminotransferase activity, the growth defect observed in the Δ*rv0812* mutant was PABA-dependent and not rescuable by supplementation with D-Glu/D-Ala, indicating that the main role of Rv0812 was not as a Dat but an ADCL. Additionally, alanine racemase (Alr) and glutamate racemase (MurI) are both predicted to be essential in this study and prior studies (Sassetti et al., 2003; Zhang et al., 2012), suggesting that racemization is the main biosynthetic pathway for D-amino acids and that D-amino acid transamination is insufficient to compensate for the loss of either of the racemases. Dat activity, either through Rv0812 or another uncharacterized enzyme, is unlikely to be physiologically important in Mtb. In retrospect, our hypothesis that Rv0812 has a major role in D-amino acid metabolism was perhaps wishful overfitting of weak structural evidence in order to establish a functional link between Rv0812 and cell envelope function.

2.5.2 The functional role of MarP

Inferring the specific functions of MarP is by no means an easy task given the disparate functions of the multiple interacting partners identified; nevertheless, there are a few functional themes among these interactors that may provide clues about its role in Mtb physiology, and possibly the nature of its uncharacterized interacting partners. Many of the characterized genetic interaction partners of MarP have known functions in cell envelope biosynthesis and function, and the implication is that MarP also contributes to cell envelope integrity as well. Admittedly, cell envelope integrity is determined by multiple interconnected functional pathways, and the conclusion that MarP fulfils parallel or redundant functions to these cell envelope genes is a vague one that sheds little light on its

specific role; MarP negatively interacts with genes involved in peptidoglycan biosynthesis and structure, mycolic acid synthesis and secretion, lipoarabinamannan biosynthesis and inorganic ion transport amongst many others, and there is not enough current evidence to pinpoint which of these particular functions is controlled by MarP.

Notable amongst the negative interactors was the peptidoglycan hydrolase RipA, which was identified in our lab to be a proteolytic substrate activated by MarP (Botella, study under review). As a protein with both essential and non-essential domains (Zhang et al., 2012), RipA violates the general rule of thumb that transposon insertion results in a complete loss of protein function, and the *ripA:tn* mutants present after the initial outgrowth on 7H10 plates are probably partial loss of function mutants. The *ripA-marP* interaction may thus be interpreted as a special case of negative interaction on the same pathway, by which the combined effect of two partial-loss of function mutants result in complete loss of function in the pathway, and hence synthetic lethality (Baryshnikova et al., 2013). This raises the secondary question as to why *marP* deletion, resulting in the complete loss of function of MarP, can be considered as a partial loss of function mutation in the context of the screen. A possible explanation is that MarP only has a partial contribution to RipA activation, and RipA may be activated by a second protease, or may have partial activity in the absence of proteolytic activation (Fig 2.10) - while a few studies have indicated that RipA is a zymogen requiring activation (Chao et al., 2013a; Ruggiero et al., 2010), a contrasting report showed that full length RipA was capable of degrading small synthetic peptidoglycan fragments, and N-terminus truncation simulating cleavage did not improve enzymatic activity (Both et al., 2011). Secondly, while the *marP* deletion mutant is viable *in vitro*, *ripA* cannot be fully deleted due to one of its domains being essential, indicating that RipA retains at least part of its essential function in the absence of MarP.

A further complication of this model arises when one considers the possibility that MarP may have multiple substrates, and may modulate separate parallel pathways that are

synthetically lethal with each other. Under this case, the combined effect of *marP* deletion with transposon insertion in the non-essential domain of RipA does not necessarily result in the complete loss of function of the RipA functional pathway, however, synthetic lethality may result from the loss of function of one of the other MarP-dependent pathways parallel in functionality to RipA (Fig. 2.11B). The multiple possible explanations of the *ripA/marP* negative interaction illustrate the difficulty in interpreting genetic interactions when certain key assumptions are violated, in this case the assumptions that transposon insertion results in a complete loss of gene function, and that MarP only regulates one proteolytic substrate, which is in turn regulated only by MarP.

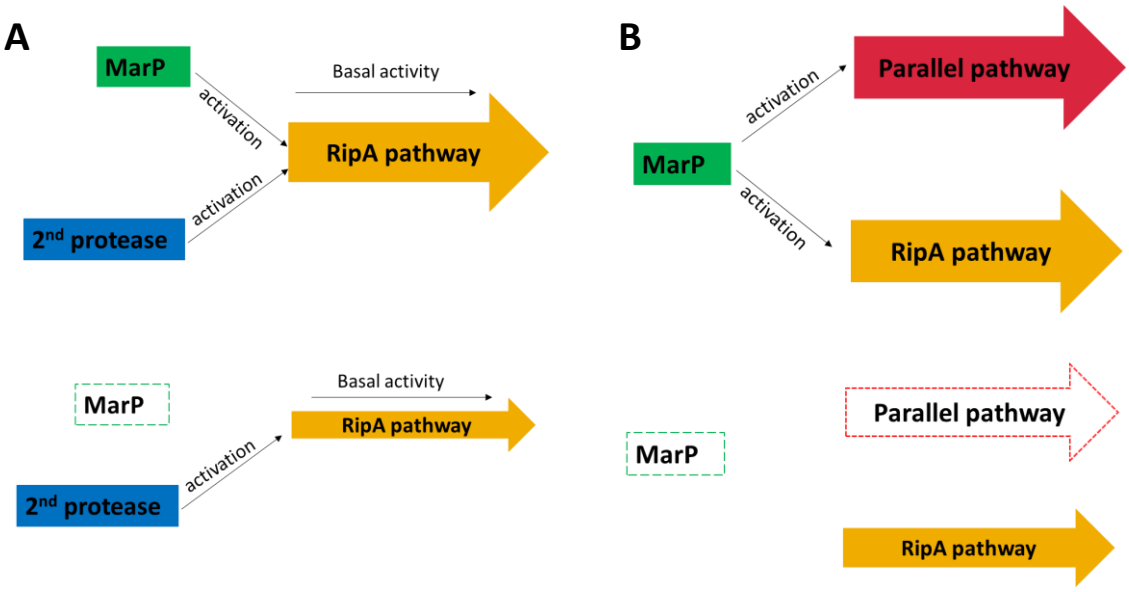

Figure 2.11 – Multi-activator/multi-substrate models of MarP/RipA negative interaction. **A**- RipA may be independently activated by multiple proteins including MarP, or may possess basal activity in the absence of proteolytic activation. Loss of MarP results in a partial loss of function in the RipA pathway, which may be aggravated to the point of synthetic lethality by a partial loss of function transposon mutation in *ripA*. **B**- MarP may activate multiple functional pathways parallel to that of RipA. While the loss of MarP does not necessarily result in lethal loss of function in the RipA pathway, loss of activity in MarP-activated parallel pathways may be synthetic lethal with any partial loss of function mutations in the RipA pathway. These two models are not mutually exclusive, and RipA may be activated by multiple proteases, which in turn activate multiple functional pathways.

The loss of *marP* is able to alleviate fitness defects caused by loss of function of multiple pathways, as seen from the group 1 positive interactions with Rv0812, the type VII secretion pathways (especially ESX-5) and mycobactin biosynthesis. The *marP*-dependent alleviation of growth defects associated with the loss of ESX-5 components mirrors a previous study by which overexpression of the mycobacterial porin MspA, or loss of pdim in *M. marinum* was able to rescue ESX-5 essentiality. The proposed model for this phenomenon was that ESX-5 may be necessary for the secretion of proteins involved in the transport of substrates across the outer membrane, and that the increase in cell envelope permeability resulting from the loss of pdim or porin overexpression is able to facilitate compensatory diffusion of substrates into the cell (Ates et al., 2015). Similarly, *marP* deletion may increase cell envelope permeability, rescuing ESX-5 essentiality; this mechanism could potentially also facilitate compensatory iron transport in the absence of mycobactin, accounting for the positive interaction observed. While these interactions represent downstream effects of *marP* deletion and do not directly illuminate the specific functions of *marP*, they show that *marP* may be an important determinant of cell envelope permeability, with far reaching effects on other aspects of Mtb physiology.

Group 2 positive interaction indicates transposon mutations that can alleviate the fitness defects of the Δ*marP* mutant, possibly revealing antagonistic functional pathways to MarP. While we were unable to determine if any of the group 2 positive interactors are proteolytic substrates of MarP, they may prove to be important determinants of cell wall structure – as the evidence thus far suggests that MarP is important in maintaining low cell envelope permeability, these group 2 interactors may have the opposite effect of promoting permeability.

2.5.3 Limitations of TnSeq-based interaction screens

As previously noted, we were unable to identify any coequal interactors (signifying proteins on the same functional pathway as MarP) under the conditions of our screen, given

the subtle nature of that class of positive interaction. The libraries in this experiment were constructed on rich, minimally selective 7H9 agar media to preserve library mutant diversity for downstream experiments; in order to better identify coequal interactions, future TnSeq interaction screens should use libraries constructed on media imposing a stronger selective pressure on mutants in the MarP functional pathway, such as higher malachite green concentration in the case of 7H10/7H11 media, or concentrations of antibiotics partially inhibitory to the ΔmarP strain, but not the WT strain.

A core weakness of screens relying on transposon mutant libraries is that essential genes are not represented in the output libraries, and their absence constitutes a critical blind spot in the screen. The RipA-MarP negative interaction could be visualized due to the presence of non-essential domains in RipA; however, other fully-essential genes that could interact with MarP may have been overlooked. The same limitation applies to any other TnSeq genetic screen seeking to identify specific functional partners of the query gene, and future experimenters need to bear in mind the possibility that the main interacting partners that they are searching for might not be present in their output datasets due to gene essentiality.

Finally, while it is relatively straightforward to perform a TnSeq screen and obtain long lists of genetic interaction partners, the true difficulty lies in the meaningful interpretation of the results. TnSeq ultimately measures mutant fitness, but unexpected changes in mutant fitness do not necessarily guarantee that the hits identified are pertinent to the specific function of the query gene. This is clearly illustrated in the case of our MarP interaction screen – MarP interacts with many different pathways with disparate mechanisms, but it is still unclear from the genetic interaction screen data which of these proteins may be a proteolytic substrate of MarP. The difficulty of interpreting the MarP genetic interaction screen may be attributed to its pleiotropic phenotype – it presumably controls cell wall permeability and integrity, which in turn affects multiple aspects of Mtb

physiology such as cell division, stress susceptibility and substrate transport across the cell envelope, resulting in downstream genetic interaction across a wide variety of pathways. Additionally, as cell envelope structure is controlled by multiple Mtb genes, trying to identify the specific process regulated by MarP becomes a task akin to finding a leaf hidden in a proverbial forest.

As TnSeq screens are by nature mechanistically agnostic, meaningful interpretation of TnSeq data demands additional context about the problem being addressed. In the case of *marP*, the TnSeq screen may be complemented by a second protein interaction screen - while both types of screen have a tendency to generate non-specific hits, focusing on hits shared between the screens may improve the chances of identifying a true functional partner of MarP. Similar to what has been done before in *E. coli* (Babu et al., 2011), aggregation of genetic interaction data from multiple screens with different query genes may allow researchers to chart the genetic interaction network of Mtb; such networks may help indicate which genes are specific to certain functional pathways and which have pleiotropic effects, allowing for a more comprehensive interpretation of TnSeq interaction data.

CHAPTER 3: SCREENING FOR GENES DETERMINING ANTIBIOTIC SUSCEPTIBILITY

3.1 Design and interpretation of a TnSeq-based antibiotic susceptibility screen

As intrinsic resistance mechanisms play an important role in the recalcitrance of Mtb to chemotherapy, we performed an antibiotic susceptibility screen to identify genes that may contribute to these processes, in particular the ones conferring the greatest effect to antibiotic susceptibility. We used a preconstructed WT Mtb transposon library (WT1) for this set of screens, the WT library was comprised of ~10^5 unique mutants and had a high library diversity with ~64% of the TA sites represented (Table 2.1). Glycerol stocks of this library were thawed and recovered in a preculture to log-phase growth, and were exposed to varying concentrations of the frontline antibiotics rifampicin, isoniazid, ethambutol and the peptidoglycan-targeting antibiotics vancomycin and meropenem. Antibiotic concentrations resulting in partial reduction of the overall library growth rate to 60-75% that of the antibiotic-free control were used in follow-up analyses (Fig. 3.1B).

Competitive outgrowth for a period of approximately 6.5 generations (100-fold expansion of the population) resulted in altered transposon mutant frequencies in the respective output libraries (Fig. 3.1A). Antibiotic susceptibility was quantified by comparing mutant frequency differences between the partially-inhibited library relative to the antibiotic free control; similar to the genetic interaction study, we used the TRANSIT analysis tool to calculate the log2Fc between the libraries and determine statistical significance of the fold-changes by resampling testing.

Interpretation of the TnSeq antibiotic-susceptibility screen is considerably more straightforward than that of the genetic interaction screen. While the MarP interaction screen aims to indirectly infer possible functional relationships between *marP* and other genes based the observed fitnesses of single and double mutants, the antibiotic-susceptibility screen directly answers the primary question as to which mutants exhibit the greatest fitness changes under antibiotic selection. Mutants with negative log2Fcs have

reduced fitness under antibiotic selection and are thus more sensitive, whereas positive log2Fcs indicate increased antibiotic resistance in the corresponding mutants. The screen does not directly address the mechanisms for the change in antibiotic susceptibility – it may be due to functional interaction between the antibiotic and gene (similar to functional pathway interaction observed in the genetic interaction screens), but can also occur because of altered repair pathway functionality, changes in antibiotic target accessibility and differences in drug metabolism (Fig. 3.2).

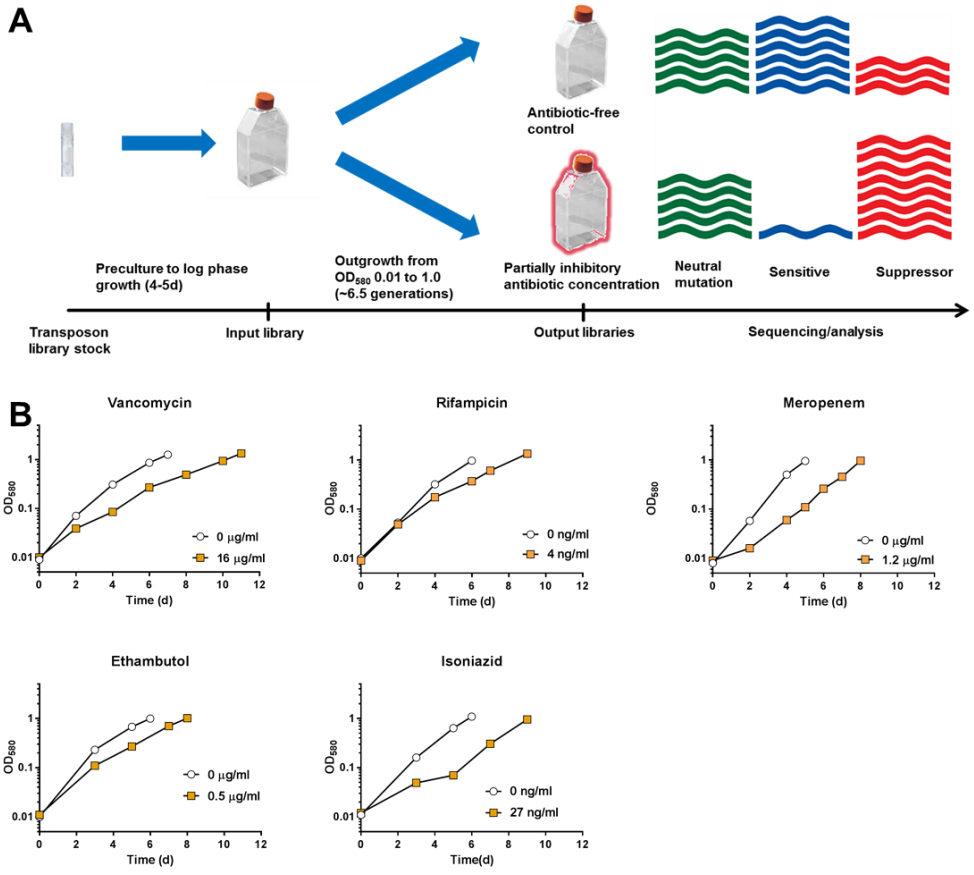

Figure 3.1 – Identification of genes associated with antibiotic susceptibility by TnSeq screening. A -Schematic of the antibiotic sensitivity screen. Briefly, an aliquot of a saturated transposon library is recovered to log-phase growth, and this input library is inoculated into media with or without a partially inhibitory concentration of antibiotic. Outgrowth in the absence/presence of antibiotic results in altered transposon mutant proportions in the output libraries, which can be determined via sequencing and analysis. **B** – Partially-inhibitory antibiotic selection of transposon libraries. Growth curves displayed are representative of the growth kinetics of transposon libraries observed in the presence or absence of antibiotic selection

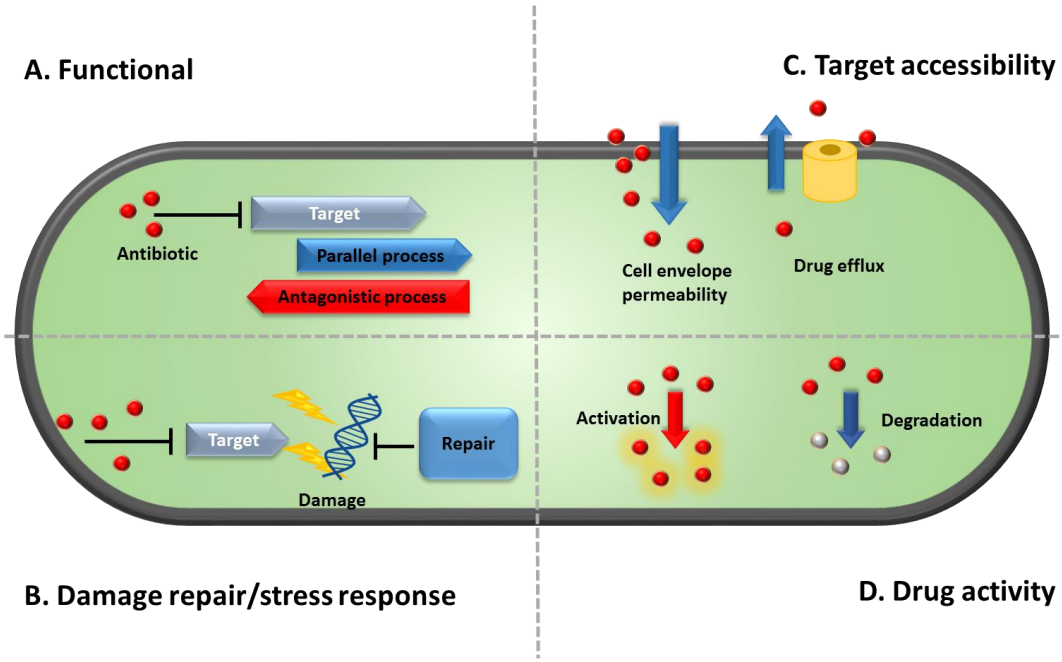

Figure 3.2 – Genetic factors determining antibiotic susceptibility in Mtb. A – Genes may buffer against/enhance the effects of antibiotic target inhibition by mediating functions parallel or antagonistic to that of the target. **B** – Repair/stress response pathways can mitigate secondary damages caused by target inhibition. **C** – Antibiotic target accessibility may be affected by changes in cell envelope permeability or active efflux of antibiotic molecules. **D** – Antibiotic activity can be modified by enzymes activating/degrading antibiotics.

3.2 Comparison of antibiotic susceptibility gene profiles indicates high similarity between the intrinsic resistance mechanisms of rifampicin and vancomycin

After calculating log2Fcs and performing resampling testing on triplicated experimental datasets, we identified 251 mutants whose change in fitness under antibiotic selection was statistically significant after false discovery rate correction ($q<0.05$) under at least one of the antibiotic selection conditions tested. Cluster analysis was performed on the different antibiotic susceptibility gene profiles to determine which antibiotics were most similar in terms of their intrinsic resistance mechanisms; we expected antibiotics with similar modes of action (e.g. cell envelope biosynthesis) to have similar susceptibility gene profiles. Unexpectedly, the vancomycin and rifampicin library profiles clustered closely together,

subsequently clustering with the meropenem profiles followed by the ethambutol profiles (Fig. 3.3). The isoniazid profiles were extant to those of the other four antibiotics.

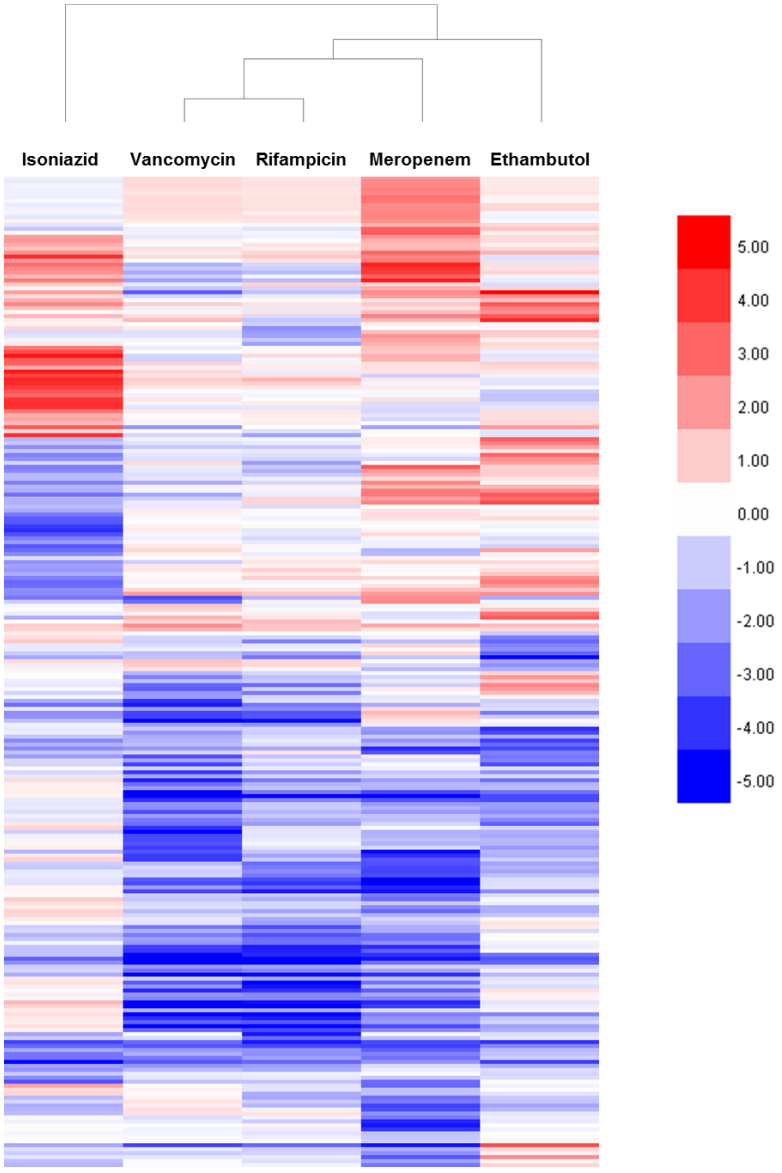

Figure 3.3 – Cluster analysis of antibiotic sensitivity profiles. Hierarchical clustering was performed on antibiotic sensitivity profiles derived from triplicated experiments, using Pearson's correlation as the similarity metric. The mean log2 TnSeq Fc in transposon mutant frequency for each gene under antibiotic selection relative to the antibiotic-free control is indicated on the colour scale, with increased mutant representation in red and reduced representation in blue. Genes that did not exhibit statistically significant differences ($q<0.05$ based on resampling testing) in transposon insertion under any of the antibiotic selection conditions tested were omitted, and the 251 remaining genes were used in this analysis

We compared the overlap of susceptibility-causing mutants in each of the antibiotics in order to identify intrinsic resistance mechanisms shared between the various antibiotics. Several mutations were observed to lead to increased sensitivity to multiple antibiotics (Fig. 3.4A) – 17 genes were linked to increased sensitivity in at least 4 out of the 5 antibiotics tested, and transposon insertions in the *fecB* gene were predicted to result cross-sensitivity to all five antibiotics.

To further determine the similarity of the mechanisms conferring intrinsic resistance to different antibiotics, we measured the overlap of sensitive mutants in one to one comparisons of each antibiotic; overlap was quantified by the number of genes shared between two sensitivity profiles and also the Jaccard index, which measures the proportional overlap between the two sets ($A \cap B / A \cup B$) (Fig. 3.4B). In agreement with the clustering analysis, there was a large degree of overlap between the vancomycin and rifampicin sensitive mutant subsets, with 47 genes in common between the vancomycin and rifampicin sensitive mutants (proportional overlap = 0.43). There was slightly less overlap between the sensitive mutant subsets of rifampicin and meropenem, with 34 genes shared between the rifampicin and meropenem subsets (proportional overlap = 0.32); despite the fact that meropenem and vancomycin both target peptidoglycan as their mechanism of action, overlap between their sensitive mutant subsets was comparatively more modest (31 genes, proportional overlap = 0.26). The ethambutol sensitivity subset overlapped more with the vancomycin subset (31 genes, proportional overlap = 0.32) than with the other antibiotics, and in agreement with the cluster analysis that the isoniazid profiles were least related to those of the other drugs, a smaller proportion of isoniazid-sensitive genes overlapped with the sensitive subsets of the other antibiotics.

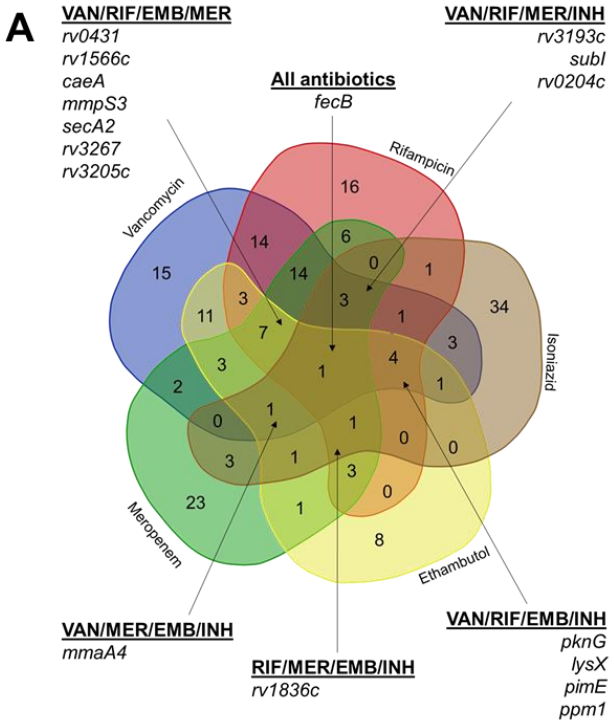

B

	Rifampicin (74 hits)	Isoniazid (54 hits)	Ethambutol (45 hits)	Meropenem (69 hits)
Vancomycin (83 hits)	47 (0.43)	14 (0.11)	31 (0.32)	31 (0.26)
Rifampicin (74 hits)		11 (0.09)	19 (0.19)	35 (0.32)
Isoniazid (54 hits)			9 (0.10)	10 (0.09)
Ethambutol (45 hits)				18 (0.19)

Figure 3.4 - Intrinsic resistance mechanisms are shared between different antibiotics A – Venn diagram of antibiotic sensitive mutants. Sets of significantly sensitive mutants (negative TnSeq-Fcs, q<0.05) for each antibiotic are represented by the coloured regions, with the number of overlapping genes indicated in their respective zones. **B** – Overlap between antibiotic sensitivity profiles. Overlap matrix indicating the number of genes shared between pairs of antibiotic sensitivity profiles (unbracketed numbers). The degree of overlap is represented in the form of the Jaccard index (bracketed numbers), i.e. the proportion of sensitivity genes shared between the two libraries over the total number of genes from both libraries ($A \cap B / A \cup B$), where A and B are different sets of sensitive mutants.

3.3 Validation of TnSeq predictions

We validated the predictions of the TnSeq screen in single strain minimum-inhibitory concentration (MIC) assays. A panel of 21 mutant strains was selected from our strain collection for MIC testing (Table 3.1), consisting of a mix of mutants predicted to have significantly altered antibiotic susceptibility to at least one of the drugs, as well as a few control mutants with no significant changes in mutant representation under the TnSeq screen. MIC decreases of up to 20-fold were observed for vancomycin, 4-fold for rifampicin and meropenem, and only up to 1.8-fold for ethambutol within the panel; none of the 21 mutants we tested displayed a detectable reduction in MIC for isoniazid (Supplementary Table ST1). While our TnSeq screen also indicated an enrichment for the *pckA* mutant under meropenem selection, we did not observe any significant increases in its MIC.

The ability of the TnSeq screens to predictively rank mutants in order of antibiotic sensitivity was of particular interest to us as it could aid in the prioritization of study candidates from within the large mutant lists typically generated by genetic screens. Spearman correlations (ρ) between TnSeq-Fc and mutant MIC-shifts for vancomycin/rifampicin/meropenem were between 0.72-0.77, illustrating a general trend that the mutants with the lowest TnSeq-Fcs are also likely to have the lowest MICs (Fig. 3.5B). Reflective of lower screen precision and the smaller range of MIC shifts observed for ethambutol, the ethambutol screen exhibited a poorer Spearman correlation (ρ=0.65). We were unable to determine the Spearman correlation for the isoniazid screen as none of mutants in our panel were isoniazid-sensitive, this could however be partly due to the scarcity of predicted isoniazid-sensitive mutants within our mutant panel.

Table 3.1 – Determination of minimum inhibitory concentrations (MICs) of a mutant strain panel. Determination of minimum inhibitory concentrations (MICs) of a mutant strain panel. Prior studies from which the respective mutants were obtained from are indicated in the reference column

	Minimum inhibitory concentration (µg/ml)					
Strain	**Vancomycin**	**Rifampicin**	**Meropenem**	**Ethambutol**	**Isoniazid**	**Source/reference**
H37Rv WT	20	0.02	7.5	0.9	0.04	
rv0007:tn	10	0.02	2.65	0.9	0.04	(Vandal et al., 2008)
pbpA:tn	1.77	0.005	2.65	0.49	0.04	(Vandal et al., 2008)
ΔponA1	5	0.02	7.5	0.6	0.04	Unpublished
ΔpckA	5	0.02	7.5	0.9	0.04	(Marrero et al., 2010)
rv0431:tn	2.5	0.01	3.75	0.6	0.04	(Vandal et al., 2008)
Δicl1	20	0.02	7.5	0.9	0.04	(Marrero et al., 2010)
Δrv0955	5	0.01	3.75	0.9	0.04	(Goodsmith et al., 2015) & unpublished
ΔglpX	40	0.02	7.5	0.9	0.04	(Ganapathy et al., 2015)
rv1272c:tn	20	0.02	7.5	0.9	0.04	(Vandal et al., 2008)
ΔlprG	2.5	0.005	7.5	0.9	0.04	(Gaur et al., 2014)
Δ*epiA*	20	0.02	7.5	0.9	0.04	Unpublished
lysX:tn	10	0.01	7.5	0.6	0.04	(Vandal et al., 2008)
ppm1:tn	20	0.02	7.5	0.6	0.04	(Vandal et al., 2008)
Δ*rv2136c*	20	0.02	7.5	0.9	0.04	(Darby et al., 2011)
glnA2:tn	20	0.02	7.5	0.9	0.04	(Vandal et al., 2008)
caeA:tn	0.88	0.0035	1.33	0.6	0.04	(Vandal et al., 2008)
Δ*fecB*	1.25	0.005	1.88	0.9	0.04	Unpublished
rv3679:tn	20	0.02	7.5	0.9	0.04	(Vandal et al., 2008)
rv3680:tn	20	0.02	7.5	0.9	0.04	(Vandal et al., 2008)
ponA2:tn	5	0.01	2.65	0.9	0.04	(Vandal et al., 2008)
Δ*rv3717*	10	0.005	7.5	0.9	0.04	Unpublished

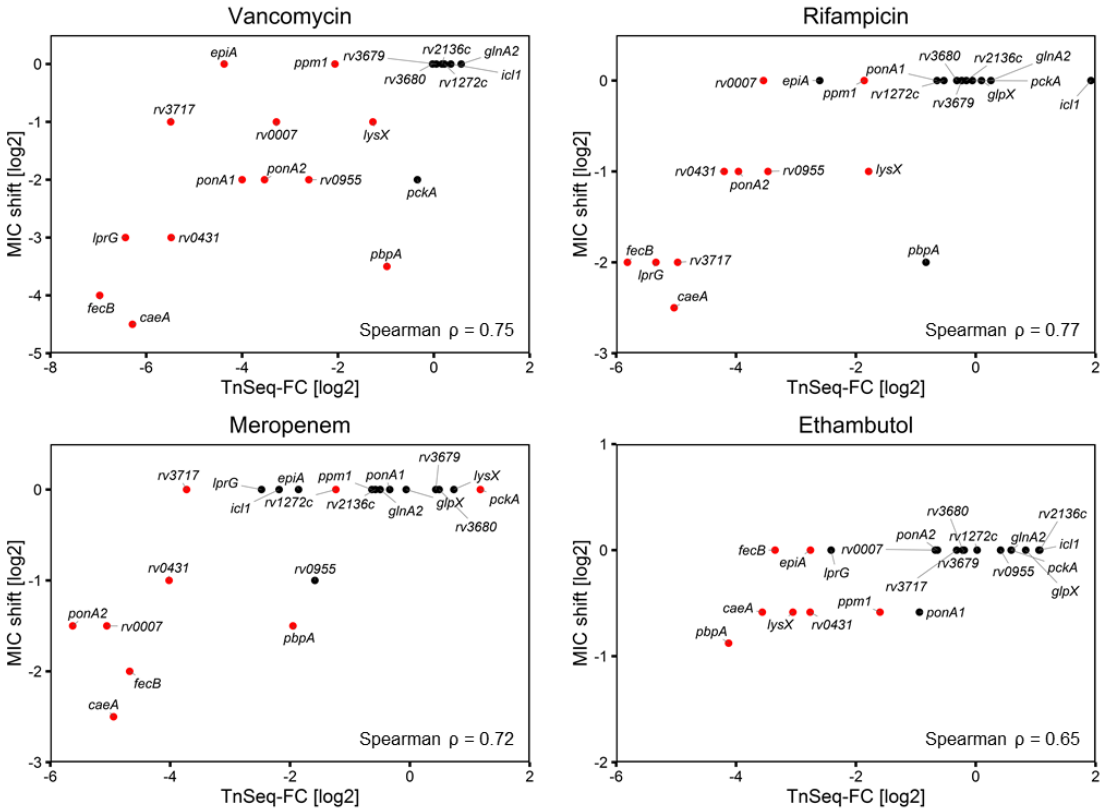

Figure 3.5 – Predictive ranking of mutant antibiotic sensitivity by TnSeq. Spearman rank correlation (ρ) between log2Fc from the antibiotic screen and the observed log2 MIC shift relative to the WT strain. TnSeq Fc values are derived from triplicate experiments, while MIC shifts for each mutant are the mean of duplicate experiments. Mutants predicted to be significantly underrepresented/enriched under the TnSeq screen (q<0.05) are colored red.

As the TnSeq screen assesses mutant fitness at a single antibiotic concentration, it does not directly measure the mutant MIC, and lowered mutant frequency within an antibiotic-selected transposon library does not necessarily require or imply a decrease in mutant MIC (Girgis et al., 2009). To verify if this was the case in the ethambutol/isoniazid screens, we performed growth assays of various mutants in the presence of the low antibiotic concentrations used in the TnSeq screens (Fig. 3.6). The *fecB*, *rv0431*, *lysX*, *rv2224c* and *pbpA* mutants displayed drastic/complete growth attenuation at an ethambutol concentration of 0.5µg/ml, whereas the *fecB* and *ponA1* mutants exhibited stronger attenuation in the presence of 40ng/ml of isoniazid relative to the WT strain; confirming

reduced mutant fitness at these partially inhibitory concentrations despite the absence of a substantial mutant MIC shift.

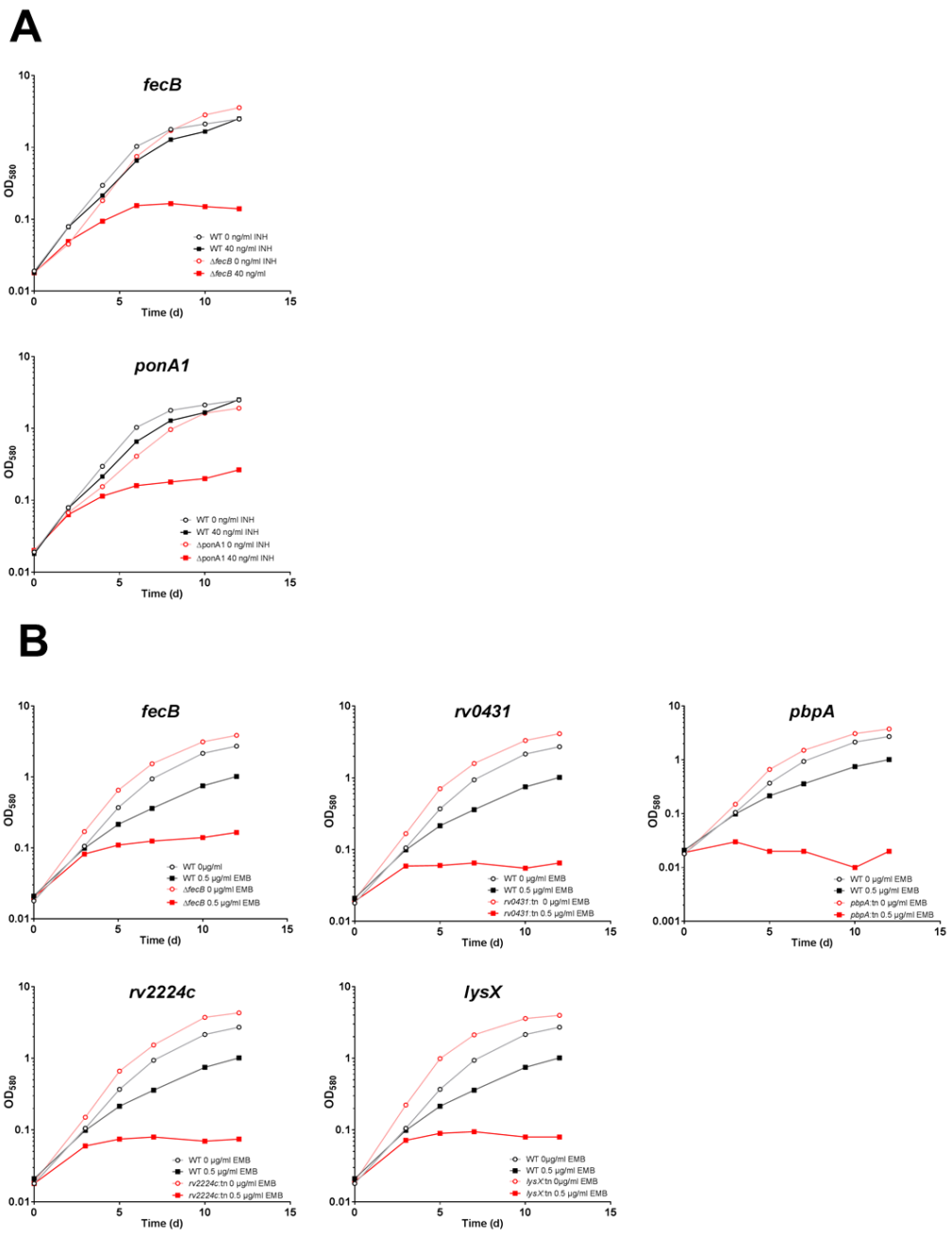

Figure 3.6 – Mutants predicted to be sensitive by the TnSeq screen exhibit greater growth attenuation at partially inhibitory antibiotic concentrations, despite minimal changes in in antibiotic MIC. Growth curves of WT (black) and mutant (red) strains under **A –** 40 ng/ml isoniazid **B-** 0.5 μg/ml ethambutol. Growth curves are representative of two independent experiments

3.4 Identification of mutations resulting in antibiotic sensitivity and resistance

We summarized the TnSeq data from transposon library selection under the five different antibiotics into a searchable annotated spreadsheet (Appendix A2). From this data, we identified genes that significantly affected fitness under antibiotic selection (Fig. 3.7A) – genes associated with particularly strong antibiotic phenotypes, cross-sensitivity to multiple antibiotics or have interesting functional annotations will be discussed in this section.

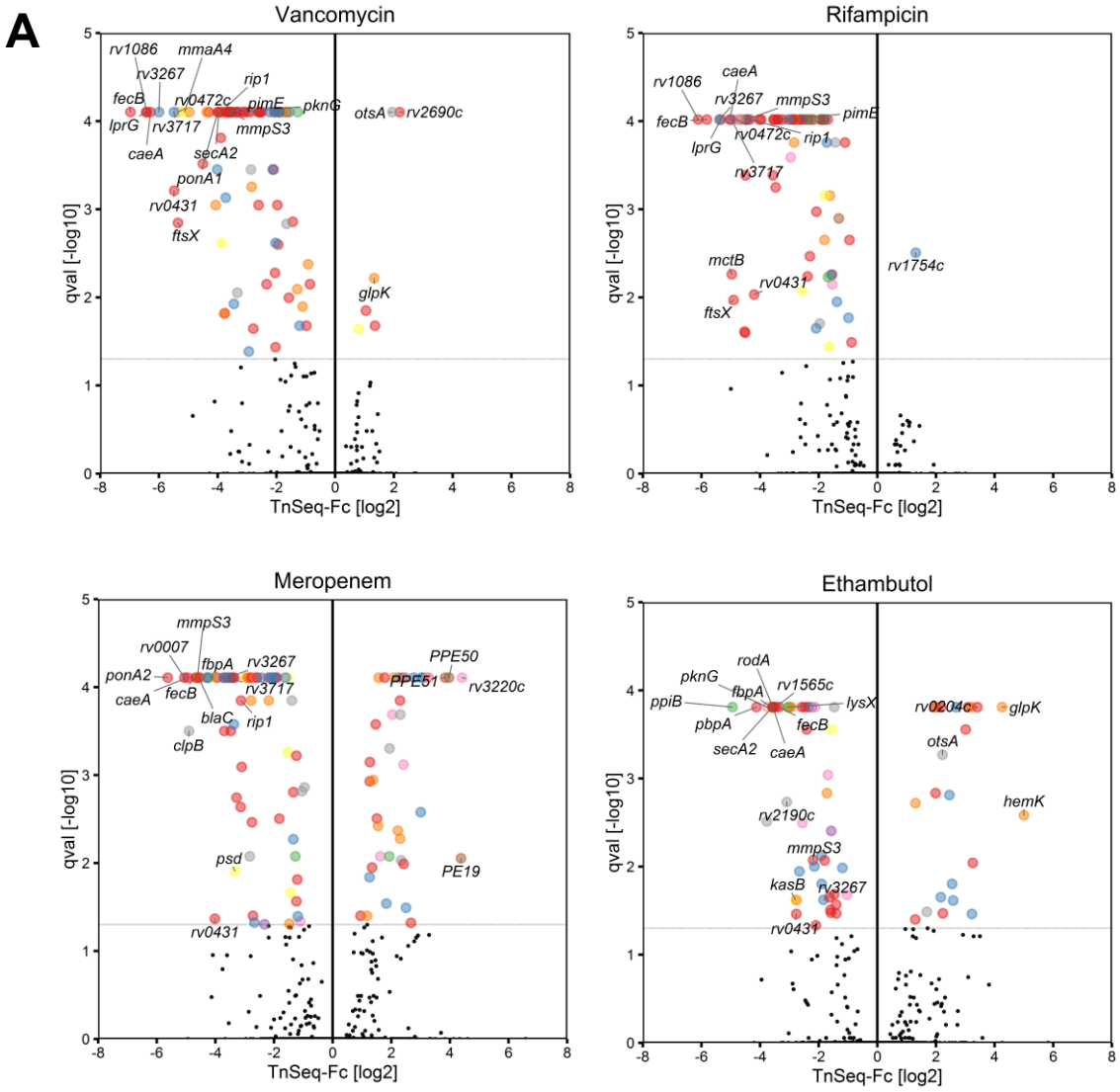

(continued)

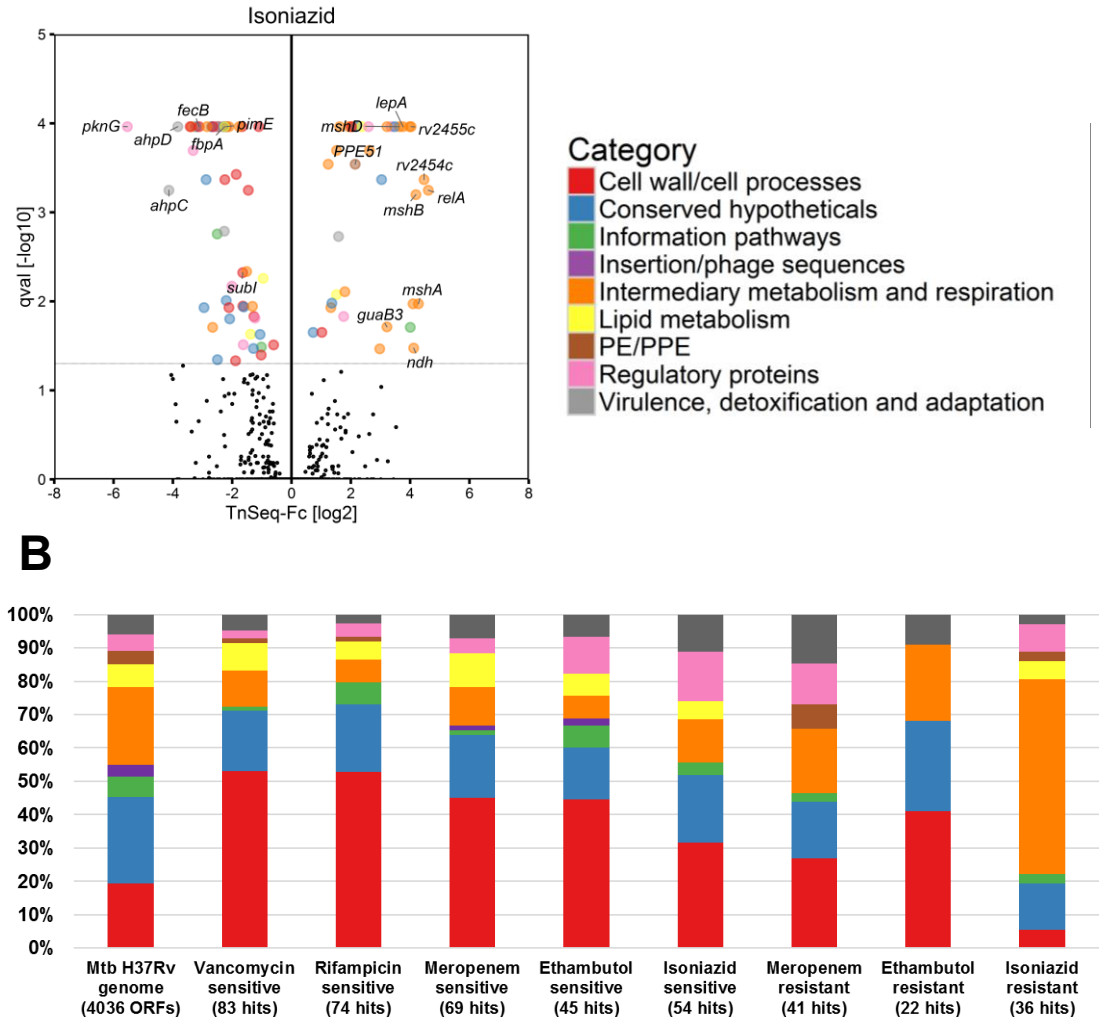

Figure 3.7 – Identification and functional categorization of genes related to antibiotic susceptibility. A – TnSeq-Fc and false-discovery rate adjusted p values (qval) from the resampling test are plotted for each genetic locus, loci meeting the significance threshold of q<0.05 are colored according to their functional categories on Tuberculist. **B –** Proportions of sensitive/resistant mutants corresponding to the different functional categories assigned by Tuberculist. The overall functional composition of the Mtb H37Rv genome is displayed to the left of the chart as a point of reference. Data for vancomycin/rifampicin resistant mutants is not displayed due to the small number of genes in these groups.

3.4.1 Cross-sensitivity to multiple antibiotics

A rough functional classification of antibiotic susceptibility determining genes (Fig. 3.7B) indicates that intrinsic antibiotic resistance is largely determined by genes in the cell wall/cell processes functional category in the Tuberculist database, comprising about 50% of the genes in the vancomycin, rifampicin, meropenem and ethambutol sensitive mutant sets

and 30% of the isoniazid sensitive mutant set. Many of these genes are shared across multiple antibiotics (Fig. 3.4B) - prominent among the genes/proteins contributing to antibiotic cross-sensitivity are FecB, annotated as an iron-dicitrate-binding periplasmic lipoprotein, Rv3267, a recently characterized LytR-CpsA-Psr (LCP) family protein that is capable of ligating arabinogalactan to peptidoglycan(Grzegorzewicz et al., 2016; Harrison et al., 2016), the protein translocase SecA2, the mannosyltransferase PimE, and Rv2224c/CaeA, a cell envelope-associated carboxyesterase/protease associated with reduced virulence(Lun and Bishai, 2007; Rengarajan et al., 2008) and increased imipenem sensitivity when disrupted (Lun et al., 2014).

We were also interested in regulatory processes involved in the control of antibiotic sensitivity - regulatory proteins linked to antibiotic cross-sensitivity include the protein kinase PknG, which was previously shown to be involved in intrinsic resistance to multiple antibiotics including erythromycin, vancomycin, ethambutol, rifampicin and imipenem(Wolff et al., 2009) , the site-2-protease Rip1, which controls transcription of multiple pathways including mycolic acid biosynthesis (Makinoshima and Glickman, 2005; Schneider et al., 2014), and the uncharacterized TetR-family transcriptional regulator Rv0472c.

3.4.2 Vancomycin, rifampicin and meropenem

As indicated by the previously mentioned cluster analysis, the vancomycin, rifampicin and meropenem sensitivity profiles possess a large degree of similarity, with 25 genes shared between the three sensitive gene subsets; the prevalence of cell envelope genes in this common group suggests a strong link between cell envelope function and antibiotic sensitivity to these drugs. In addition to the genes previously mentioned, transposon insertions in *ponA2*, encoding a penicillin binding protein and *moeA1*, which encodes a molybdopterin biosynthesis protein were associated with increased sensitivity in all three drugs.

In contrast to the shared genes, genes that are unique to each of the susceptibility profiles may be indicative of mechanistic pathways specific to each drug. Transposon insertions in *ponA1*, a penicillin binding protein gene, were associated with increased sensitivity to vancomycin but not meropenem, highlighting that while both drugs act on peptidoglycan biosynthesis, they may differentially affect various functional aspects of the process. As to be expected, mutations in the broad-spectrum beta-lactamase gene *blaC* specifically led to increased sensitivity to meropenem but not any of the other drugs. Transposon insertions in the *mce1* locus and the PE/PPE protein genes *pe19*, *ppe50* and *ppe51* were specifically enriched under meropenem selection; *ppe51* mutant enrichment was also observed under isoniazid selection. Overexpression of PE19 was previously shown to result in increased cell envelope permeability (Ramakrishnan et al., 2016), which could possibly account for the link with meropenem sensitivity.

3.4.3 Ethambutol

While the ethambutol antibiotic sensitivity profile shares many common elements with the vancomycin/rifampicin/meropenem sensitivity cluster (e.g. genes in the *pknG* operon, *fecB* and *pimE*), the ranking of the sensitivity-related genes in this subset differ by a notable degree. The top ranking ethambutol sensitivity genes include *ppiB,* a peptidyl-prolyl isomerase involved in protein folding that also possesses chaperone-like activity(Pandey et al., 2016), *fbpA*, a gene involved in trehalose dimycolate/cord factor biosynthesis, the cell division gene *rodA* and the penicillin binding protein encoding gene *pbpA*; these mutants are predicted to have weaker and often statistically insignificant levels of sensitivity to vancomycin and rifampicin. Ethambutol resistance was also predicted for multiple transposon mutants involved in metabolism – we observed increased frequencies of mutants in carbon metabolism (glycerol kinase GlpK, polyphosphate glucokinase PpgK and trehalose-synthase OtsA) and the putative methyltransferase HemK.

3.4.4 Isoniazid

The resistance mechanisms of *Mtb* against isoniazid have been well-established in previous studies. Our screen confirmed previously reported isoniazid resistance phenotypes associated with loss-of-function mutations in various genes - these include the mycothiol biosynthesis genes *mshA*, *mshB* and *mshD* (Xu et al., 2011), and the NADH dehydrogenase *ndh(Miesel et al., 1998; Vilcheze et al., 2005)*. While the catalase KatG has been reported to be necessary for the activation of isoniazid (Heym et al., 1993), we did not see an enrichment in the proportion of *katG* mutants under isoniazid selection, possibly due to a pronounced growth defect of *katG* mutants in Middlebrook 7H9 media. The isoniazid sensitivity profile also predicts a few novel mechanisms potentially associated with isoniazid resistance – these include the stringent response regulator RelA, genes in sulfur metabolism (*cysQ, cysG* and *sirA*) and various oxidoreductases (2-oxoglutarate oxidoreductase subunits KorA/KorB (Rv2455c/2454c) and the putative oxidoreductase GuaB3).

Promoter mutations resulting in the overexpression of the alkyl hydroperoxide reductase AhpC were previously identified in multiple isoniazid-resistant clinical strains(Miesel et al., 1998). Transposon mutations in the *ahpC* and also the adjacent *ahpD* loci were underrepresented in the isoniazid selected library, suggesting that loss of peroxidase and peroxynitrite reductase function may indeed be associated with increased isoniazid sensitivity.

3.4.5 Efflux pumps

We also aimed to identify the major efflux systems contributing towards resistance of the antibiotics tested (Table 3.2). Contrary to our expectations, disruption of individual efflux pump genes generally did not affect fitness under the antibiotic concentrations tested. While transposon insertions in the ABC transporter membrane protein gene *rv1272c* were underrepresented after meropenem selection, we did not observe any decrease in the MIC for meropenem in the *rv1272*:tn mutant (Table 3.1). Mutant frequencies for *rv1747* were

significantly reduced under outgrowth in vancomycin, whereas *rv1410c* insertions were underrepresented under selection with vancomycin, rifampicin and meropenem; however, both genes have been previously implicated in cell wall biosynthesis (Martinot et al., 2016; Spivey et al., 2013)and may thus be contributing to drug resistance in a drug-efflux independent manner.

Table 3.2 – TnSeq data summary for putative efflux pump genes. This list is based on previously published lists of putative efflux pump genes (Black et al., 2014; Louw et al., 2009). Mutations resulting in statistically significant antibiotic sensitivity (log_2 Fc <0, q<0.05) are highlighted in yellow.

	Vancomycin		Rifampicin		Meropenem		Ethambutol		Isoniazid		
Gene	FC [log2]	qval	FC [log2]	qval	FC [log2]	qval	FC [log2]	qval	FC [log2]	qval	Description
rv0037c	0.34	1	0.59	1	0.91	1	1.48	1	0.19	1	integral membrane protein
rv0194	0.04	1	0.07	1	0.02	1	0.11	1	0.13	1	transmembrane multidrug efflux pump
mmpL11	1.05	0.014126	0.29	1	0.18	1	0.26	1	0.14	1	transmembrane transporter MmpL11
mmpL3	3.79	1	0.63	1	1.73	1	3.03	1	0.04	1	transmembrane transporter MmpL3
iniB	0.08	1	0.08	1	0.12	1	0.72	1	0.21	1	isoniazid inducible protein IniB
iniA	0.05	1	0.12	1	0.18	1	0.94	0.880197	0.00	1	isoniazid inducible protein IniA
iniC	0.04	1	0.26	1	0.32	1	0.91	1	0.05	1	isoniazid inducible protein IniC
mmpL4	0.10	1	0.12	1	0.95	0.039806	0.68	0.086673	0.08	1	transmembrane transporter MmpL4
mmpL5	0.00	1	0.10	1	0.11	1	0.06	1	0.22	1	transmembrane transporter MmpL5
mmpS5	0.11	1	0.09	1	0.00	1	0.40	1	0.09	1	membrane protein MmpS5
emrB	0.02	1	0.28	1	0.06	1	0.02	1	0.07	1	multidrug resistance integral membrane efflux protein EmrB
pstB	0.15	1	0.26	1	0.02	1	0.02	1	0.03	1	phosphate-transport ABC transporter ATP-binding protein PstB
mmpL13b	0.02	1	0.05	1	0.13	1	0.22	1	0.10	1	transmembrane transporter MmpL13b
papA3	0.21	1	0.09	1	0.03	1	1.09	1	0.03	1	polyketide synthase associated protein PapA3
rv1218c	0.08	1	0.26	1	0.07	1	0.31	1	0.04	1	antibiotic transporter ATP-binding protein
rv1250	0.06	1	0.04	1	0.24	1	0.10	1	0.05	1	drug:H+ antiporter-2 (14 Spanner) (DHA2) family drug resistance MFS transporter
rv1258c	0.03	1	0.25	1	0.25	1	0.08	1	0.11	1	H+ antiporter protein
rv1272c	0.22	1	0.53	1	1.24	0.027264	0.02	1	0.68	1	ABC transporter membrane protein
rv1273c	0.15	1	0.69	1	0.36	1	0.20	1	0.25	1	ABC transporter membrane protein
irtA	0.18	1	0.08	1	0.83	1	0.43	1	0.86	1	iron-regulated transporter IrtA
irtB	0.06	1	0.74	1	1.53	1	0.24	1	1.01	0.948299	iron-regulated transporter IrtB
rv1410c	3.07	0	3.23	0	1.91	0	0.75	1	0.32	1	MFS drug efflux transporter P55
rv1456c	0.00	1	0.00	1	0.00	1	1.00	1	0.32	1	cytochrome C oxidase subunit XV assembly protein
rv1457c	1.91	1	2.78	1	2.13	1	1.56	1	3.86	1	ABC transporter efflux protein DrrB
rv1458c	0.18	1	0.22	1	2.58	0.087426	2.23	0.033915	1.56	0.653063	antibiotic transporter ATP-binding protein
rv1463	0.00	1	1.09	1	0.00	1	0.00	1	0.00	1	ABC transporter ATP-binding protein
rv1634	0.05	1	0.15	1	0.12	1	0.45	1	0.92	0.601054	drug efflux membrane protein
rv1686c	0.18	1	0.01	1	0.26	1	0.18	1	0.23	1	ABC transporter efflux protein DrrB
rv1687c	0.11	1	0.10	1	0.11	1	0.08	1	0.03	1	ABC transporter ATP-binding protein
rv1747	3.13	0	0.90	1	0.35	1	1.97	0	0.13	1	transmembrane ABC transporter ATP-binding protein
bacA	0.17	1	0.37	1	0.43	1	0.10	1	0.03	1	drug-transport transmembrane ABC transporter ATP-binding protein BacA
rv1877	0.01	1	0.12	1	0.52	1	0.01	1	0.14	1	drug:H+ antiporter-2 (14 Spanner) (DHA2) family drug resistance MFS transporter
rv2209	0.08	1	0.00	1	0.17	1	0.10	1	0.09	1	integral membrane protein
stp	0.14	1	0.13	1	0.00	1	0.27	1	0.85	1	integral membrane drug efflux protein Stp
rv2459	0.16	1	0.09	1	0.46	1	0.01	1	0.09	1	drug:H+ antiporter-2 (14 Spanner) (DHA2) family drug resistance MFS transporter
rv2477c	0.00	1	1.09	1	0.00	1	1.64	1	0.00	1	ChvD family ATP-binding cassette protein
rv2686c	0.02	1	0.25	1	0.42	1	0.09	1	0.04	1	antibiotic-transport ABC transporter
rv2687c	0.04	1	0.40	1	1.16	1	0.10	1	0.32	1	antibiotic-transport ABC transporter
rv2688c	0.23	1	0.44	1	0.97	1	0.06	1	0.23	1	antibiotic-transport ABC transporter
efpA	0.00	1	0.00	1	0.00	1	0.15	1	0.32	1	integral membrane efflux protein EfpA
drrA	0.15	1	0.05	1	0.02	1	0.29	1	0.07	1	doxorubicin resistance ATP-binding protein DrrA
drrB	0.28	1	0.15	1	0.03	1	0.18	1	0.01	1	doxorubicin resistance ABC transporter permease DrrB
drrC	0.51	1	0.58	1	0.04	1	0.22	1	0.18	1	ABC transporter efflux protein DrrB
mmpL7	0.44	1	0.10	1	0.17	1	0.01	1	0.21	1	RND superfamily inner membrane transporter MmpL7
rv2994	0.07	1	0.22	1	0.10	1	0.19	1	0.07	1	integral membrane protein
rv3000	0.21	1	0.07	1	0.97	1	0.32	1	0.04	1	ABC transporter permease
mmr	0.33	1	0.08	1	0.35	1	0.58	1	0.81	1	multidrug resistance protein Mmr
whiB7	0.37	1	0.11	1	0.08	1	0.38	1	0.31	1	transcriptional regulator WhiB-like WhiB7
rv3239c	0.06	1	0.16	1	0.09	1	0.17	1	0.11	1	drug:H+ antiporter-2 (14 Spanner) (DHA2) family drug resistance MFS transporter
rv3679	0.05	1	0.23	1	0.43	1	0.19	1	1.32	0.111722	anion transporter ATPase
rv3728	0.13	1	0.11	1	0.12	1	0.32	1	0.36	1	drug:H+ antiporter-2 (14 Spanner) (DHA2) family drug resistance MFS transporter

3.5 Characterization of FecB (Rv3044)

fecB transposon mutants were strongly underrepresented in libraries selected under partially inhibitory concentrations of all the antibiotics tested, suggesting its importance in intrinsic antibiotic cross-resistance (Fig. 3.4A, Table 3.3). We thus chose FecB as a follow-up study candidate from our antibiotic susceptibility screens. Based on sequence homology, FecB has been annotated as a putative iron(III) dicitrate binding lipoprotein similar to the substate binding protein in the FecBCDE iron-citrate ABC transporter system in *E. coli* (Banerjee et al., 2016; Braun and Herrmann, 2007; Staudenmaier et al., 1989); however, the other components of this system are absent in the Mtb genome, indicating that *fecB* may be an orphaned gene fulfilling a different function. We generated a Δ*fecB* deletion strain where *fecB* was replaced with a hygromycin resistance cassette, which we confirmed by Southern blot analysis (Fig. 3.8). From the Δ*fecB* mutant, we also generated a complementation strain constitutively expressing *fecB* under the control of the hsp60 promoter.

Table 3.3 – *fecB* mutants are predicted to be strongly sensitive to all five antibiotics studied in the screen. Summary of TnSeq data for *fecB*

	Vancomycin		Rifampicin		Isoniazid		Ethambutol		Meropenem	
Gene nam	FC [log2]	qval	FC [log2]	qval	FC [log2]	qval	FC [log2]	qval	FC [log2]	qval
fecB	-6.97	0	-5.81	0	-3.11	0	-3.35	0	-4.68	0

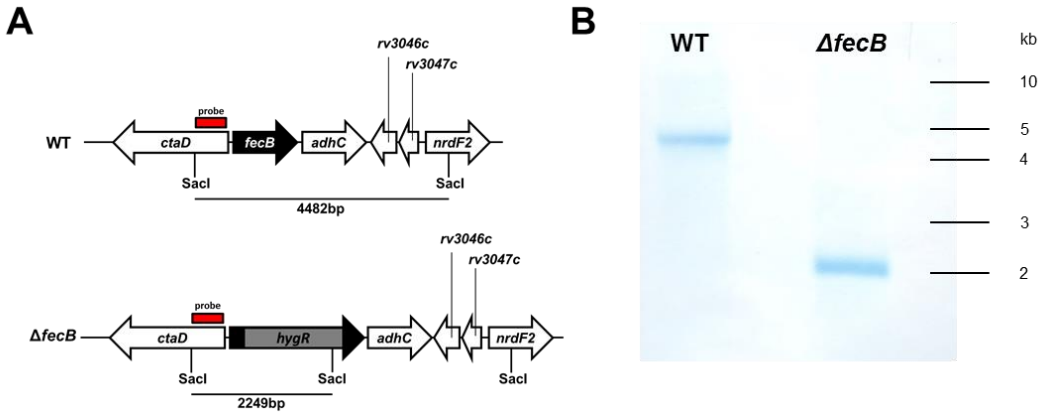

Figure 3.8 Construction of the Δ*fecB* mutant. A – Genomic maps of *fecB* and adjacent genes in WT H37Rv Mtb and the *fecB* deletion strain, showing SacI restriction sites and probe binding sites. **B-** Southern blot of SacI digested genomic DNA from WT H37Rv and Δ*fecB* strains.

3.5.1 FecB is important for intrinsic resistance to multiple antibiotics

We validated the predictions of the TnSeq screen by MIC assays. The MIC for the Δ*fecB* strain was reduced by 16-fold for vancomycin and 4-fold in rifampicin and meropenem, however, we did not observe a reduction in MIC of at least 1.5-fold for isoniazid and ethambutol (Table 3.1/3.4, Fig 3.5). Despite the lack of a strong MIC shift, the growth rate of the Δ*fecB* mutant was reduced relative to the WT strain under partially inhibitory concentrations of isoniazid and ethambutol (Fig. 3.6), confirming the TnSeq predictions of reduced Δ*fecB* fitness.

Further MIC assays showed that the Δ*fecB* mutant is hypersensitive to multiple antibiotics to varying degrees, and that the increased antibiotic sensitivity could be complemented by constitutive expression of *fecB* from an integrative plasmid (Table 3.4). The fold-reduction in antibiotic MIC in the Δ*fecB* mutant was correlated with antibiotic molecular weight (Pearson r = 0.734), suggesting that FecB is important in intrinsic resistance to higher molecular weight antibiotics (Fig. 3.9).

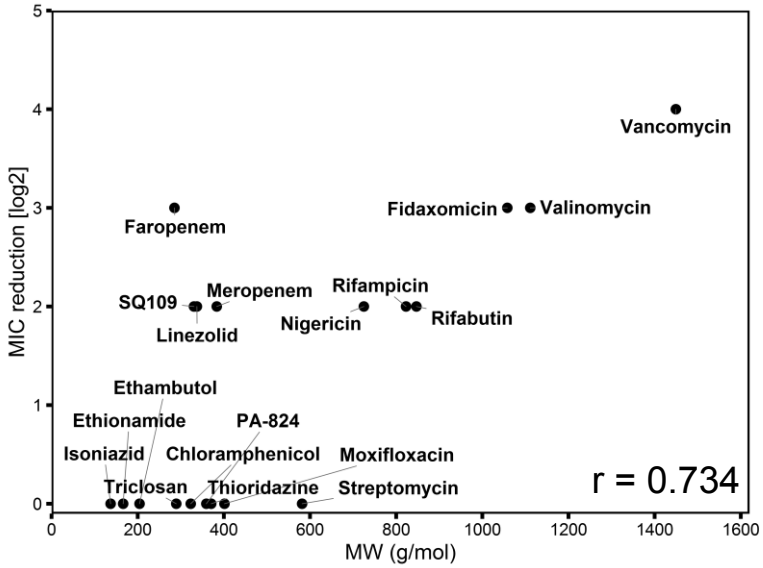

Figure 3.9 – The Δ*fecB* mutant exhibits greater hypersensitivity to higher molecular-weight antibiotics. Correlation plot of the relative reduction in MIC of the ΔfecB mutant versus antibiotic molecular weight

3.5.2 FecB is not likely to be a major iron transporter

As FecB is annotated as a putative iron (III) dicitrate binding lipoprotein, we tested if the Δ*fecB* mutant exhibited any iron-dependent growth effects. We used the Δ*mbtK* mutant as a positive reference control for deficient iron uptake – the Δ*mbtK* strain is unable to synthesize mycobactins, major siderophores important for iron transport in Mtb, and was shown to be impaired in iron scavenging and growth *in vitro* (Madigan et al., 2015). In growth curves using chelated Sauton's medium as the base medium, the Δ*fecB* mutant showed growth comparable to the WT and complementation strains at ammonium ferric citrate concentrations of 0.5µM, 50µM and 500 µM; in contrast, the Δ*mbtK* mutant was unable to grow at 0.5µM of ferric ammonium citrate and was growth defective relative to the WT strain at the higher iron concentrations (Fig. 3.10A). We were unable to conclude if the Δ*fecB* mutant was slightly attenuated relative to the WT/complementation strains in the base Sauton's media without iron supplementation because of experimental variability (Fig. 3.10A/3.10B), this was likely due to variations in residual trace amounts of iron in the base media, and also possible carryover of iron from the preculture. However, the WT, Δ*fecB*, and complementation strains all exhibited slow growth in the absence of iron supplementation, while the Δ*mbtK* was completely unable to grow at concentrations below 0.5µM of ferric ammonium citrate – this suggested FecB was not as important as the mycobactin pathway in iron transport.

We also performed growth assays using Sauton's medium supplemented with hemin, an iron source that can be taken up by Mtb independently of the mycobactin pathway (Owens et al., 2013; Tullius et al., 2011). Hemin supplementation was able to rescue the growth defect of the Δ*mbtK* strain in Sauton's medium and 7H9 (which contains ammonium ferric citrate as an iron source), but did not further improve growth of Δ*fecB* (Fig. 3.10B, Fig. 3.10C). We conclude that Δ*fecB* does not have a significant iron utilization defect under the

conditions of the screen (which uses 7H9 as the culture medium), and the increased antibiotic susceptibility is not likely to be related to iron deficiency.

Figure 3.10 – FecB is not likely to be a major iron transporter. Growth curves of Mtb strains under different iron supplementation conditions: **A**- Sauton's medium supplemented with ammonium ferric citrate (AFC). **B**- Sauton's medium supplemented with hemin. **C**- Middlebrook 7H9 media supplemented with hemin

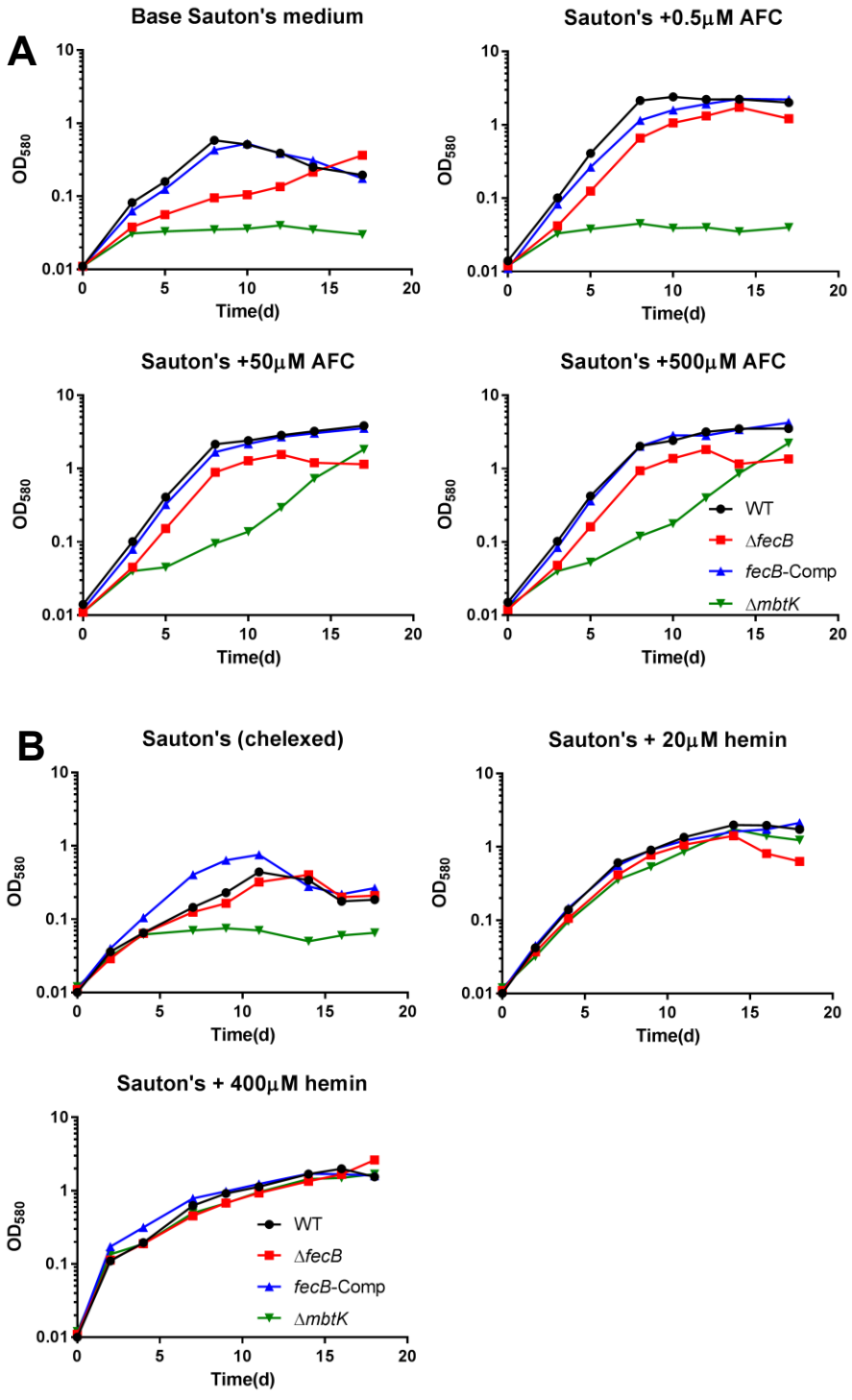
A
Base Sauton's medium
Sauton's +0.5μM AFC
Sauton's +50μM AFC
Sauton's +500μM AFC
OD580
Time(d)
WT
ΔfecB
fecB-Comp
ΔmbtK
B
Sauton's (chelexed)
Sauton's + 20μM hemin
Sauton's + 400μM hemin

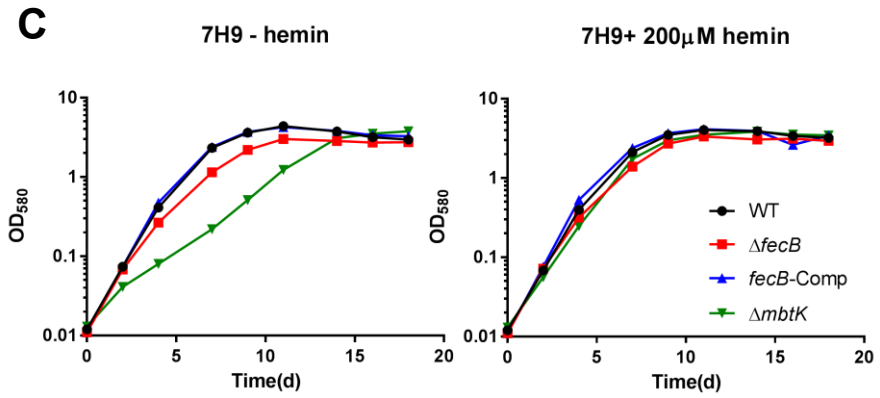

3.5.3 The Δ*fecB* mutant has a more permeable and less lipophilic cell envelope

Given the large proportion of cell envelope processes represented in the antibiotic-sensitive mutants predicted by TnSeq, and also the negative interaction between *fecB* and *marP*, we hypothesized that *fecB* was also important in determining the integrity of the cell envelope. We tested for increased cell envelope permeability in the Δ*fecB* mutant by the ethidium bromide (EtBr) uptake assay (Rodrigues et al., 2015). The Δ*fecB* mutant exhibited a 4-5-fold increase in ethidium bromide uptake relative to the WT and complemented strains based on fluorescence measurements, suggesting that loss of *fecB* results in increased cell envelope permeability (Fig. 3.11A). To investigate the possibility that the loss of *fecB* may have resulted in greater EtBr uptake due to reduced efflux, we treated the cells with the efflux inhibitor verapamil (Fig. 3.11B) – all three strains experienced a 50% increase in EtBr uptake, with the Δ*fecB* mutant still exhibiting a 4-5 fold greater uptake relative to the other strains, showing that the increased EtBr uptake in the Δ*fecB* was independent of verapamil-sensitive efflux mechanisms, and likely due to increased cell envelope permeability

To confirm if increased cell envelope permeability could result in increased antibiotic uptake, we measured the uptake of fluorescent-tagged vancomycin in the various Mtb strains. The Δ*fecB* mutant exhibited a similar 4-5-fold increase in vancomycin uptake relative to the WT and complemented strains, implying that the observed vancomycin sensitivity could be attributed to an increase in cell envelope permeability.

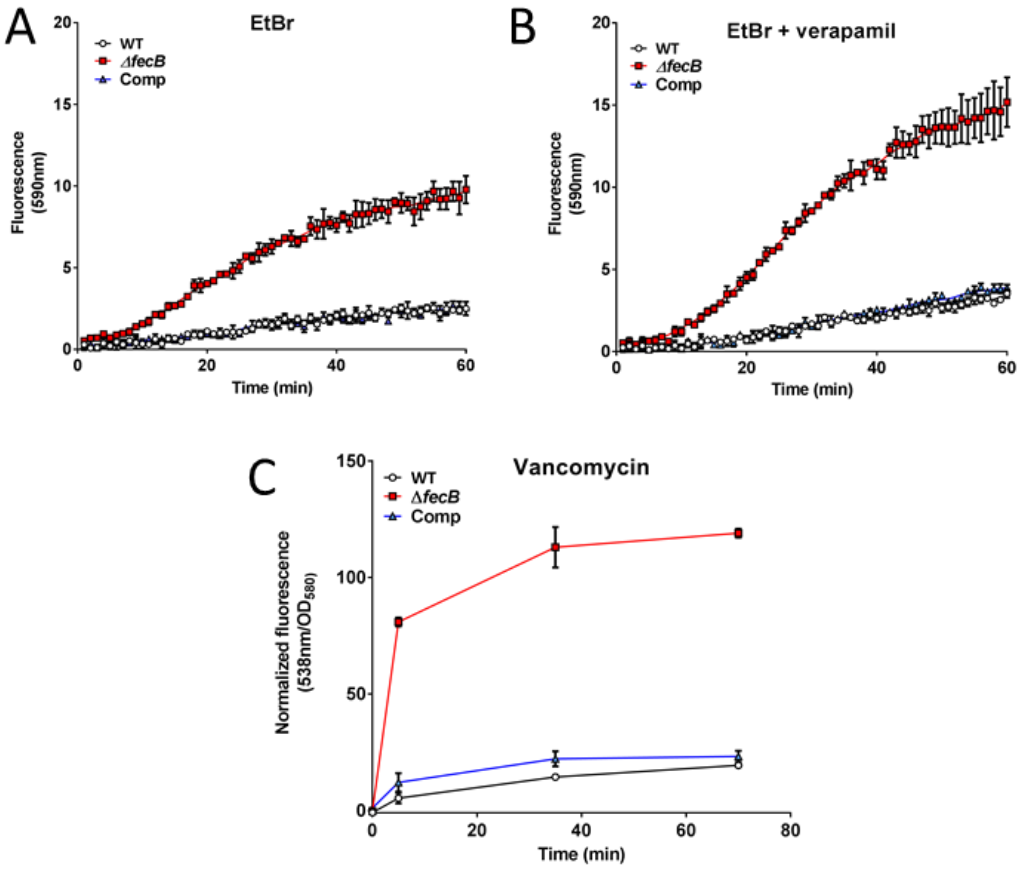

Figure 3.11 - The ΔfecB mutant exhibits increased uptake of exogenous substrates. A/B – Uptake of ethidium bromide by WT (black), Δ*fecB*(red) and complemented (blue) strains in the absence (A) and presence (B) of 100µg/ml verapamil. Fluorescent emission at 590nm was measured at 1min intervals from triplicated wells, and the data shown is representative of two independent experiments. **C**- Uptake of BODIPY-FL tagged vancomycin. A suspension of Mtb in PBS/tagged vancomycin was sampled at the timepoints indicated and washed, and emission at 538nm normalized to the OD of the washed suspension was measured. Datapoints shown are the means of triplicated measurements ± SD and are representative of two independent experiments

The increase in cell envelope permeability implies a change in cell envelope structure and physical properties. Previous studies have indicated that mycobacterial mutants in *pknG, fbpA* and mycolic acid biosynthesis have less hydrophobic cell walls and increased sensitivity to multiple antibiotics (Liu and Nikaido, 1999; Nguyen et al., 2005; Wolff and Nguyen, 2012). We assayed the cell envelope hydrophobicity of the Δ*fecB* mutant by the hexadecane partition procedure (Etienne et al., 2002; Rosenberg et al., 1980) – the Δ*fecB* mutant was significantly less hydrophobic than the WT strain (but not the complementation strain),

suggesting a change in the composition of the cell envelope that could possibly account for the increased permeability and antibiotic sensitivity.

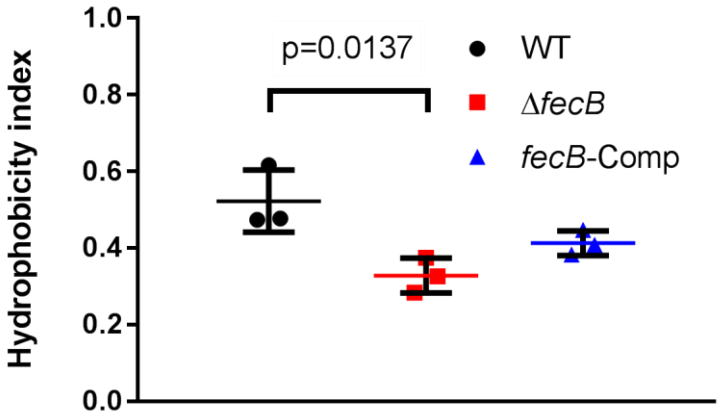

Figure 3.12 – The Δ*fecB* mutant has a less hydrophobic cell envelope. The hydrophobicity of the WT, Δ*fecB* and complementation strains was assessed by the hexadecane partition procedure. Triplicate measurements were taken for each strain.

3.5.4 The Δ*fecB* mutant has a growth defect on solid media that may be cell density dependent

In the process of experimentation, we noticed that the Δ*fecB* mutant had problems forming colonies on solid media. We confirmed this effect by plating spots of various dilutions of mid-log phase cultures onto 7H10 media (Fig. 3.13) – there appeared to be a density dependent growth defect in the Δ*fecB* mutant, which failed to grow at spot dilutions of ~10^4 cfu per spot or less. Spot morphology was also altered in the Δ*fecB* mutant – Δ*fecB* mutant spots had a smoother appearance, in contrast to the reticulated appearance of the WT and complementation strain spots and colonies. We did not observe Δ*fecB* colonies at the lower spot concentrations after up to 8 weeks of outgrowth. We tested a variety of different conditions to determine if any media specific component might be affecting the growth of the Δ*fecB* mutant. There was no improvement from the removal of potentially toxic media components (achieved by the omission of malachite green or oleic acid supplementation; and also by the addition of activated charcoal to adsorb unknown toxic

agents), supplementation with iron sources (hemin and ferric ammonium citrate) or lowering the atmospheric oxygen concentration in the incubator (data not shown).

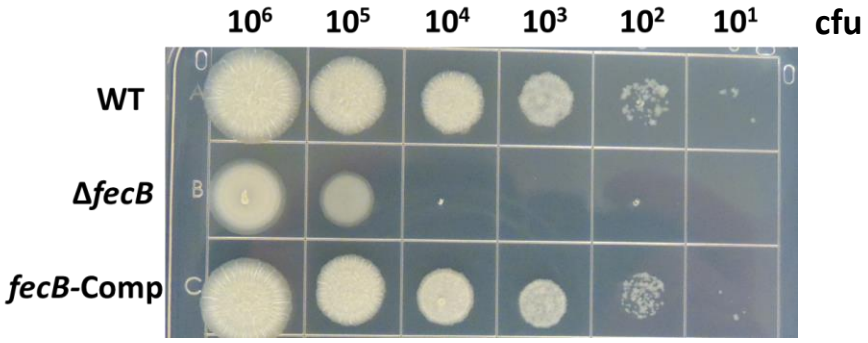

Figure 3.13 – The Δ*fecB* mutant is defective for growth on solid media. Volumes of Mtb culture containing 10^1 – 10^6 cfu were spotted onto 7H10 media. The spot dilutions shown here are from after 12 days of outgrowth.

The severe growth defect of the Δ*fecB* mutant on solid media was incongruous with the TnSeq data indicating that it was not essential on solid media, and our ability to isolate the mutant in the first place. As the plate phenotype that we observed implied cell-density dependent Δ*fecB* mutant growth, we hypothesized that we were able to previously able isolate *fecB* mutants due to the presence of high densities of untransformed bacteria on the plate. To recapitulate these conditions, we plated a high density of WT bacteria onto 7H10 plates containing hygromycin before performing the spot dilutions. This addition of WT bacteria was able to rescue the growth defect of the Δ*fecB* mutant (Fig. 3.14). Treatment with culture supernatant was however unable to rescue the growth defect, suggesting that a cell-associated component was involved in alleviating the Δ*fecB* phenotype. We were unable to rescue growth with either heat-killed Mtb or lysate obtained from mechanically-disrupted cultures; however, WT cells pre-killed by hygromycin could alleviate the growth defect (data not shown), suggesting a requirement for intact cells for rescue.

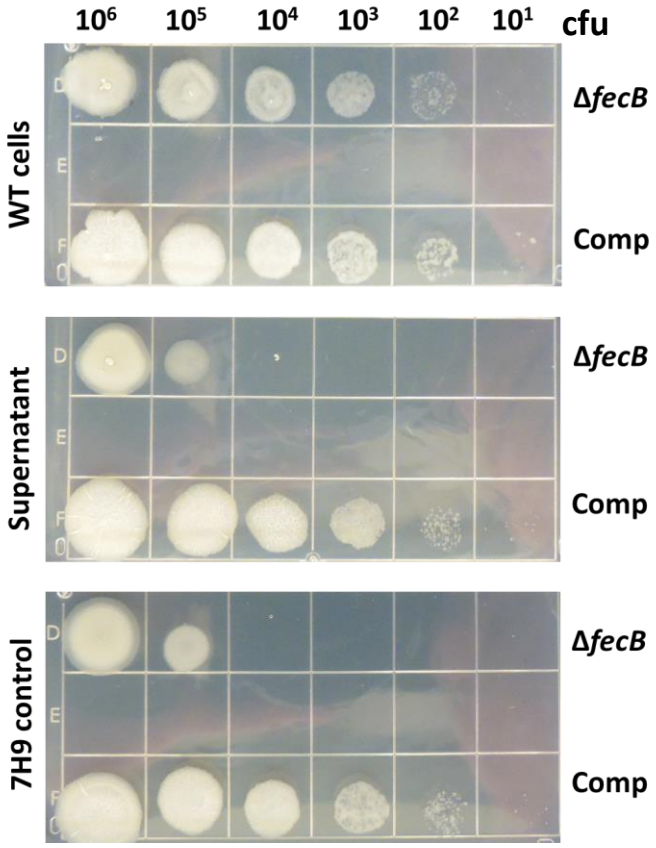

Figure 3.14– The ΔfecB mutant is able to grow on solid media in the presence of WT cells.

1ml of an OD1.0 WT culture (~5x10^8 cfu) or an equivalent volume of WT culture supernatant or 7H9 was spread onto 7H10-hygromycin plates, and different concentrations of Δ*fecB* and complementation strain culture were spotted onto the plate

3.5.5 The *ΔfecB* mutant is attenuated *in vivo*

fecB was previously predicted to be required for *in vivo* growth (Zhang et al., 2013). We infected C57BL/6 mice with the WT, Δ*fecB* and complementation strains via aerosol; we subsequently measured bacterial burdens in the lung and spleen, and also assessed lung pathology. 7H10- hygromycin plates pre-treated with WT cells were used in the enumeration of Δ*fecB* colonies. Δ*fecB* burden in the lung was reduced by at least 2-3 orders of magnitude relative to infection with the WT/complementation strains at the d16, d28 and d56 timepoints; we were also unable to recover Δ*fecB* lung colonies in half of the mice in the d16, d28, and d56 timepoints, indicating either a failure to establish infection or incomplete

rescue of the plate attenuation phenotype. We did not recover any Δ*fecB* colonies from the spleens (Fig. 3.15A).

Due to the uncertainty about colony enumeration in the Δ*fecB* strain, we assessed lung pathology as a secondary indicator of strain virulence (Fig. 3.15B-D). Mice infected with Δ*fecB* did not have granulomatous lung lesions at d56 post-infection, indicating reduced virulence of the Δ*fecB* strain.

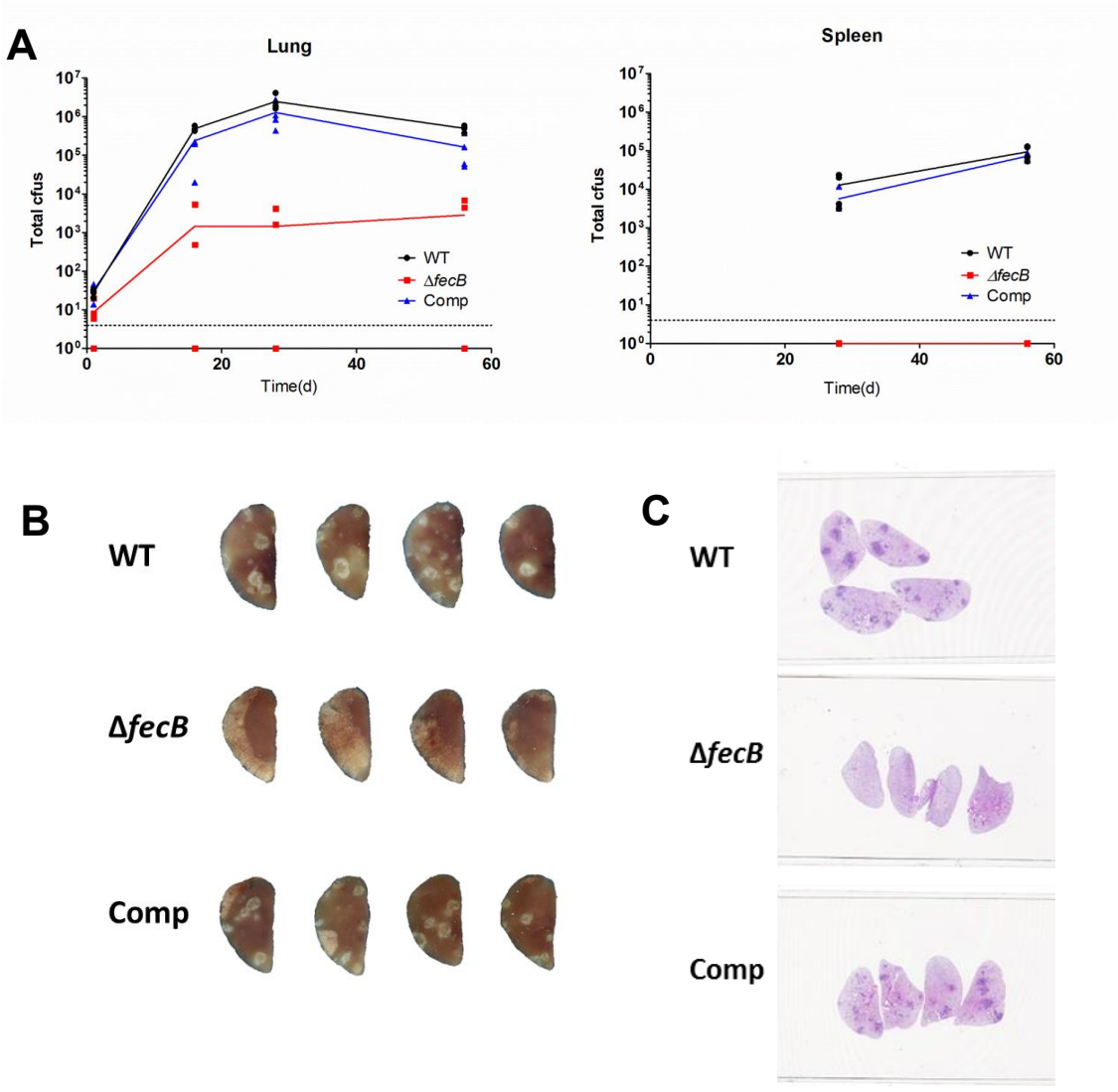

(continued)

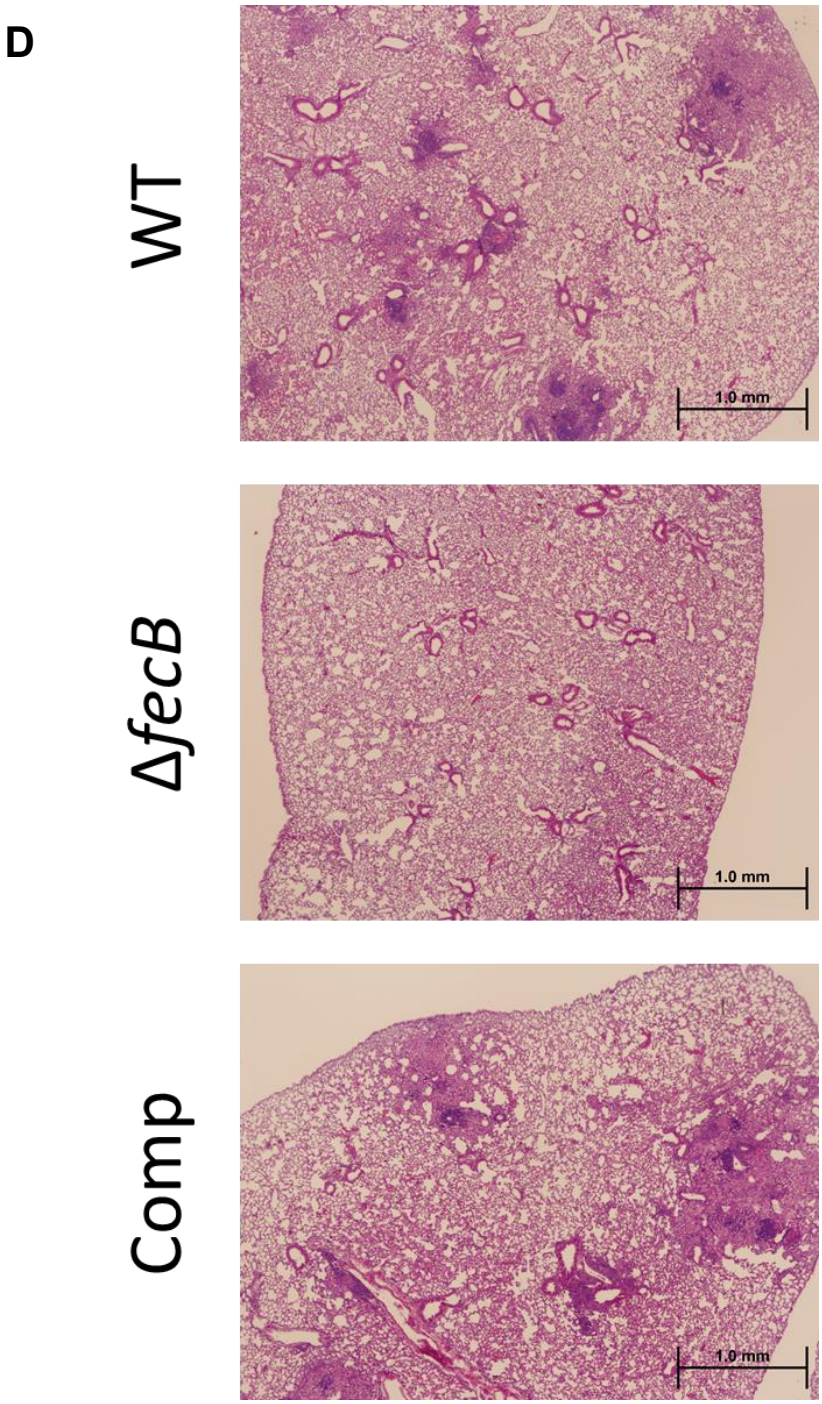

Figure 3.15 – The Δ*fecB* mutant is attenuated *in vivo*. A- Lung and spleen cfu counts from mice infected with the WT, Δ*fecB* and complementation strains. **B-** Gross lung pathology of infected mice. **C,D-** Hematoxylin and eosin (H&E) staining of lung sections at **C**- 1x and **D**- 4x magnification

3.6 Discussion

3.6.1 The functional role of FecB

From our screen, we identified *fecB* to be a gene important in cross-resistance to multiple antibiotics. Loss of *fecB* resulted in increased cell envelope permeability and a slight reduction in cell envelope hydrophobicity, suggesting a role for FecB in cell envelope structure and integrity. Despite its annotation as an iron transport protein, we did not see any major requirement of FecB in the utilization of iron; this may be due to the absence of the other components of the ferric-citrate ABC transporter system in the Mtb genome. FecB in *E. coli* has been shown to different species of ferric citrate as well as other trivalent metal ion complexes with citrate, and also a variety of tricarboxylic acids in complex or not complexed with metal ions (Banerjee et al., 2016). While our studies do not suggest that FecB is majorly involved in iron transport, it could possibly be involved in the regulation of periplasmic iron concentrations, or alternatively be involved in the transport of other metal ions or tricarboxylic acids. The construction of structural mutants of FecB in its ligand binding site could potentially help us confirm if its ligand binding activity is important in determining the cell envelope structure of Mtb.

In addition to increased susceptibility to multiple antibiotics, the Δ*fecB* mutant was attenuated *in vivo* and displayed a density-dependent growth defect on solid media. It is unknown at this point why the Δ*fecB* mutant has such a profound growth defect on plates, but we speculate that altered cell envelope properties/composition in the Δ*fecB* mutant might lead to deficiency in colony/biofilm formation, which may be rescued by unknown factors secreted by other Mtb cells in a high-density culture. In-depth lipidomic and metabolomic analysis may help us identify deficient metabolites in the *fecB* mutant that may inform us on the processes required for colony and biofilm formation.

Finally, in light of the pleiotropic multi-stress sensitivity phenotypes of other cell envelope mutants such as the Δ*marP*, it is likely that FecB may also be important in resisting

multiple stresses such as low pH, detergent and oxidative/nitrosative stress. Assays quantifying bacteriocidal effects on the Δ*fecB* mutant are currently subject to uncertainty due to the difficulty in recovering Δ*fecB* colonies on solid media. The construction of a conditionally-regulated *fecB* mutant could permit the reliable enumeration of colonies on solid media inducing FecB expression, and thus allow bacteriocidal assays to be performed. Alternatively, a liquid media based bacterial quantification method such as the most-probable-number (MPN) assay could be used. Future work involving bacteriocidal concentrations of antibiotics could help determine if killing kinetics are accelerated in the Δ*fecB* mutant and whether persister frequency is altered, which could indicate the suitability of FecB as a synergistic target potentiating the action of antibiotics.

3.6.2 Key conclusions of the antibiotic susceptibility screen

In this study, we used a TnSeq-based approach to identify and rank the genetic determinants of Mtb fitness under multiple antibiotic selection pressures. One of the aims of our study was to determine if the mechanisms governing antibiotic sensitivity are generally antibiotic-specific or largely shared across the different antibiotics. Cell envelope/cell division genes featured predominantly amongst the mutants sensitive toward the five antibiotics tested, with genes such as *fecB*, *pknG* and *caeA* determining susceptibility to multiple antibiotics within the test panel. This could possibly be due to increased cell envelope permeability and antibiotic uptake resulting from a compromised cell envelope; alternatively, loss of function of these non-essential cell envelope genes could sensitize *Mtb* to normally sub-lethal levels of cell envelope damage induced by antibiotics. While the antibiotics tested shared multiple intrinsic resistance mechanisms, we were also able to identify sensitivity genes specific to each antibiotic, which could be informative about the mode of action of their respective antibiotics.

The antibiotic susceptibility gene profile of rifampicin was highly similar to that of vancomycin and meropenem; this result was somewhat intriguing given that rifampicin

inhibits RNA polymerase whereas vancomycin and meropenem act on peptidoglycan biosynthesis. The large overlap between the vancomycin/rifampicin sensitivity genes may indicate the higher importance of cell envelope permeability in intrinsic resistance to these drugs, possibly related to their larger molecular sizes. These results also suggest the possibility that sub-inhibitory concentrations of rifampicin may result in cell envelope stress that becomes synthetically lethal in combination with the loss of function of certain cell envelope genes. Recent studies have shown that point mutations in *rpoB*, a target gene of rifampicin, result in altered fatty acid metabolism(du Preez and Loots, 2012) and profound changes in cell wall lipid composition, suggesting that inhibition of RNA polymerase by rifampicin is also likely to affect cell envelope structure and integrity. Following this line of argument, cell envelope damage could possibly be a major downstream effect of RNA polymerase inhibition leading to bacteriocidality, and potential synergistic combinations of rifampicin and cell-envelope targeting drugs (in particular the peptidoglycan-actives) could lead to more effective anti-TB treatment regimens; this is supported by a recent study demonstrating a synergistic effect between rifampicin and carbapenem antibiotics (Kaushik et al., 2015).

We sought to identify the main efflux pump systems contributing to intrinsic antibiotic resistance, but contrary to our expectations, we did not observe a major requirement for efflux pump genes in the presence of antibiotic selection. There are many possible explanations for this conspicuous absence -this may be due to the high level of redundancy between the multiple efflux pump systems, which could buffer against the effects of single efflux-gene disruption in our TnSeq study. Alternatively, our inability to detect significantly important efflux genes may be due to the limitations of our screen – drug efflux may be mostly mediated by the few essential efflux genes (*efpA*, *irtB*, *rv1463* or *rv3806c*), which are not detectable in our transposon libraries, or that the partly inhibitory antibiotic concentrations were insufficient to induce the induction of efflux pumps. Finally,

and most simply, it is entirely possible that efflux pumps do not play a key role in intrinsic resistance to the antibiotics tested. It was previously noted that treatment with the efflux inhibitors reserpine or verapamil did not affect the overall uptake of ofloxacin or rifampicin in both replicating and non-replicating Mtb (Piddock et al., 2000; Sarathy et al., 2013). The authors of these studies did however suggest the possibility that efficacious induction of efflux pumps may be specific to certain drug-resistant strains, and that efflux may be comparatively less important in the laboratory H37Rv strain used in the current study. In the face of all these possibilities, it is still reasonable to conclude that single-gene inhibition of the efflux genes covered by our screen is unlikely to result in any major change in sensitivity to the antibiotics tested, and it would thus be unproductive to design inhibitors for individual efflux pumps for adjunctive chemotherapy with these drugs. We note that our study does not necessarily rule out efflux pumps as important determinants of resistance toward other antibiotics, and further screening needs to be done to address this.

An influential but oft-debated study by Kohanski et al. suggested that the bacteriocidal activity of certain antibiotics is due to hydroxyl radical production occurring as a consequence of antibiotic-target interaction, resulting in oxidative damage. The study also suggested that mechanisms remediating hydroxyl radical damage such as antioxidant systems or repair pathways could play an important role in intrinsic antibiotic resistance (Kohanski et al., 2007). We did not observe increased sensitivity resulting from mutations in the mycothiol biosynthesis pathway, the main antioxidant system in Mtb, as well as in the DNA repair genes (e.g. RecA); however, *clpB* mutants showed an increase in sensitivity to the peptidoglycan-targeting drugs vancomycin and meropenem. ClpB is a chaperonin involved in the degradation or sequestration of irreversibly oxidized proteins (Vaubourgeix et al., 2015), suggesting that the action of vancomycin or meropenem may be associated with increased protein damage. Similar to the case of the efflux pumps, the paucity of repair mechanisms represented in mutants with increased antibiotic sensitivity may indicate redundancy

between repair pathways, an inability of the screen to detect essential repair genes, the antibiotic conditions being too low to induce major oxidative damage, or the general non-involvement of these repair pathways in mitigating damage caused by the antibiotics tested.

The observation that certain genes affect antibiotic susceptibility in replicating Mtb cultures raises the question as to whether they also contribute to antibiotic resistance in non-replicating persister populations. Environmental stresses such as hypoxia, oxidative stress and nutrient deprivation are known to induce global transcriptional changes resulting in altered metabolism, reduced cellular replication, and structural changes to the cell envelope, leading to a state of phenotypic drug tolerance (Gengenbacher et al., 2010; Nathan and Barry, 2015; Sarathy et al., 2013). It was previously shown that the sulfate transport system proteins CysT, CysW, CysA1 and SubI were upregulated under starvation conditions (Betts et al., 2002); our observation that transposon insertions in *subI-cysTWA1* (*rv2400c-rv2397c*) were associated with antibiotic cross-sensitivity suggests a possible mechanism by which the upregulation of sulfate utilization pathways may promote antibiotic tolerance, by increased synthesis of sulfolipids or other sulfated metabolites that contribute to intrinsic resistance. Further characterization of antibiotic-susceptibility determining genes may reveal novel mechanisms contributing to phenotypic drug resistance in Mtb.

3.6.3 Antibiotic susceptibility screen design and troubleshooting

In order to identify genes determining antibiotic susceptibility, we expanded transposon libraries in the presence or absence of partially inhibitory antibiotic concentrations close to the MIC, for a period of ~6.5 generations. The rationale for this particular screen design is as follows:

1. By using a partially-inhibitory antibiotic concentration, library selection and outgrowth occurs in the same phase of the screen, eliminating the need for a secondary outgrowth step. While we could alternatively have performed the screen under bacteriocidal conditions and identified mutants with altered killing kinetics,

this would have necessitated a secondary outgrowth phase to identify viable mutants at the end of the selection period. This could potentially introduce selection-independent variation in mutant frequencies in the output libraries, if the extent of the outgrowth is not well standardized between the experimental and control groups. Standardization of the outgrowth phase is particularly complicated post-antibiotic selection due to delayed recovery of antibiotic-treated cultures and potential carryover of antibiotics from the selection culture to the outgrowth plate. A secondary outgrowth phase would also result in a loss of library diversity due to selection against slow-growing mutants in the outgrowth phase.

2. Partially inhibitory selection was carried out at an antibiotic concentration close to the MIC – this would maximize the selection pressure on the mutant libraries, allowing for the identification of a large number of both sensitive and resistant mutants. Increasing antibiotic selection pressure would also reduce the extent of outgrowth required to obtain a significant change in mutant frequencies.
3. By reducing the outgrowth duration to 6.5 generations, library diversity is improved due to reduced loss of mutants that are growth-defective in culture, even in the absence of antibiotic selection. This improves screen coverage and reduces the number of "blind-spot" genes that cannot be reliably tested statistically. Secondarily, reducing the outgrowth duration ensures that the screens can be completed in 1-2 weeks, improving experimental efficiency.

This screen design prioritizes greater genomic coverage, reduced experimental noise and a faster execution time; however, the main tradeoff of this design is that it identifies multiple trivial hits with minimal impact on antibiotic susceptibility, as defined by standard measures of sensitivity such as the MIC or the minimum bacteriocidal concentration (MBC). The possible reasons for this non-specificity will be discussed in this section.

While our TnSeq screen assesses mutant fitness at a single partially inhibitory antibiotic concentration, we chose to assess screen performance based on its ability to predict mutants with reduced MICs. The distribution of antibiotics in tuberculosis lesions is highly variable (Dartois, 2014; Prideaux et al., 2015), and the MIC is thus more reflective of a mutant's ability to survive and replicate in the diversity of niches in a host undergoing TB chemotherapy. Despite the fact that single-concentration mutant fitness and mutant MIC are related, they are far from perfectly correlated – multiple hits in this screen and previous similar studies (Dorr et al., 2016; Girgis et al., 2009) exhibit no reduction in MICs despite showing reduced mutant fitness under specific antibiotic concentrations. It is also possible that the significant changes in mutant frequency and the implied changes in antibiotic sensitivity may be particular to the culture conditions of the TnSeq screen (e.g. inter-mutant competition/cooperation in mixed culture, insufficient recovery time from thawing) and not necessarily reproducible in the context of the single-strain MIC assay.

Nevertheless, our screen demonstrates reasonable predictive ability in the identification and ranking of mutants with MIC reductions for vancomycin, rifampicin and meropenem. Screen performance was significantly poorer for ethambutol and isoniazid, with none of the mutants within our 21 mutant validation panel exhibiting an MIC reduction of greater than 1.5-fold for isoniazid. The comparatively poor performance of the isoniazid screen could possibly be attributed to the steep Hill slope of the isoniazid Mtb-inhibition curve (i.e. the difference between the lowest concentration required to fully inhibit Mtb growth and the highest concentration that does not inhibit growth at all is very small), which results in major fitness changes over a narrow window of isoniazid concentrations. The growth curves of selected mutants under partially inhibitory antibiotic conditions of ethambutol and isoniazid (Fig. 3.) illustrate that large changes in growth rates and consequently mutant frequencies can occur in spite of miniscule/non-apparent MIC shifts. To improve precision in the identification of "non-trivial" hits with significant reductions in MICs,

more stringent TnSeq-Fc cutoffs could be imposed, or alternatively, much lower antibiotic concentrations could be used to ensure the specific selection of mutants with significant MIC reductions. The use of lower antibiotic concentrations would however necessitate a longer outgrowth duration, which could reduce library diversity and genomic coverage of the screen.

The problem of trivial hits raises the question as to whether the antibiotic susceptibility screen design should be aligned to more clinically relevant measures of antibiotic susceptibility. A main aim of this screen was to identify targets that could potentiate the activity of existing antibiotics and reduce treatment duration. Relevant quantifiers of antibiotic synergy would thus include a reduction in MIC, faster killing kinetics and reduced persister populations; particularly under environmental conditions similar to those *in vivo*. Screening of libraries under bacteriocidal antibiotic concentrations would directly address the question of which mutations lead to faster killing and possibly reduced persister formation. However, bacteriocidal screens would be more difficult to implement due to the above-mentioned problems of reduced library diversity and increased experimental noise; in particular, a screen for mutants with reduced persister formation would require selection on a much greater mutant population than in this screen to avoid bottlenecking effects, due to the low frequency of persisters in the population. At this point, it is unknown which screen design performs better in the identification of relevant hits, and extensive screen testing and mutant validation would be required to determine optimal screen conditions.

CHAPTER 4: CONCLUDING REMARKS

4.1 The convergence of screens

This work adds two new datasets to the vast body of genetic screen studies in Mtb. If one were to step back and look at all the genetic screen data as a whole, he/she might notice the recurrence of certain hits across multiple screens. For example, of the 20 other acid-susceptible mutants identified in the Vandal screen, 8 were found to be negative interactors of *marP* (Table 2.3), which is not altogether surprising given that they could mediate parallel redundant processes contributing to acid resistance. More intriguing are hits that span over multiple screens that are seemingly unrelated at first glance – comparison of a previous *in vivo* essentiality screen (Zhang et al., 2013) with our antibiotic susceptibility screens identifies 20 mutants in common that are more susceptible to at least three antibiotics and are also attenuated *in vivo;* of these 20 genes, 18 are genetic interaction partners of *marP* (the majority of these are negative interactors, with the exception of the positively interacting *ponA2*) (Fig. 4.1). The convergence of these three screens points at a functional cluster of genes that is important in the tolerance of the two major sources of stress in a clinical setting – antibiotics and the host.

The unifying theme between these genes appears to their involvement in cell envelope processes. As stated in previous sections, we hypothesize the loss of cell envelope integrity leads to pleiotropic stress phenotypes, possibly due to increased permeability to toxic agents such as antibiotics, weak acids, reactive oxidative/nitrosative species and antimicrobial peptides. The interaction of these genes with *marP* suggests parallel functionality between members in this gene cluster, and it would be interesting to verify if these mutants share other common phenotypes, such as antibiotic hypersusceptibility correlated with antibiotic molecular weight as observed in the Δ*fecB* mutant.

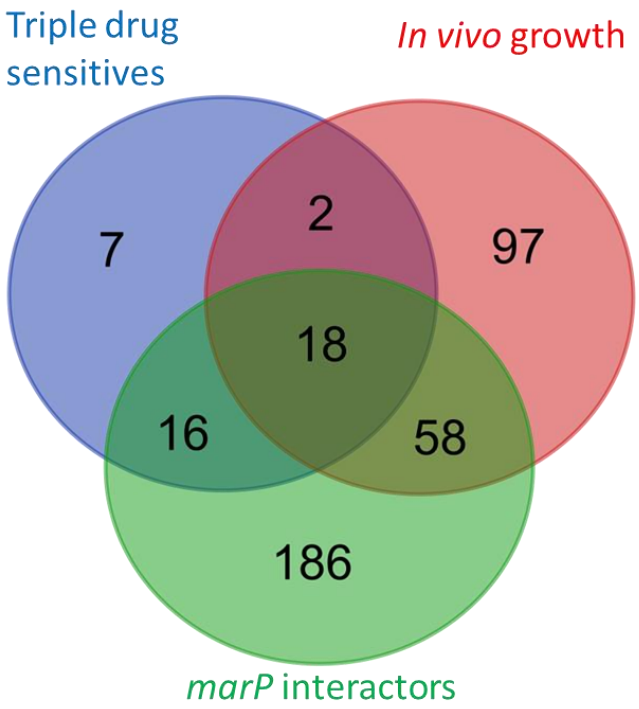

Gene	Annotation
pbpA	penicillin-binding protein PbpA
pssA	CDP-diacylglycerol-serine O-phosphatidyltransferase PssA
rv0472c	transcriptional regulator TetR-family
moeA1	molybdopterin biosynthesis protein MoeA1
rv1086	short-chain Z-isoprenyl diphosphate synthase
pimE	mannosyltransferase PimE
rv1566c	invasion-associated protein RipD
secA2	preprotein translocase ATPase subunit SecA2
ppm1	polyprenol-monophosphomannose synthase Ppm1
mmpS3	membrane protein MmpS3
caeA	carboxylesterase CaeA
sigB	RNA polymerase sigma factor SigB
rip1	metalloprotease Rip1
fecB	Fe(III)-dicitrate-binding periplasmic lipoprotein FecB
rv3193c	transmembrane protein
rv3205c	hypothetical protein
rv3267	hypothetical protein (CpsA related protein)
ponA2	bifunctional membrane-associated penicillin-binding protein 1A/1B PonA2

Figure 4.1 – Overlapping hits between *in vivo* essentiality, antibiotic susceptibility and *marP* genetic interaction screens. **A-** Overlap of mutants that are significantly more sensitive to at least three antibiotics, genetic interaction partners of *marP* ($q<0.05$ under the resampling test), or required for optimal growth *in vivo* (based on the criteria defined by Zhang et al. 2013, in which mutants are underrepresented 10-fold *in vivo* relative to an *in vitro* control and are significant under the Mann-Whitney-U (MWU) test at $q<0.01$, at D10 and D45 post-aerosol infection). **B-** List of 18 hits shared between the screens. Detailed TnSeq statistics are available in Appendix A2.

The end of many a bacterial genetics study is marked with the tired refrain of "our gene may prove to be valuable antibiotic target" – might the genes we have identified be of therapeutic value, and if so, what distinguishes them from the multitudes of other potential chemotherapeutic options? Based on current drug development paradigms, the answer is a resounding "no" – the most ideal antibiotic targets are essential in vitro, and the critical weakness of transposon library-based screens is that the vast majority of the genes represented in the library are non-essential (with the exception of genes with both essential/non-essential genes such as RipA), and are presumably less potent antibiotic targets. To advocate for the devil, one could possibly argue the targets we have identified may be vulnerable in an in vivo context, and also possess the attractive quality of synergizing with existing antibiotic regimens, which may give them an edge over more conventional candidates. On a more theoretical note, genetic interaction screens could identify synthetically lethal combinations of non-essential targets – for example, a hypothetical combination of MarP and FecB inhibitor could have potent anti-mycobacterial activity, if one manages to get around the logistical problem of developing two different inhibitors. Ultimately, what decides the success of an antibiotic target is not genetics but chemistry, and the points raised are moot in the absence of a pharmacologically-suitable inhibitor.

4.2 The future of genetic screens in Mtb

At this point in time, TnSeq is one of the more powerful methodologies for high-throughput genome-wide screening of Mtb mutants, but it is unable to comprehensively characterize the genes that are essential *in vitro*. These essential genes are likely to represent critical weak points in the physiology of Mtb, and future genetic screens will need to reach past the low-hanging fruit of non-essential genes in order to expose these vulnerabilities.

The study of essential genes is hindered by the non-viability of gene deletion mutants, and requires the construction of viable partial-loss-of-function mutants.

Conditional-knockdown systems regulated by transcriptional/proteolytic control (Kim et al., 2013; Lin et al., 2016) have opened the way for the study of essential Mtb genes; however, large collections of these conditionally-regulated mutants need to be constructed and amassed to attain high-throughput screening capabilities comparable to that of TnSeq, an enormous undertaking that would require at least a few more years (and a lot of money) to complete. Recent advances in CRISPR interference (CRISPRi) hint at a possible fast-track for the rapid assembly of an essential gene knockdown library in Mtb, it is likely that much more optimization is needed to attain effective and reliable knockdown, and to control for possible off-target effects (Choudhary et al., 2015; Peters et al., 2016; Singh et al., 2016). The realization of a comprehensive knockdown library in Mtb could pave the way for the discovery of more complete genetic interaction networks, the identification of specific targets of novel antibiotic candidates (Kim et al., 2013), and also targets that synergize with existing antibiotic regimens while possessing potent bacteriocidal/bacteriostatic activity themselves.

All in all, this TnSeq study may just be a prelude for the greater things that are yet to come. It does however provide some key lessons that may aid in the execution and interpretation of future genetic screens encompassing essential genes:

1. **Expect pleiotropy.** Our study has shown that there are multiple non-essential genes that mediate susceptibility to different antimicrobial agents and stresses, and are identified across multiple screens; additionally, the *marP* screen highlights the fact that a single gene can genetically interact with multiple pathways of disparate function. We predict that pleiotropy may be even more common in essential genes given their physiological importance, and knockdown of these genes may lead to broad perturbations across multiple physiological systems, as has been observed in mutants of the RNA polymerase gene *rpoB* (du Preez and Loots, 2012; Lahiri et al., 2016). The identification of pleiotropic genes is both a blessing and a curse – genes

mediating pleiotropic susceptibility to multiple stresses could be potent antibiotic targets synergizing with existing antibiotic regimens and host-induced stresses, however, the potentially large number of non-specific genetic and chemical-genomic interactions could frustrate efforts to identify specific functional gene targets, as illustrated in our *marP* interaction screen. The curation of a list of "usual suspects" mediating multiple phenotypes could help narrow down the list of specific targets, but might be inherently misleading – a gene may possess the specific function targeted by the screen, but may be discarded due to guilt by association with other pleiotropic genes

2. **Context is important.** Interpretation of data from high-throughput genetic screens is not straightforward – this is in part due to the highly-interconnected nature of genetic and chemical-genetic interaction networks and gene pleiotropy as described above, and also due to the quantification of interactions by simple numerical measures that do not necessarily correspond to the aims of the screen; a case in the point is our identification of mutants with miniscule shifts in isoniazid MIC, despite the large difference in mutant fitness at the single concentration used in the screen. Screen data should never be taken at face value on its own, but independently verified and interpreted through other screens and experiments. For example, cross-referencing of multiple genetic/chemical-genomic screens could help identify specific and non-specific screen hits, and specific genetic interactions could be revealed by supplemental protein-protein interaction screens.

CHAPTER 5: MATERIALS AND METHODS

5.1 Bacteria strains and culture conditions

M. tuberculosis H37Rv and derivative strains were routinely cultured in Middlebrook 7H9 medium (BD Difco) supplemented with 0.2% glycerol, 0.05% Tween 80, 0.5% bovine serum albumin (Roche), 0.2% dextrose and 0.085% NaCl. The antibiotics hygromycin B (50µg/ml), kanamycin (50µg/ml) and zeocin were added to media when selection was required.

The ΔmarP strain was obtained from a previous study (Vandal et al., 2008). Gene deletion mutants of *rv0812* and *fecB* were constructed by a recombineering strategy of allelic exchange as previously described (Murphy et al., 2015), and confirmed by Southern blotting. In the case of the *rv0812* mutant, 1µg/ml of PABA or 1µg/ml of D-glutamate/D-alanine (Sigma) were added to plate media to rescue auxotrophy. Complementation strains of *rv0812* and *fecB* were generated from their respective gene deletions strain by reintroducing a copy of *rv0812/fecB* under the control of the hsp60 promoter into the attL5 site. All complementation plasmids were created using Gateway Cloning Technology (Invitrogen). Additional mutant strains used in antibiotic susceptibility validation are listed in Table 3.1.

5.2 Transposon library construction

Mtb transposon libraries were constructed in quadruplicate in the WT H37Rv /Δ*marP* backgrounds by *himar1* mutagenesis as previously described (Long et al., 2015). Briefly, 100ml mid-log phase *Mtb* cultures (OD_{600} ~0.7-1.0) were incubated with 1-2x10^{11} pfu of ΦMycoMarT7 phage(Sassetti et al., 2001) at 37°C for 4h. Cultures were then washed and plated on Middlebrook 7H9 media in 1.5% agar supplemented with OADC (BD BBL), 0.5% glycerol and 0.05% Tween 80, and incubated for 19 days for the WT strain and 21 days for the Δ*marP* strain at 37°C, yielding libraries consisting of ~10^5 mutants each. Libraries was

harvested by scraping and stored as frozen stocks in Middlebrook 7H9 media in 15% glycerol at -80°C for downstream experiments.

5.3 TnSeq antibiotic-susceptibility screen

A WT transposon library frozen stock was thawed and incubated in Middlebrook 7H9 media for 4 days at 37°C to allow the library to recover to log-phase growth. This library starter culture was subcultured into 25ml cultures at a starting OD_{580} of 0.01, at varying antibiotic concentrations including an antibiotic-free control. Cultures were incubated at 37°C until an OD_{580} of ~1.0 as to standardize the number of outgrowth generations between libraries at approximately 6.5 generations. A partially-inhibitory concentration inhibiting the library growth rate to between 60-75% of that of the antibiotic-free library was determined for each antibiotic, this concentration was typically between 0.25x-0.5x of the antibiotic MIC; the selection concentrations used were 16 µg/ml for vancomycin, 4 ng/ml for rifampicin, 1.2 µg/ml for meropenem, 20-30 ng/ml for isoniazid and 0.4-0.6 µg/ml for ethambutol.

5.4 Sequencing of transposon mutant libraries

Genomic DNA was extracted from selected transposon libraries and mutant composition was determined by sequencing amplicons of the transposon-genome junctions as previously described (Long et al., 2015). Briefly, genomic DNA was sheared into ~500bp fragments by ultrasonication by a Covaris® E220 system, and fragments were subjected to end-repair and A-tailing with Taq polymerase, and ligated to T-tailed adapters bearing random 7-nucleotide barcodes to distinguish between unique fragments before subsequent PCR amplification. Fragments containing transposon-genome junctions were selectively enriched in a first PCR amplification, size-selected at a 400-600bp range and amplified in a second hemi-nested PCR to add adapter sequences for Illumina® sequencing. PCR amplicons were subjected to 75-100bp paired-end sequencing on an Illumina® HiSeq platform and raw sequence data was exported to .fastq files for further analysis.

5.5 Mapping and quantification of transposon insertions

Raw sequence data was processed using the TPP tool from the TRANSIT TnSeq analysis platform (DeJesus et al., 2015) – transposon genome junctions were mapped to the *Mtb* H37Rv reference genome NC_018143.1 using the Burroughs-Wheeler Aligner (BWA). To account for possible PCR amplication biases, reads corresponding to the same TA site and possessing the same 7-nucleotide barcode were considered to be derived from the same template, and these duplicate reads were discarded from the final template counts. Gene essentiality calls were assigned using a 4-state Hidden Markov Model (DeJesus and Ioerger, 2013) based on library datasets obtained from 4 independently constructed libraries outgrown on 7H9 agar plates (Plate essentiality), and the 13 libraries outgrown in 7H9 used as antibiotic-free controls for the TnSeq antibiotic screen (7H9 essentiality).

5.6 Identification of genes affecting fitness under antibiotic selection

Genes conditionally affecting fitness in the presence of antibiotic selection were identified using the resampling test module in the TRANSIT analysis platform as previously described(DeJesus et al., 2015). Briefly, triplicated libraries outgrown in the presence of antibiotics were compared to their corresponding antibiotic-free controls derived from the same starter cultures; differences in template-counts between libraries were normalized using Trimmed Total Reads (TTR) normalization. Significant differences between the sum of read-counts in the antibiotic-free and antibiotic-selected conditions were evaluated by comparison to a resampling distribution derived by randomly permutation of the observed counts of TA sites within a particular genetic locus among all datasets; p-values were defined as the proportion of values within 10^6 permutations that had a value more extreme than the observed experimental result, and these p-values were adjusted for multiple comparisons (qval) using the Benjamini-Hochberg procedure. TnSeq fold changes (TnSeq-Fc) were computed as log2 transformed ratios of the normalized read-counts between the antibiotic-selected and antibiotic-free libraries; to facilitate logarithmic transformation, zero-values

within the read counts were replaced with a pseudocount corresponding to the detection limit of the sequencing data.

We defined genes having a qval <0.05 from the resampling/permutation test to be significant determinants of fitness under antibiotic selection. For antibiotics which had two different selection conditions sequenced (isoniazid, ethambutol and meropenem), the higher of the two concentrations was used as the reference dataset for downstream analysis due to the higher sensitivity in identifying significant loci.

5.7 Additional data analysis and representation

Similarity between the various antibiotic-sensitivity profiles was determined based on average-linkage clustering of uncentered Pearson correlations with Cluster 3.0(de Hoon et al., 2004). Data arrays and cluster trees were visualized using Java Treeview (Saldanha, 2004).

Overlap between antibiotic sensitivity profiles was quantified in terms of the Jaccard index (i.e. the proportion of shared genes over the total number of genes in both profiles, or A∩B/A∪B). Venn diagrams were generated using the Venn Diagrams webtool (Universiteit_Gent_Bioinformatics)

Spearman correlation between MIC-shifts and TnSeq-Fcs were calculated in Prism 7.0. Numerical data and figures were presented using Microsoft Excel, Prism 7.0 and R.

5.8 Proteolysis assay for possible MarP substrates

Gateway Cloning Technology was used to generate episomal plasmids expressing C-terminal FLAG-tagged versions of Rv0012, Rv0537 and Rv0538, and transformed into WT and Δ*marP M. smegmatis* mc^2155.

50ml cultures were grown to mid-log phase (OD 0.8-1.2) in Sauton's medium and washed in 1xPBS. Protein lysates were prepared by 3 cycles of mechanical lysis of at 4500rpm for 30 seconds each with 0.1mm zirconia/silica beads. The cell wall fraction was obtained by centrifuging the toal lysate at 13000rpm at 4^oC for 60min, and boiled in 10% SDS for 10min to solubilize the pellet. Protein concentrations were estimated using the BioRad Lowry assay

kit, and approximately 50µg of each sample was loaded and separated on a 15% SDS-PAGE gel, and transferred to a nitrocellulose membrane. The Western blot was stained in Odyssey blocking buffer with mouse anti-FLAG antibody (Sigma, 1:250) and anti-Dlat (1:10000) as a loading control, and visualized using the Odyssey Infra-red Imaging System (LI-COR Biosciences)

5.9 Growth/auxotrophy assays for PABA/D-amino acids

Growth curves were performed in Middlebrook 7H9 media supplemented with either 1µg/ml PABA or 1µg/ml each of D-Ala/D-Glu. Growth curves were also performed in defined Sauton's medium containing 0.05% monobasic potassium phosphate, 0.05% magnesium sulfate heptahydrate, 0.2% citric acid, 0.005% ammonium ferric citrate, 0.05% ammonium sulfate, 0.0001% zinc sulfate, and 0.05% Tween-80 adjusted to pH 7.4. Growth assays on solid media were done on 7H10 media supplemented with 1µg/ml PABA or 1µg/ml each of D-Ala/D-Glu.

5.10 Antibiotic sensitivity assay

Minimum inhibitory concentrations (MIC) for the various *Mtb* strains were determined using the microbroth dilution technique – *Mtb* strains were grown to mid-log phase (OD_{580} = 0.6-1.0) and equal volumes of *Mtb* suspension were dispensed into a 4-fold/2-fold/1.5-fold dilution series in Middlebrook 7H9 media to a final OD of 0.01-0.025 per well. OD_{580} in each well was measured after 10-14 days of outgrowth, and the MIC_{90} was determined at the concentration of antibiotic at which bacterial growth was inhibited by 90% relative to the antibiotic-free control wells. Assays were repeated with a minimum of two replicates for each strain.

5.11 Growth assays in different iron sources

Strains were grown in iron-defined Sauton's medium – nominally iron-free Sauton's medium was prepared as described above minus the dicationic salts, adjusted to pH 7.4, chelated overnight with 20g/L of Chelex-100 resin (Bio-Rad), filtered and supplemented with

, 0.05% magnesium sulfate heptahydrate and 0.0001% zinc sulfate. Media was supplemented with varying concentrations of ammonium ferric citrate and hemin as indicated. Similarly, growth curves were also performed in 7H9 media with the hemin concentrations indicated.

5.12 Cell envelope permeability assay

Cell envelope permeability was determined using the ethidium bromide (EtBr) uptake assay as previously described (Rodrigues et al., 2015). Briefly, mid-log phase *Mtb* cultures were washed once in PBS + 0.05% Tween 80, and adjusted to an OD of 0.8 in PBS supplemented with 0.4% glucose. 100µl of bacteria were added to triplicate wells in black 96-well plate with clear bottomed wells (Costar), and an equal volume of 2µg/ml EtBr in PBS+0.4% glucose was added to each well to a final EtBr concentration of 1µg/ml and an OD_{580} of 0.4. EtBr fluorescence was measured at an excitation wavelength of 530nm and emission wavelength of 590nm at one minute intervals over a course of 60 min. To investigate possible effects of efflux inhibition, the experiment was repeated with the addition of 100µg/ml of verapamil to the test wells.

A similar assay was performed to determine permeability to fluorescent-tagged vancomycin. *Mtb* suspensions at an OD_{580} of 0.4 in PBS+0.4% glucose were incubated with 2µg/ml of BODIPY-FL® vancomycin (Thermo Scientific), and 200µl sample aliquots were taken at the 5,30 and 60min incubation timepoints, washed twice and finally resuspended in 200 µl PBS. Fluorescence was measured at an excitation of 485nm and emission at 538nm, and normalized to the OD_{580} of the final suspension to account for cell losses during the washing.

5.13 Cell envelope hydrophobicity assay

Cell envelope hydrophobicity was assayed by the hexadecane partition procedure (Etienne et al., 2002; Rosenberg et al., 1980) – briefly, mid-log phase cultures of the various strains were washed in 1xPBS and adjusted to an OD of 1.0 in PBS. 0.3ml of hexadecane (Sigma) was added to 0.9ml of each cell suspension in PBS, vortexed for 10s and left to stand for 20min to allow the aqueous/organic phases to separate. The OD of the aqueous phase

was measured, and the percentage reduction in OD relative to the input was taken as the hydrophobicity index.

5.14 Solid media spot dilution assays

Mid-log phase cultures (OD0.8-1.2) were diluted to an OD 0.2, and 10-fold serial dilutions were prepared. 10µl of each dilution was spotted onto solid media, producing spots containing between 10-10^6 cfu each. Solid media tested this way include 7H9 agar, 7H10 agar supplemented with OADC or fatty-acid free ADN, 7H10 agar with 0.4% activated charcoal, 7H10 supplemented with 20µM hemin, 50µM of ammonium ferric citrate or 20ng/ml mycobactin or Sauton's media + 1.5% Bacto agar.

For cell-based plate phenotype rescue experiments, 5x10^8 cfu of mid-log phase WT Mtb in 500µl 7H9 were spread onto 7H10 plates with 50µg/ml hygromycin added, as controls, equivalent volumes of mid and late log phase (OD 2.5-3.0) culture supernatant or 7H9 media were added to plates before the addition of spot dilutions. We also treated plates with biomass-equivalent amounts of WT bacteria heat-killed at 80^{o}C for 1h, WT lysate obtained from 3 cycles of mechanical lysis of at 4500rpm for 30 seconds each with 0.1mm zirconia/silica beads or bacteria pre-killed in 100µg/ml hygromycin in 7H9 for a period of 14 days.

5.15 Mouse infection

Female C57BL/6 mice (Jackson Laboratory) were infected with *Mtb* aerosolized using the Glass-Col inhalation exposure system – 5ml each of OD 0.2 single-cell suspensions of the WT, Δ*fecB* and complementation strains were injected into the nebulized, delivering approximately 100-200 bacilli per mouse. Four mice were sacrificed at each timepoint - lungs were harvested at D1, D16, D28 and D56 post-infection, while spleens were harvested at D28 and D56 post-infection. Organs were homogenized and plated on 7H10 media to enumerate cfus, to permit Δ*fecB* colony growth, 5x10^8 cfu of WT Mtb was spread on each plate prior to the application of organ homogenates. To visualize lung pathology, the left lung lobes was

obtained on D28/D56 and fixed in 10% formalin in PBS, and subsequently sectioned and stained with hematoxylin and eosin (H&E) under standard protocols. All mouse procedures were reviewed and approved by the Weill Cornell Medical College Institutional Animal Care and Use Committee (IACUC)

APPENDICES

APPENDIX A1 – Summary of *marP* interaction screen data

APPENDIX A2 – Summary of antibiotic susceptibility screen data

REFERENCES

Ainsa, J.A., Martin, C., Gicquel, B., and Gomez-Lus, R. (1996). Characterization of the chromosomal aminoglycoside 2'-N-acetyltransferase gene from Mycobacterium fortuitum. Antimicrob Agents Chemother *40*, 2350-2355.

Aldridge, B.B., Fernandez-Suarez, M., Heller, D., Ambravaneswaran, V., Irimia, D., Toner, M., and Fortune, S.M. (2012). Asymmetry and aging of mycobacterial cells lead to variable growth and antibiotic susceptibility. Science *335*, 100-104.

Andersson, D.I. (2006). The biological cost of mutational antibiotic resistance: any practical conclusions? Curr Opin Microbiol *9*, 461-465.

Armstrong, J.A., and Hart, P.D. (1971). Response of cultured macrophages to Mycobacterium tuberculosis, with observations on fusion of lysosomes with phagosomes. J Exp Med *134*, 713-740.

Ates, L.S., Ummels, R., Commandeur, S., van de Weerd, R., Sparrius, M., Weerdenburg, E., Alber, M., Kalscheuer, R., Piersma, S.R., Abdallah, A.M.*, et al.* (2015). Essential Role of the ESX-5 Secretion System in Outer Membrane Permeability of Pathogenic Mycobacteria. PLoS Genet *11*, e1005190.

Babu, M., Diaz-Mejia, J.J., Vlasblom, J., Gagarinova, A., Phanse, S., Graham, C., Yousif, F., Ding, H., Xiong, X., Nazarians-Armavil, A.*, et al.* (2011). Genetic interaction maps in Escherichia coli reveal functional crosstalk among cell envelope biogenesis pathways. PLoS Genet *7*, e1002377.

Bai, Y.L., Yang, J., Zhou, X., Ding, X.X., Eisele, L.E., and Bai, G.C. (2012). Mycobacterium tuberculosis Rv3586 (DacA) Is a Diadenylate Cyclase That Converts ATP or ADP into c-di-AMP. Plos One *7*.

Banerjee, S., Paul, S., Nguyen, L.T., Chu, B.C., and Vogel, H.J. (2016). FecB, a periplasmic ferric-citrate transporter from E. coli, can bind different forms of ferric-citrate as well as a wide variety of metal-free and metal-loaded tricarboxylic acids. Metallomics *8*, 125-133.

Bansal-Mutalik, R., and Nikaido, H. (2014). Mycobacterial outer membrane is a lipid bilayer and the inner membrane is unusually rich in diacyl phosphatidylinositol dimannosides. Proc Natl Acad Sci U S A *111*, 4958-4963.

Baryshnikova, A., Costanzo, M., Myers, C.L., Andrews, B., and Boone, C. (2013). Genetic interaction networks: toward an understanding of heritability. Annu Rev Genomics Hum Genet *14*, 111-133.

Basset, G.J., Ravanel, S., Quinlivan, E.P., White, R., Giovannoni, J.J., Rebeille, F., Nichols, B.P., Shinozaki, K., Seki, M., Gregory, J.F., 3rd*, et al.* (2004). Folate synthesis in plants: the last step of the p-aminobenzoate branch is catalyzed by a plastidial aminodeoxychorismate lyase. Plant J *40*, 453-461.

Beste, D.J., Espasa, M., Bonde, B., Kierzek, A.M., Stewart, G.R., and McFadden, J. (2009). The genetic requirements for fast and slow growth in mycobacteria. PLoS One *4*, e5349.

Betts, J.C., Lukey, P.T., Robb, L.C., McAdam, R.A., and Duncan, K. (2002). Evaluation of a nutrient starvation model of Mycobacterium tuberculosis persistence by gene and protein expression profiling. Mol Microbiol *43*, 717-731.

Bigger, J.W. (1944). Treatment of staphylococcal infections with penicillin - By intermittent sterilisation. Lancet *2*, 497-500.

Billington, O.J., McHugh, T.D., and Gillespie, S.H. (1999). Physiological cost of rifampin resistance induced in vitro in Mycobacterium tuberculosis. Antimicrob Agents Chemother *43*, 1866-1869.

Bisson, G.P., Mehaffy, C., Broeckling, C., Prenni, J., Rifat, D., Lun, D.S., Burgos, M., Weissman, D., Karakousis, P.C., and Dobos, K. (2012). Upregulation of the phthiocerol dimycocerosate biosynthetic pathway by rifampin-resistant, rpoB mutant Mycobacterium tuberculosis. J Bacteriol *194*, 6441-6452.

Biswas, T., Small, J., Vandal, O., Odaira, T., Deng, H., Ehrt, S., and Tsodikov, O.V. (2010). Structural insight into serine protease Rv3671c that Protects M. tuberculosis from oxidative and acidic stress. Structure *18*, 1353-1363.

Black, P.A., Warren, R.M., Louw, G.E., van Helden, P.D., Victor, T.C., and Kana, B.D. (2014). Energy metabolism and drug efflux in Mycobacterium tuberculosis. Antimicrob Agents Chemother *58*, 2491-2503.

Both, D., Schneider, G., and Schnell, R. (2011). Peptidoglycan remodeling in Mycobacterium tuberculosis: comparison of structures and catalytic activities of RipA and RipB. J Mol Biol *413*, 247-260.

Bottger, E.C., Springer, B., Pletschette, M., and Sander, P. (1998). Fitness of antibiotic-resistant microorganisms and compensatory mutations. Nat Med *4*, 1343-1344.

Braun, V., and Herrmann, C. (2007). Docking of the periplasmic FecB binding protein to the FecCD transmembrane proteins in the ferric citrate transport system of Escherichia coli. J Bacteriol *189*, 6913-6918.

Brennan, P.J. (2003). Structure, function, and biogenesis of the cell wall of Mycobacterium tuberculosis. Tuberculosis (Edinb) *83*, 91-97.

Brennan, P.J., and Nikaido, H. (1995). The envelope of mycobacteria. Annu Rev Biochem *64*, 29-63.

Brites, D., and Gagneux, S. (2015). Co-evolution of Mycobacterium tuberculosis and Homo sapiens. Immunol Rev *264*, 6-24.

Brossier, F., Veziris, N., Truffot-Pernot, C., Jarlier, V., and Sougakoff, W. (2011). Molecular investigation of resistance to the antituberculous drug ethionamide in

multidrug-resistant clinical isolates of Mycobacterium tuberculosis. Antimicrob Agents Chemother *55*, 355-360.

Buriankova, K., Doucet-Populaire, F., Dorson, O., Gondran, A., Ghnassia, J.C., Weiser, J., and Pernodet, J.L. (2004). Molecular basis of intrinsic macrolide resistance in the Mycobacterium tuberculosis complex. Antimicrob Agents Chemother *48*, 143-150.

Canetti, G., Parrot, R., Porven, G., and Le Lirzin, M. (1969). [Rifomycin levels in the lung and tuberculous lesions in man]. Acta Tuberc Pneumol Belg *60*, 315-322.

Casali, N., Nikolayevskyy, V., Balabanova, Y., Ignatyeva, O., Kontsevaya, I., Harris, S.R., Bentley, S.D., Parkhill, J., Nejentsev, S., Hoffner, S.E.*, et al.* (2012). Microevolution of extensively drug-resistant tuberculosis in Russia. Genome Res *22*, 735-745.

Chakraborty, S., Gruber, T., Barry, C.E., 3rd, Boshoff, H.I., and Rhee, K.Y. (2013). Para-aminosalicylic acid acts as an alternative substrate of folate metabolism in Mycobacterium tuberculosis. Science *339*, 88-91.

Chambers, H.F., Moreau, D., Yajko, D., Miick, C., Wagner, C., Hackbarth, C., Kocagoz, S., Rosenberg, E., Hadley, W.K., and Nikaido, H. (1995). Can Penicillins and Other Beta-Lactam Antibiotics Be Used to Treat Tuberculosis. Antimicrobial Agents and Chemotherapy *39*, 2620-2624.

Chao, M.C., Abel, S., Davis, B.M., and Waldor, M.K. (2016). The design and analysis of transposon insertion sequencing experiments. Nat Rev Microbiol *14*, 119-128.

Chao, M.C., Kieser, K.J., Minami, S., Mavrici, D., Aldridge, B.B., Fortune, S.M., Alber, T., and Rubin, E.J. (2013a). Protein complexes and proteolytic activation of the cell wall hydrolase RipA regulate septal resolution in mycobacteria. PLoS Pathog *9*, e1003197.

Chao, M.C., Pritchard, J.R., Zhang, Y.J., Rubin, E.J., Livny, J., Davis, B.M., and Waldor, M.K. (2013b). High-resolution definition of the Vibrio cholerae essential gene set with hidden Markov model-based analyses of transposon-insertion sequencing data. Nucleic Acids Res *41*, 9033-9048.

Chim, N., Habel, J.E., Johnston, J.M., Krieger, I., Miallau, L., Sankaranarayanan, R., Morse, R.P., Bruning, J., Swanson, S., Kim, H.*, et al.* (2011). The TB Structural Genomics Consortium: a decade of progress. Tuberculosis (Edinb) *91*, 155-172.

Choudhary, E., Thakur, P., Pareek, M., and Agarwal, N. (2015). Gene silencing by CRISPR interference in mycobacteria. Nat Commun *6*, 6267.

Cole, S.T., Brosch, R., Parkhill, J., Garnier, T., Churcher, C., Harris, D., Gordon, S.V., Eiglmeier, K., Gas, S., Barry, C.E., 3rd*, et al.* (1998). Deciphering the biology of Mycobacterium tuberculosis from the complete genome sequence. Nature *393*, 537-544.

Comas, I., Borrell, S., Roetzer, A., Rose, G., Malla, B., Kato-Maeda, M., Galagan, J., Niemann, S., and Gagneux, S. (2011). Whole-genome sequencing of rifampicin-

resistant Mycobacterium tuberculosis strains identifies compensatory mutations in RNA polymerase genes. Nat Genet *44*, 106-110.

Comas, I., Coscolla, M., Luo, T., Borrell, S., Holt, K.E., Kato-Maeda, M., Parkhill, J., Malla, B., Berg, S., Thwaites, G.*, et al.* (2013). Out-of-Africa migration and Neolithic coexpansion of Mycobacterium tuberculosis with modern humans. Nat Genet *45*, 1176-1182.

Coscolla, M., and Gagneux, S. (2014). Consequences of genomic diversity in Mycobacterium tuberculosis. Semin Immunol *26*, 431-444.

Cox, G., and Wright, G.D. (2013). Intrinsic antibiotic resistance: Mechanisms, origins, challenges and solutions. International Journal of Medical Microbiology *303*, 287-292.

Crofton, J., and Mitchison, D.A. (1948). Streptomycin resistance in pulmonary tuberculosis. Br Med J *2*, 1009-1015.

Da Silva, P.E.A., and Palomino, J.C. (2011). Molecular basis and mechanisms of drug resistance in Mycobacterium tuberculosis: classical and new drugs. J Antimicrob Chemoth *66*, 1417-1430.

da Silva, P.E.A., Von Groll, A., Martin, A., and Palomino, J.C. (2011). Efflux as a mechanism for drug resistance in Mycobacterium tuberculosis. Fems Immunol Med Mic *63*, 1-9.

Daffe, M., and Etienne, G. (1999). The capsule of Mycobacterium tuberculosis and its implications for pathogenicity. Tuber Lung Dis *79*, 153-169.

Daniel, T.M. (2006). The history of tuberculosis. Respir Med *100*, 1862-1870.

Daniel, V.S., and Daniel, T.M. (1999). Old Testament biblical references to tuberculosis. Clin Infect Dis *29*, 1557-1558.

Danilchanka, O., Pavlenok, M., and Niederweis, M. (2008). Role of porins for uptake of antibiotics by Mycobacterium smegmatis. Antimicrob Agents Chemother *52*, 3127-3134.

Danilchanka, O., Pires, D., Anes, E., and Niederweis, M. (2015). The Mycobacterium tuberculosis outer membrane channel protein CpnT confers susceptibility to toxic molecules. Antimicrob Agents Chemother *59*, 2328-2336.

Danilchanka, O., Sun, J., Pavlenok, M., Maueroder, C., Speer, A., Siroy, A., Marrero, J., Trujillo, C., Mayhew, D.L., Doornbos, K.S.*, et al.* (2014). An outer membrane channel protein of Mycobacterium tuberculosis with exotoxin activity. Proc Natl Acad Sci U S A *111*, 6750-6755.

Darby, C.M., and Nathan, C.F. (2010). Killing of non-replicating Mycobacterium tuberculosis by 8-hydroxyquinoline. J Antimicrob Chemother *65*, 1424-1427.

Darby, C.M., Venugopal, A., Ehrt, S., and Nathan, C.F. (2011). Mycobacterium tuberculosis gene Rv2136c is dispensable for acid resistance and virulence in mice. Tuberculosis (Edinb) *91*, 343-347.

Dartois, V. (2014). The path of anti-tuberculosis drugs: from blood to lesions to mycobacterial cells. Nat Rev Microbiol *12*, 159-167.

Dartois, V., and Barry, C.E., 3rd (2013). A medicinal chemists' guide to the unique difficulties of lead optimization for tuberculosis. Bioorg Med Chem Lett *23*, 4741-4750.

de Hoon, M.J.L., Imoto, S., Nolan, J., and Miyano, S. (2004). Open source clustering software. Bioinformatics *20*, 1453-1454.

de Knegt, G.J., Bruning, O., ten Kate, M.T., de Jong, M., van Belkum, A., Endtz, H.P., Breit, T.M., Bakker-Woudenberg, I.A., and de Steenwinkel, J.E. (2013). Rifampicin-induced transcriptome response in rifampicin-resistant Mycobacterium tuberculosis. Tuberculosis (Edinb) *93*, 96-101.

De Rossi, E., Arrigo, P., Bellinzoni, M., Silva, P.A., Martin, C., Ainsa, J.A., Guglierame, P., and Riccardi, G. (2002). The multidrug transporters belonging to major facilitator superfamily in Mycobacterium tuberculosis. Mol Med *8*, 714-724.

DeJesus, M.A., Ambadipudi, C., Baker, R., Sassetti, C., and Ioerger, T.R. (2015). TRANSIT--A Software Tool for Himar1 TnSeq Analysis. PLoS Comput Biol *11*, e1004401.

DeJesus, M.A., and Ioerger, T.R. (2013). A Hidden Markov Model for identifying essential and growth-defect regions in bacterial genomes from transposon insertion sequencing data. BMC Bioinformatics *14*, 303.

DeJesus, M.A., and Ioerger, T.R. (2015). Capturing Uncertainty by Modeling Local Transposon Insertion Frequencies Improves Discrimination of Essential Genes. IEEE/ACM Trans Comput Biol Bioinform *12*, 92-102.

DeJesus, M.A., Zhang, Y.J., Sassetti, C.M., Rubin, E.J., Sacchettini, J.C., and Ioerger, T.R. (2013). Bayesian analysis of gene essentiality based on sequencing of transposon insertion libraries. Bioinformatics *29*, 695-703.

Diacon, A.H., Donald, P.R., Pym, A., Grobusch, M., Patientia, R.F., Mahanyele, R., Bantubani, N., Narasimooloo, R., De Marez, T., van Heeswijk, R.*, et al.* (2012). Randomized pilot trial of eight weeks of bedaquiline (TMC207) treatment for multidrug-resistant tuberculosis: long-term outcome, tolerability, and effect on emergence of drug resistance. Antimicrob Agents Chemother *56*, 3271-3276.

Dixon, S.J., Costanzo, M., Baryshnikova, A., Andrews, B., and Boone, C. (2009). Systematic mapping of genetic interaction networks. Annu Rev Genet *43*, 601-625.

Domenech, P., Reed, M.B., and Barry, C.E., 3rd (2005). Contribution of the Mycobacterium tuberculosis MmpL protein family to virulence and drug resistance. Infect Immun *73*, 3492-3501.

Dorr, T., Delgado, F., Umans, B.D., Gerding, M.A., Davis, B.M., and Waldor, M.K. (2016). A Transposon Screen Identifies Genetic Determinants of Vibrio cholerae Resistance to High-Molecular-Weight Antibiotics. Antimicrob Agents Chemother *60*, 4757-4763.

Doster, B., Murray, F.J., Newman, R., and Woolpert, S.F. (1973). Ethambutol in the initial treatment of pulmonary tuberculosis. U.S. Public Health Service tuberculosis therapy trials. Am Rev Respir Dis *107*, 177-190.

du Preez, I., and Loots, D. (2012). Altered Fatty Acid Metabolism Due to Rifampicin-Resistance Conferring Mutations in the rpoB Gene of Mycobacterium tuberculosis: Mapping the Potential of Pharmaco-metabolomics for Global Health and Personalized Medicine. Omics *16*, 596-603.

Dutta, N.K., Bandyopadhyay, N., Veeramani, B., Lamichhane, G., Karakousis, P.C., and Bader, J.S. (2014). Systems biology-based identification of Mycobacterium tuberculosis persistence genes in mouse lungs. MBio *5*.

Ehlers, S., and Schaible, U.E. (2012). The granuloma in tuberculosis: dynamics of a host-pathogen collusion. Front Immunol *3*, 411.

Ehrt, S., and Schnappinger, D. (2009). Mycobacterial survival strategies in the phagosome: defence against host stresses. Cell Microbiol *11*, 1170-1178.

Ernst, J.D. (2012). The immunological life cycle of tuberculosis. Nat Rev Immunol *12*, 581-591.

Escribano, I., Rodriguez, J.C., Llorca, B., Garcia-Pachon, E., Ruiz, M., and Royo, G. (2007). Importance of the efflux pump systems in the resistance of Mycobacterium tuberculosis to fluoroquinolones and linezolid. Chemotherapy *53*, 397-401.

Etienne, G., Villeneuve, C., Billman-Jacobe, H., Astarie-Dequeker, C., Dupont, M.A., and Daffe, M. (2002). The impact of the absence of glycopeptidolipids on the ultrastructure, cell surface and cell wall properties, and phagocytosis of Mycobacterium smegmatis. Microbiology *148*, 3089-3100.

Flores, A.R., Parsons, L.M., and Pavelka, M.S., Jr. (2005). Characterization of novel Mycobacterium tuberculosis and Mycobacterium smegmatis mutants hypersusceptible to beta-lactam antibiotics. J Bacteriol *187*, 1892-1900.

Ford, C.B., Shah, R.R., Maeda, M.K., Gagneux, S., Murray, M.B., Cohen, T., Johnston, J.C., Gardy, J., Lipsitch, M., and Fortune, S.M. (2013). Mycobacterium tuberculosis mutation rate estimates from different lineages predict substantial differences in the emergence of drug-resistant tuberculosis. Nat Genet *45*, 784-790.

Gagneux, S., Long, C.D., Small, P.M., Van, T., Schoolnik, G.K., and Bohannan, B.J. (2006). The competitive cost of antibiotic resistance in Mycobacterium tuberculosis. Science *312*, 1944-1946.

Ganapathy, U., Marrero, J., Calhoun, S., Eoh, H., de Carvalho, L.P., Rhee, K., and Ehrt, S. (2015). Two enzymes with redundant fructose bisphosphatase activity sustain gluconeogenesis and virulence in Mycobacterium tuberculosis. Nat Commun *6*, 7912.

Gao, L.Y., Laval, F., Lawson, E.H., Groger, R.K., Woodruff, A., Morisaki, J.H., Cox, J.S., Daffe, M., and Brown, E.J. (2003). Requirement for kasB in Mycobacterium mycolic acid biosynthesis, cell wall impermeability and intracellular survival: implications for therapy. Mol Microbiol *49*, 1547-1563.

Gaur, R.L., Ren, K., Blumenthal, A., Bhamidi, S., Gonzalez-Nilo, F.D., Jackson, M., Zare, R.N., Ehrt, S., Ernst, J.D., and Banaei, N. (2014). LprG-mediated surface expression of lipoarabinomannan is essential for virulence of Mycobacterium tuberculosis. PLoS Pathog *10*, e1004376.

Gengenbacher, M., Rao, S.P., Pethe, K., and Dick, T. (2010). Nutrient-starved, non-replicating Mycobacterium tuberculosis requires respiration, ATP synthase and isocitrate lyase for maintenance of ATP homeostasis and viability. Microbiology *156*, 81-87.

Girgis, H.S., Harris, K., and Tavazoie, S. (2012). Large mutational target size for rapid emergence of bacterial persistence. Proc Natl Acad Sci U S A *109*, 12740-12745.

Girgis, H.S., Hottes, A.K., and Tavazoie, S. (2009). Genetic architecture of intrinsic antibiotic susceptibility. PLoS One *4*, e5629.

Gold, B., Warrier, T., and Nathan, C. (2015). A multi-stress model for high throughput screening against non-replicating Mycobacterium tuberculosis. Methods Mol Biol *1285*, 293-315.

Gonzalo-Asensio, J., Mostowy, S., Harders-Westerveen, J., Huygen, K., Hernandez-Pando, R., Thole, J., Behr, M., Gicquel, B., and Martin, C. (2008). PhoP: a missing piece in the intricate puzzle of Mycobacterium tuberculosis virulence. PLoS One *3*, e3496.

Goodsmith, N., Guo, X.V., Vandal, O.H., Vaubourgeix, J., Wang, R., Botella, H., Song, S., Bhatt, K., Liba, A., Salgame, P.*, et al.* (2015). Disruption of an M. tuberculosis membrane protein causes a magnesium-dependent cell division defect and failure to persist in mice. PLoS Pathog *11*, e1004645.

Goren, M.B., D'Arcy Hart, P., Young, M.R., and Armstrong, J.A. (1976). Prevention of phagosome-lysosome fusion in cultured macrophages by sulfatides of Mycobacterium tuberculosis. Proc Natl Acad Sci U S A *73*, 2510-2514.

Griffin, J.E., Gawronski, J.D., Dejesus, M.A., Ioerger, T.R., Akerley, B.J., and Sassetti, C.M. (2011). High-resolution phenotypic profiling defines genes essential for mycobacterial growth and cholesterol catabolism. PLoS Pathog *7*, e1002251.

Grzegorzewicz, A.E., de Sousa-d'Auria, C., McNeil, M.R., Huc-Claustre, E., Jones, V., Petit, C., Angala, S.K., Zemanova, J., Wang, Q., Belardinelli, J.M.*, et al.* (2016). Assembling of the Mycobacterium tuberculosis Cell Wall Core. J Biol Chem *291*, 18867-18879.

Harrison, J., Lloyd, G., Joe, M., Lowary, T.L., Reynolds, E., Walters-Morgan, H., Bhatt, A., Lovering, A., Besra, G.S., and Alderwick, L.J. (2016). Lcp1 Is a Phosphotransferase Responsible for Ligating Arabinogalactan to Peptidoglycan in Mycobacterium tuberculosis. MBio *7*.

Hartkoorn, R.C., Chandler, B., Owen, A., Ward, S.A., Bertel Squire, S., Back, D.J., and Khoo, S.H. (2007). Differential drug susceptibility of intracellular and extracellular tuberculosis, and the impact of P-glycoprotein. Tuberculosis (Edinb) *87*, 248-255.

Hazbon, M.H., Brimacombe, M., Bobadilla del Valle, M., Cavatore, M., Guerrero, M.I., Varma-Basil, M., Billman-Jacobe, H., Lavender, C., Fyfe, J., Garcia-Garcia, L.*, et al.* (2006). Population genetics study of isoniazid resistance mutations and evolution of multidrug-resistant Mycobacterium tuberculosis. Antimicrob Agents Chemother *50*, 2640-2649.

Heym, B., Zhang, Y., Poulet, S., Young, D., and Cole, S.T. (1993). Characterization of the Katg Gene Encoding a Catalase-Peroxidase Required for the Isoniazid Susceptibility of Mycobacterium-Tuberculosis. Journal of Bacteriology *175*, 4255-4259.

HKCS (1981). Controlled trial of four thrice-weekly regimens and a daily regimen all given for 6 months for pulmonary tuberculosis. Lancet *1*, 171-174.

Hoff, D.R., Ryan, G.J., Driver, E.R., Ssemakulu, C.C., De Groote, M.A., Basaraba, R.J., and Lenaerts, A.J. (2011). Location of intra- and extracellular M. tuberculosis populations in lungs of mice and guinea pigs during disease progression and after drug treatment. PLoS One *6*, e17550.

Hoffmann, C., Leis, A., Niederweis, M., Plitzko, J.M., and Engelhardt, H. (2008). Disclosure of the mycobacterial outer membrane: cryo-electron tomography and vitreous sections reveal the lipid bilayer structure. Proc Natl Acad Sci U S A *105*, 3963-3967.

Huynh, K.K., and Grinstein, S. (2007). Regulation of vacuolar pH and its modulation by some microbial species. Microbiol Mol Biol Rev *71*, 452-462.

Jackson, M. (2014). The mycobacterial cell envelope-lipids. Cold Spring Harb Perspect Med *4*.

Jamieson, S.R. (1950). Combined streptomycin-para-aminosalicylic acid treatment of pulmonary tuberculosis. Tubercle *31*, 155-156.

Jarlier, V., and Nikaido, H. (1990). Permeability barrier to hydrophilic solutes in Mycobacterium chelonei. J Bacteriol *172*, 1418-1423.

Jarlier, V., and Nikaido, H. (1994). Mycobacterial cell wall: structure and role in natural resistance to antibiotics. FEMS Microbiol Lett *123*, 11-18.

Jones, W.M., Soper, T.S., Ueno, H., and Manning, J.M. (1985). D-Glutamate-D-amino acid transaminase from bacteria. Methods Enzymol *113*, 108-113.

Kang, D.D., Lin, Y.Y., Moreno, J.R., Randall, T.D., and Khader, S.A. (2011). Profiling Early Lung Immune Responses in the Mouse Model of Tuberculosis. Plos One *6*.

Kaur, D., Guerin, M.E., Skovierova, H., Brennan, P.J., and Jackson, M. (2009). Chapter 2: Biogenesis of the cell wall and other glycoconjugates of Mycobacterium tuberculosis. Adv Appl Microbiol *69*, 23-78.

Kaushik, A., Makkar, N., Pandey, P., Parrish, N., Singh, U., and Lamichhane, G. (2015). Carbapenems and Rifampin Exhibit Synergy against Mycobacterium tuberculosis and Mycobacterium abscessus. Antimicrob Agents Chemother *59*, 6561-6567.

Keren, I., Minami, S., Rubin, E., and Lewis, K. (2011). Characterization and transcriptome analysis of Mycobacterium tuberculosis persisters. MBio *2*, e00100-00111.

Keshavjee, S., and Farmer, P.E. (2012). Tuberculosis, drug resistance, and the history of modern medicine. N Engl J Med *367*, 931-936.

Kieser, K.J., Baranowski, C., Chao, M.C., Long, J.E., Sassetti, C.M., Waldor, M.K., Sacchettini, J.C., Ioerger, T.R., and Rubin, E.J. (2015). Peptidoglycan synthesis in Mycobacterium tuberculosis is organized into networks with varying drug susceptibility. Proc Natl Acad Sci U S A *112*, 13087-13092.

Kim, J.H., O'Brien, K.M., Sharma, R., Boshoff, H.I.M., Rehren, G., Chakraborty, S., Wallach, J.B., Monteleone, M., Wilson, D.J., Aldrich, C.C.*, et al.* (2013). A genetic strategy to identify targets for the development of drugs that prevent bacterial persistence. P Natl Acad Sci USA *110*, 19095-19100.

Kislitsyna, N.A., and Kotova, N.I. (1980). [Rifampicin and isoniazid concentration in the blood and resected lungs in tuberculosis with combined use of the preparations]. Probl Tuberk, 63-65.

Kjellsson, M.C., Via, L.E., Goh, A., Weiner, D., Low, K.M., Kern, S., Pillai, G., Barry, C.E., and Dartois, V. (2012). Pharmacokinetic Evaluation of the Penetration of Antituberculosis Agents in Rabbit Pulmonary Lesions. Antimicrobial Agents and Chemotherapy *56*, 446-457.

Koch, R. (1952). [Tuberculosis etiology]. Dtsch Gesundheitsw *7*, 457-465.

Kohanski, M.A., Dwyer, D.J., Hayete, B., Lawrence, C.A., and Collins, J.J. (2007). A common mechanism of cellular death induced by bactericidal antibiotics. Cell *130*, 797-810.

Konno, K., Feldmann, F.M., and Mcdermott, W. (1967). Pyrazinamide Susceptibility and Amidase Activity of Tubercle Bacilli. American Review of Respiratory Disease *95*, 461-+.

Kumar, P., Arora, K., Lloyd, J.R., Lee, I.Y., Nair, V., Fischer, E., Boshoff, H.I., and Barry, C.E., 3rd (2012). Meropenem inhibits D,D-carboxypeptidase activity in Mycobacterium tuberculosis. Mol Microbiol *86*, 367-381.

Lahiri, N., Shah, R.R., Layre, E., Young, D., Ford, C., Murray, M.B., Fortune, S.M., and Moody, D.B. (2016). Rifampin Resistance Mutations Are Associated with Broad Chemical Remodeling of Mycobacterium tuberculosis. J Biol Chem *291*, 14248-14256.

Lehmann, J. (1964). Twenty Years Afterward Historical Notes on the Discovery of the Antituberculosis Effect of Paraaminosalicylic Acid (Pas) and the First Clinical Trials. Am Rev Respir Dis *90*, 953-956.

Lenaerts, A., Barry, C.E., 3rd, and Dartois, V. (2015). Heterogeneity in tuberculosis pathology, microenvironments and therapeutic responses. Immunol Rev *264*, 288-307.

Lenaerts, A.J., Hoff, D., Aly, S., Ehlers, S., Andries, K., Cantarero, L., Orme, I.M., and Basaraba, R.J. (2007). Location of persisting mycobacteria in a Guinea pig model of tuberculosis revealed by r207910. Antimicrob Agents Chemother *51*, 3338-3345.

Levin, B.R., and Rozen, D.E. (2006). Non-inherited antibiotic resistance. Nat Rev Microbiol *4*, 556-562.

Levitte, S., Adams, K.N., Berg, R.D., Cosma, C.L., Urdahl, K.B., and Ramakrishnan, L. (2016). Mycobacterial Acid Tolerance Enables Phagolysosomal Survival and Establishment of Tuberculous Infection In Vivo. Cell Host Microbe *20*, 250-258.

Li, X.Z., Zhang, L., and Nikaido, H. (2004). Efflux pump-mediated intrinsic drug resistance in Mycobacterium smegmatis. Antimicrob Agents Chemother *48*, 2415-2423.

Lin, K., O'Brien, K.M., Trujillo, C., Wang, R.J., Wallach, J.B., Schnappinger, D., and Ehrt, S. (2016). Mycobacterium tuberculosis Thioredoxin Reductase Is Essential for Thiol Redox Homeostasis but Plays a Minor Role in Antioxidant Defense. Plos Pathogens *12*.

Lin, P.L., Coleman, T., Carney, J.P., Lopresti, B.J., Tomko, J., Fillmore, D., Dartois, V., Scanga, C., Frye, L.J., Janssen, C*., et al.* (2013). Radiologic responses in cynomolgous macaques for assessing tuberculosis chemotherapy regimens. Antimicrob Agents Chemother.

Lin, P.L., Ford, C.B., Coleman, M.T., Myers, A.J., Gawande, R., Ioerger, T., Sacchettini, J., Fortune, S.M., and Flynn, J.L. (2014). Sterilization of granulomas is common in active and latent tuberculosis despite within-host variability in bacterial killing. Nature Medicine *20*, 75-+.

Liu, J., Barry, C.E., 3rd, Besra, G.S., and Nikaido, H. (1996a). Mycolic acid structure determines the fluidity of the mycobacterial cell wall. J Biol Chem *271*, 29545-29551.

Liu, J., and Nikaido, H. (1999). A mutant of Mycobacterium smegmatis defective in the biosynthesis of mycolic acids accumulates meromycolates. Proc Natl Acad Sci U S A *96*, 4011-4016.

Liu, J., Takiff, H.E., and Nikaido, H. (1996b). Active efflux of fluoroquinolones in Mycobacterium smegmatis mediated by LfrA, a multidrug efflux pump. J Bacteriol *178*, 3791-3795.

Long, J.E., DeJesus, M., Ward, D., Baker, R.E., Ioerger, T., and Sassetti, C.M. (2015). Identifying essential genes in Mycobacterium tuberculosis by global phenotypic profiling. Methods Mol Biol *1279*, 79-95.

Louw, G.E., Warren, R.M., Gey van Pittius, N.C., Leon, R., Jimenez, A., Hernandez-Pando, R., McEvoy, C.R., Grobbelaar, M., Murray, M., van Helden, P.D*., et al.* (2011). Rifampicin reduces susceptibility to ofloxacin in rifampicin-resistant Mycobacterium tuberculosis through efflux. Am J Respir Crit Care Med *184*, 269-276.

Louw, G.E., Warren, R.M., Gey van Pittius, N.C., McEvoy, C.R., Van Helden, P.D., and Victor, T.C. (2009). A balancing act: efflux/influx in mycobacterial drug resistance. Antimicrob Agents Chemother *53*, 3181-3189.

Lun, S., Miranda, D., Kubler, A., Guo, H., Maiga, M.C., Winglee, K., Pelly, S., and Bishai, W.R. (2014). Synthetic lethality reveals mechanisms of Mycobacterium tuberculosis resistance to beta-lactams. MBio *5*, e01767-01714.

Lun, S.C., and Bishai, W.R. (2007). Characterization of a novel cell wall-anchored protein with carboxylesterase activity required for virulence in Mycobacterium tuberculosis. Journal of Biological Chemistry *282*, 18348-18356.

MacMicking, J.D., Taylor, G.A., and McKinney, J.D. (2003). Immune control of tuberculosis by IFN-gamma-inducible LRG-47. Science *302*, 654-659.

Madigan, C.A., Martinot, A.J., Wei, J.R., Madduri, A., Cheng, T.Y., Young, D.C., Layre, E., Murry, J.P., Rubin, E.J., and Moody, D.B. (2015). Lipidomic analysis links mycobactin synthase K to iron uptake and virulence in M. tuberculosis. PLoS Pathog *11*, e1004792.

Madsen, C.T., Jakobsen, L., Buriankova, K., Doucet-Populaire, F., Pernodet, J.L., and Douthwaite, S. (2005). Methyltransferase Erm(37) slips on rRNA to confer atypical resistance in Mycobacterium tuberculosis. J Biol Chem *280*, 38942-38947.

Magnani, G., Lomazzi, M., and Peracchi, A. (2013). Completing the folate biosynthesis pathway in Plasmodium falciparum: p-aminobenzoate is produced by a highly divergent promiscuous aminodeoxychorismate lyase. Biochem J *455*, 149-155.

Makinoshima, H., and Glickman, M.S. (2005). Regulation of Mycobacterium tuberculosis cell envelope composition and virulence by intramembrane proteolysis. Nature *436*, 406-409.

Mani, R., St Onge, R.P., Hartman, J.L.t., Giaever, G., and Roth, F.P. (2008). Defining genetic interaction. Proc Natl Acad Sci U S A *105*, 3461-3466.

Marrero, J., Rhee, K.Y., Schnappinger, D., Pethe, K., and Ehrt, S. (2010). Gluconeogenic carbon flow of tricarboxylic acid cycle intermediates is critical for Mycobacterium tuberculosis to establish and maintain infection. Proc Natl Acad Sci U S A *107*, 9819-9824.

Martinot, A.J., Farrow, M., Bai, L., Layre, E., Cheng, T.Y., Tsai, J.H., Iqbal, J., Annand, J.W., Sullivan, Z.A., Hussain, M.M.*, et al.* (2016). Mycobacterial Metabolic Syndrome: LprG and Rv1410 Regulate Triacylglyceride Levels, Growth Rate and Virulence in Mycobacterium tuberculosis. PLoS Pathog *12*, e1005351.

McDermott, W. (1969). The story of INH. J Infect Dis *119*, 678-683.

Merker, M., Blin, C., Mona, S., Duforet-Frebourg, N., Lecher, S., Willery, E., Blum, M.G., Rusch-Gerdes, S., Mokrousov, I., Aleksic, E.*, et al.* (2015). Evolutionary history and global spread of the Mycobacterium tuberculosis Beijing lineage. Nat Genet *47*, 242-249.

Miesel, L., Weisbrod, T.R., Marcinkeviciene, J.A., Bittman, R., and Jacobs, W.R. (1998). NADH dehydrogenase defects confer isoniazid resistance and conditional lethality in Mycobacterium smegmatis. Journal of Bacteriology *180*, 2459-2467.

Morlock, G.P., Metchock, B., Sikes, D., Crawford, J.T., and Cooksey, R.C. (2003). ethA, inhA, and katG loci of ethionamide-resistant clinical Mycobacterium tuberculosis isolates. Antimicrob Agents Chemother *47*, 3799-3805.

Morris, R.P., Nguyen, L., Gatfield, J., Visconti, K., Nguyen, K., Schnappinger, D., Ehrt, S., Liu, Y., Heifets, L., Pieters, J.*, et al.* (2005). Ancestral antibiotic resistance in Mycobacterium tuberculosis. Proc Natl Acad Sci U S A *102*, 12200-12205.

Murphy, K.C., Papavinasasundaram, K., and Sassetti, C.M. (2015). Mycobacterial recombineering. Methods Mol Biol *1285*, 177-199.

Nambi, S., Long, J.E., Mishra, B.B., Baker, R., Murphy, K.C., Olive, A.J., Nguyen, H.P., Shaffer, S.A., and Sassetti, C.M. (2015). The Oxidative Stress Network of Mycobacterium tuberculosis Reveals Coordination between Radical Detoxification Systems. Cell Host Microbe *17*, 829-837.

Nathan, C. (2012). Fresh approaches to anti-infective therapies. Sci Transl Med *4*, 140sr142.

Nathan, C., and Barry, C.E., 3rd (2015). TB drug development: immunology at the table. Immunol Rev *264*, 308-318.

Neihardt, F.C., Parker, J., and McKeever, W.G. (1975). Function and regulation of aminoacyl-tRNA synthetases in prokaryotic and eukaryotic cells. Annu Rev Microbiol *29*, 215-250.

Nguyen, L. (2016). Antibiotic resistance mechanisms in M. tuberculosis: an update. Arch Toxicol *90*, 1585-1604.

Nguyen, L., Chinnapapagari, S., and Thompson, C.J. (2005). FbpA-dependent biosynthesis of trehalose dimycolate is required for the intrinsic multidrug resistance, cell wall structure, and colonial morphology of Mycobacterium smegmatis. Journal of Bacteriology *187*, 6603-6611.

Nguyen, L., and Pieters, J. (2009). Mycobacterial subversion of chemotherapeutic reagents and host defense tactics: challenges in tuberculosis drug development. Annu Rev Pharmacol Toxicol *49*, 427-453.

Niederweis, M., Ehrt, S., Heinz, C., Klocker, U., Karosi, S., Swiderek, K.M., Riley, L.W., and Benz, R. (1999). Cloning of the mspA gene encoding a porin from Mycobacterium smegmatis. Mol Microbiol *33*, 933-945.

Nikaido, H. (2003). Molecular basis of bacterial outer membrane permeability revisited. Microbiol Mol Biol Rev *67*, 593-656.

O'Sullivan, D.M., McHugh, T.D., and Gillespie, S.H. (2005). Analysis of rpoB and pncA mutations in the published literature: an insight into the role of oxidative stress in Mycobacterium tuberculosis evolution? J Antimicrob Chemother *55*, 674-679.

Ohkuma, S., and Poole, B. (1978). Fluorescence probe measurement of the intralysosomal pH in living cells and the perturbation of pH by various agents. Proc Natl Acad Sci U S A *75*, 3327-3331.

Orme, I.M. (2014). A new unifying theory of the pathogenesis of tuberculosis. Tuberculosis (Edinb) *94*, 8-14.

Owens, C.P., Chim, N., Graves, A.B., Harmston, C.A., Iniguez, A., Contreras, H., Liptak, M.D., and Goulding, C.W. (2013). The Mycobacterium tuberculosis secreted protein Rv0203 transfers heme to membrane proteins MmpL3 and MmpL11. J Biol Chem *288*, 21714-21728.

Pages, J.M., James, C.E., and Winterhalter, M. (2008). The porin and the permeating antibiotic: a selective diffusion barrier in Gram-negative bacteria. Nat Rev Microbiol *6*, 893-903.

Pandey, S., Sharma, A., Tripathi, D., Kumar, A., Khubaib, M., Bhuwan, M., Chaudhuri, T.K., Hasnain, S.E., and Ehtesham, N.Z. (2016). Mycobacterium tuberculosis Peptidyl-Prolyl Isomerases Also Exhibit Chaperone like Activity In-Vitro and In-Vivo. PLoS One *11*, e0150288.

Pasca, M.R., Guglierame, P., Arcesi, F., Bellinzoni, M., De Rossi, E., and Riccardi, G. (2004). Rv2686c-Rv2687c-Rv2688c, an ABC fluoroquinolone efflux pump in Mycobacterium tuberculosis. Antimicrob Agents Chemother *48*, 3175-3178.

Percudani, R., and Peracchi, A. (2003). A genomic overview of pyridoxal-phosphate-dependent enzymes. EMBO Rep *4*, 850-854.

Peters, J.M., Colavin, A., Shi, H.D., Czarny, T.L., Larson, M.H., Wong, S., Hawkins, J.S., Lu, C.H.S., Koo, B.M., Marta, E.*, et al.* (2016). A Comprehensive, CRISPR-based Functional Analysis of Essential Genes in Bacteria. Cell *165*, 1493-1506.

Piddock, L.J., Williams, K.J., and Ricci, V. (2000). Accumulation of rifampicin by Mycobacterium aurum, Mycobacterium smegmatis and Mycobacterium tuberculosis. J Antimicrob Chemother *45*, 159-165.

Prideaux, B., Via, L.E., Zimmerman, M.D., Eum, S., Sarathy, J., O'Brien, P., Chen, C., Kaya, F., Weiner, D.M., Chen, P.Y.*, et al.* (2015). The association between sterilizing activity and drug distribution into tuberculosis lesions. Nat Med *21*, 1223-1227.

Pritchard, J.R., Chao, M.C., Abel, S., Davis, B.M., Baranowski, C., Zhang, Y.J., Rubin, E.J., and Waldor, M.K. (2014). ARTIST: high-resolution genome-wide assessment of fitness using transposon-insertion sequencing. PLoS Genet *10*, e1004782.

Protopopova, M., Bogatcheva, E., Nikonenko, B., Hundert, S., Einck, L., and Nacy, C.A. (2007). In search of new cures for tuberculosis. Med Chem *3*, 301-316.

Pule, C.M., Sampson, S.L., Warren, R.M., Black, P.A., van Helden, P.D., Victor, T.C., and Louw, G.E. (2016). Efflux pump inhibitors: targeting mycobacterial efflux systems to enhance TB therapy. J Antimicrob Chemother *71*, 17-26.

Radkov, A.D., and Moe, L.A. (2014). Bacterial synthesis of D-amino acids. Appl Microbiol Biotechnol *98*, 5363-5374.

Ramakrishnan, P., Aagesen, A.M., McKinney, J.D., and Tischler, A.D. (2016). Mycobacterium tuberculosis Resists Stress by Regulating PE19 Expression. Infect Immun *84*, 735-746.

Ramaswamy, S.V., Reich, R., Dou, S.J., Jasperse, L., Pan, X., Wanger, A., Quitugua, T., and Graviss, E.A. (2003). Single nucleotide polymorphisms in genes associated with isoniazid resistance in Mycobacterium tuberculosis. Antimicrob Agents Chemother *47*, 1241-1250.

Rana, A., Rub, A., and Akhter, Y. (2014). Proteome-scale identification of outer membrane proteins in Mycobacterium avium subspecies paratuberculosis using a structure based combined hierarchical approach. Mol Biosyst *10*, 2329-2337.

Rengarajan, J., Murphy, E., Park, A., Krone, C.L., Hett, E.C., Bloom, B.R., Glimcher, L.H., and Rubin, E.J. (2008). Mycobacterium tuberculosis Rv2224c modulates innate immune responses. P Natl Acad Sci USA *105*, 264-269.

Restrepo, B.I., and Schlesinger, L.S. (2014). Impact of diabetes on the natural history of tuberculosis. Diabetes Res Clin Pract *106*, 191-199.

Ribeiro-Guimaraes, M.L., and Pessolani, M.C. (2007). Comparative genomics of mycobacterial proteases. Microb Pathog *43*, 173-178.

Riley, R.L. (1957). Aerial dissemination of pulmonary tuberculosis. Am Rev Tuberc *76*, 931-941.

Riva, M.A. (2014). From milk to rifampicin and back again: history of failures and successes in the treatment for tuberculosis. J Antibiot (Tokyo) *67*, 661-665.

Rodrigues, L., Viveiros, M., and Ainsa, J.A. (2015). Measuring efflux and permeability in mycobacteria. Methods Mol Biol *1285*, 227-239.

Rosenberg, M., Gutnick, D., and Rosenberg, E. (1980). Adherence of Bacteria to Hydrocarbons - a Simple Method for Measuring Cell-Surface Hydrophobicity. Fems Microbiology Letters *9*, 29-33.

Ruggiero, A., Marasco, D., Squeglia, F., Soldini, S., Pedone, E., Pedone, C., and Berisio, R. (2010). Structure and functional regulation of RipA, a mycobacterial enzyme essential for daughter cell separation. Structure *18*, 1184-1190.

Russell, D.G., Barry, C.E., and Flynn, J.L. (2010). Tuberculosis: What We Don't Know Can, and Does, Hurt Us. Science *328*, 852-856.

Sala, C., Dhar, N., Hartkoorn, R.C., Zhang, M., Ha, Y.H., Schneider, P., and Cole, S.T. (2010). Simple model for testing drugs against nonreplicating Mycobacterium tuberculosis. Antimicrob Agents Chemother *54*, 4150-4158.

Saldanha, A.J. (2004). Java Treeview--extensible visualization of microarray data. Bioinformatics *20*, 3246-3248.

Sander, P., De Rossi, E., Boddinghaus, B., Cantoni, R., Branzoni, M., Bottger, E.C., Takiff, H., Rodriquez, R., Lopez, G., and Riccardi, G. (2000). Contribution of the multidrug efflux pump LfrA to innate mycobacterial drug resistance. FEMS Microbiol Lett *193*, 19-23.

Sander, P., Springer, B., Prammananan, T., Sturmfels, A., Kappler, M., Pletschette, M., and Bottger, E.C. (2002). Fitness cost of chromosomal drug resistance-conferring mutations. Antimicrob Agents Chemother *46*, 1204-1211.

Sani, M., Houben, E.N., Geurtsen, J., Pierson, J., de Punder, K., van Zon, M., Wever, B., Piersma, S.R., Jimenez, C.R., Daffe, M.*, et al.* (2010). Direct visualization by cryo-EM of the mycobacterial capsular layer: a labile structure containing ESX-1-secreted proteins. PLoS Pathog *6*, e1000794.

Sarathy, J., Dartois, V., Dick, T., and Gengenbacher, M. (2013). Reduced Drug Uptake in Phenotypically Resistant Nutrient-Starved Nonreplicating Mycobacterium tuberculosis. Antimicrobial Agents and Chemotherapy *57*, 1648-1653.

Sarathy, J.P., Dartois, V., and Lee, E.J. (2012). The role of transport mechanisms in mycobacterium tuberculosis drug resistance and tolerance. Pharmaceuticals (Basel) *5*, 1210-1235.

Sassetti, C.M., Boyd, D.H., and Rubin, E.J. (2001). Comprehensive identification of conditionally essential genes in mycobacteria. Proc Natl Acad Sci U S A *98*, 12712-12717.

Sassetti, C.M., Boyd, D.H., and Rubin, E.J. (2003). Genes required for mycobacterial growth defined by high density mutagenesis. Mol Microbiol *48*, 77-84.

Schatz, A., Bugie, E., and Waksman, S.A. (1944). Streptomycin, a substance exhibiting antibiotic activity against gram positive and gram-negative bacteria. P Soc Exp Biol Med *55*, 66-69.

Schnappinger, D., Ehrt, S., Voskuil, M.I., Liu, Y., Mangan, J.A., Monahan, I.M., Dolganov, G., Efron, B., Butcher, P.D., Nathan, C*., et al.* (2003). Transcriptional Adaptation of Mycobacterium tuberculosis within Macrophages: Insights into the Phagosomal Environment. J Exp Med *198*, 693-704.

Schneider, J.S., Sklar, J.G., and Glickman, M.S. (2014). The Rip1 Protease of Mycobacterium tuberculosis Controls the SigD Regulon. Journal of Bacteriology *196*, 2638-2645.

Scorpio, A., and Zhang, Y. (1996). Mutations in pncA, a gene encoding pyrazinamidase/nicotinamidase, cause resistance to the antituberculous drug pyrazinamide in tubercle bacillus. Nature Medicine *2*, 662-667.

Segura, C., Salvado, M., Collado, I., Chaves, J., and Coira, A. (1998). Contribution of beta-lactamases to beta-lactam susceptibilities of susceptible and multidrug-resistant Mycobacterium tuberculosis clinical isolates. Antimicrob Agents Chemother *42*, 1524-1526.

Senaratne, R.H., Mobasheri, H., Papavinasasundaram, K.G., Jenner, P., Lea, E.J., and Draper, P. (1998). Expression of a gene for a porin-like protein of the OmpA family from Mycobacterium tuberculosis H37Rv. J Bacteriol *180*, 3541-3547.

Sensi, P. (1983). History of the development of rifampin. Rev Infect Dis *5 Suppl 3*, S402-406.

Singh, A., Jain, S., Gupta, S., Das, T., and Tyagi, A.K. (2003). mymA operon of Mycobacterium tuberculosis: its regulation and importance in the cell envelope. FEMS Microbiol Lett *227*, 53-63.

Singh, A.K., Carette, X., Potluri, L.P., Sharp, J.D., Xu, R., Prisic, S., and Husson, R.N. (2016). Investigating essential gene function in Mycobacterium tuberculosis using an efficient CRISPR interference system. Nucleic Acids Res.

Siroy, A., Mailaender, C., Harder, D., Koerber, S., Wolschendorf, F., Danilchanka, O., Wang, Y., Heinz, C., and Niederweis, M. (2008). Rv1698 of Mycobacterium

tuberculosis represents a new class of channel-forming outer membrane proteins. Journal of Biological Chemistry *283*, 17827-17837.

Small, J.L., O'Donoghue, A.J., Boritsch, E.C., Tsodikov, O.V., Knudsen, G.M., Vandal, O., Craik, C.S., and Ehrt, S. (2013). Substrate specificity of MarP, a periplasmic protease required for resistance to acid and oxidative stress in Mycobacterium tuberculosis. J Biol Chem *288*, 12489-12499.

Song, H., Huff, J., Janik, K., Walter, K., Keller, C., Ehlers, S., Bossmann, S.H., and Niederweis, M. (2011). Expression of the ompATb operon accelerates ammonia secretion and adaptation of Mycobacterium tuberculosis to acidic environments. Mol Microbiol *80*, 900-918.

Song, H., Sandie, R., Wang, Y., Andrade-Navarro, M.A., and Niederweis, M. (2008). Identification of outer membrane proteins of Mycobacterium tuberculosis. Tuberculosis (Edinb) *88*, 526-544.

Sonnhammer, E.L., von Heijne, G., and Krogh, A. (1998). A hidden Markov model for predicting transmembrane helices in protein sequences. Proc Int Conf Intell Syst Mol Biol *6*, 175-182.

Soper, T.S., Jones, W.M., Lerner, B., Trop, M., and Manning, J.M. (1977). Inactivation of bacterial D-amino acid transaminase by beta-chloro-D-alanine. J Biol Chem *252*, 3170-3175.

Spivey, V.L., Whalan, R.H., Hirst, E.M., Smerdon, S.J., and Buxton, R.S. (2013). An attenuated mutant of the Rv1747 ATP-binding cassette transporter of Mycobacterium tuberculosis and a mutant of its cognate kinase, PknF, show increased expression of the efflux pump-related iniBAC operon. FEMS Microbiol Lett *347*, 107-115.

Stahl, C., Kubetzko, S., Kaps, I., Seeber, S., Engelhardt, H., and Niederweis, M. (2001). MspA provides the main hydrophilic pathway through the cell wall of Mycobacterium smegmatis. Molecular Microbiology *40*, 451-464.

Staudenmaier, H., Van Hove, B., Yaraghi, Z., and Braun, V. (1989). Nucleotide sequences of the fecBCDE genes and locations of the proteins suggest a periplasmic-binding-protein-dependent transport mechanism for iron(III) dicitrate in Escherichia coli. J Bacteriol *171*, 2626-2633.

Steiner, M., Chaves, A.D., Lyons, H.A., Steiner, P., and Portugaleza, C. (1970). Primary drug-resistant tuberculosis. Report of an outbreak. N Engl J Med *283*, 1353-1358.

Stephan, J., Mailaender, C., Etienne, G., Daffe, M., and Niederweis, M. (2004). Multidrug resistance of a porin deletion mutant of Mycobacterium smegmatis. Antimicrob Agents Chemother *48*, 4163-4170.

Stolz, M., Peters-Wendisch, P., Etterich, H., Gerharz, T., Faurie, R., Sahm, H., Fersterra, H., and Eggeling, L. (2007). Reduced folate supply as a key to enhanced L-

serine production by Corynebacterium glutamicum. Appl Environ Microbiol *73*, 750-755.

Sun, J., Siroy, A., Lokareddy, R.K., Speer, A., Doornbos, K.S., Cingolani, G., and Niederweis, M. (2015). The tuberculosis necrotizing toxin kills macrophages by hydrolyzing NAD. Nat Struct Mol Biol *22*, 672-678.

Tatusova, T., DiCuccio, M., Badretdin, A., Chetvernin, V., Nawrocki, E.P., Zaslavsky, L., Lomsadze, A., Pruitt, K.D., Borodovsky, M., and Ostell, J. (2016). NCBI prokaryotic genome annotation pipeline. Nucleic Acids Res *44*, 6614-6624.

Teriete, P., Yao, Y., Kolodzik, A., Yu, J., Song, H., Niederweis, M., and Marassi, F.M. (2010). Mycobacterium tuberculosis Rv0899 adopts a mixed alpha/beta-structure and does not form a transmembrane beta-barrel. Biochemistry-Us *49*, 2768-2777.

Tewari, Y.B., Jensen, P.Y., Kishore, N., Mayhew, M.P., Parsons, J.F., Eisenstein, E., and Goldberg, R.N. (2002). Thermodynamics of reactions catalyzed by PABA synthase. Biophys Chem *96*, 33-51.

Tiberi, S., Payen, M.C., Sotgiu, G., D'Ambrosio, L., Alarcon Guizado, V., Alffenaar, J.W., Abdo Arbex, M., Caminero, J.A., Centis, R., De Lorenzo, S.*, et al.* (2016). Effectiveness and safety of meropenem/clavulanate-containing regimens in the treatment of MDR- and XDR-TB. Eur Respir J *47*, 1235-1243.

Ting, H., Kouzminova, E.A., and Kuzminov, A. (2008). Synthetic lethality with the dut defect in Escherichia coli reveals layers of DNA damage of increasing complexity due to uracil incorporation. J Bacteriol *190*, 5841-5854.

Torrey, H.L., Keren, I., Via, L.E., Lee, J.S., and Lewis, K. (2016). High Persister Mutants in Mycobacterium tuberculosis. PLoS One *11*, e0155127.

Tullius, M.V., Harmston, C.A., Owens, C.P., Chim, N., Morse, R.P., McMath, L.M., Iniguez, A., Kimmey, J.M., Sawaya, M.R., Whitelegge, J.P.*, et al.* (2011). Discovery and characterization of a unique mycobacterial heme acquisition system. Proc Natl Acad Sci U S A *108*, 5051-5056.

Universiteit_Gent_Bioinformatics. Venn Diagrams.

van Opijnen, T., Bodi, K.L., and Camilli, A. (2009). Tn-seq: high-throughput parallel sequencing for fitness and genetic interaction studies in microorganisms. Nat Methods *6*, 767-772.

van Opijnen, T., and Camilli, A. (2013). Transposon insertion sequencing: a new tool for systems-level analysis of microorganisms. Nat Rev Microbiol *11*, 435-442.

van Opijnen, T., Lazinski, D.W., and Camilli, A. (2014). Genome-Wide Fitness and Genetic Interactions Determined by Tn-seq, a High-Throughput Massively Parallel Sequencing Method for Microorganisms. Curr Protoc Mol Biol *106*, 7 16 11-17 16 24.

Vandal, O.H., Pierini, L.M., Schnappinger, D., Nathan, C.F., and Ehrt, S. (2008). A membrane protein preserves intrabacterial pH in intraphagosomal Mycobacterium tuberculosis. Nature Medicine *14*, 849-854.

Vaubourgeix, J., Lin, G., Dhar, N., Chenouard, N., Jiang, X., Botella, H., Lupoli, T., Mariani, O., Yang, G., Ouerfelli, O.*, et al.* (2015). Stressed mycobacteria use the chaperone ClpB to sequester irreversibly oxidized proteins asymmetrically within and between cells. Cell Host Microbe *17*, 178-190.

Vetting, M., Roderick, S.L., Hegde, S., Magnet, S., and Blanchard, J.S. (2003). What can structure tell us about in vivo function? The case of aminoglycoside-resistance genes. Biochem Soc T *31*, 520-522.

Vilcheze, C., and Jacobs, W.R., Jr. (2007). The mechanism of isoniazid killing: clarity through the scope of genetics. Annu Rev Microbiol *61*, 35-50.

Vilcheze, C., Weisbrod, T.R., Chen, B., Kremer, L., Hazbon, M.H., Wang, F., Alland, D., Sacchettini, J.C., and Jacobs, W.R., Jr. (2005). Altered NADH/NAD+ ratio mediates coresistance to isoniazid and ethionamide in mycobacteria. Antimicrob Agents Chemother *49*, 708-720.

Villet, R., Fonvielle, M., Busca, P., Chemama, M., Maillard, A.P., Hugonnet, J.E., Dubost, L., Marie, A., Josseaume, N., Mesnage, S.*, et al.* (2007). Idiosyncratic features in tRNAs participating in bacterial cell wall synthesis. Nucleic Acids Res *35*, 6870-6883.

Viveiros, M., Martins, M., Rodrigues, L., Machado, D., Couto, I., Ainsa, J., and Amaral, L. (2012). Inhibitors of mycobacterial efflux pumps as potential boosters for anti-tubercular drugs. Expert Rev Anti Infect Ther *10*, 983-998.

Voladri, R.K., Lakey, D.L., Hennigan, S.H., Menzies, B.E., Edwards, K.M., and Kernodle, D.S. (1998). Recombinant expression and characterization of the major beta-lactamase of Mycobacterium tuberculosis. Antimicrob Agents Chemother *42*, 1375-1381.

Voskuil, M.I., Visconti, K.C., and Schoolnik, G.K. (2004). Mycobacterium tuberculosis gene expression during adaptation to stationary phase and low-oxygen dormancy. Tuberculosis (Edinb) *84*, 218-227.

Wakamoto, Y., Dhar, N., Chait, R., Schneider, K., Signorino-Gelo, F., Leibler, S., and McKinney, J.D. (2013). Dynamic Persistence of Antibiotic-Stressed Mycobacteria. Science *339*, 91-95.

Waksman, S.A. (1964). The conquest of tuberculosis (Berkeley,: University of California Press).

Wayne, L.G., and Hayes, L.G. (1996). An in vitro model for sequential study of shiftdown of Mycobacterium tuberculosis through two stages of nonreplicating persistence. Infect Immun *64*, 2062-2069.

Wayne, L.G., and Sramek, H.A. (1994). Metronidazole Is Bactericidal to Dormant Cells of Mycobacterium-Tuberculosis. Antimicrobial Agents and Chemotherapy *38*, 2054-2058.

White, M.J., Savaryn, J.P., Bretl, D.J., He, H., Penoske, R.M., Terhune, S.S., and Zahrt, T.C. (2011). The HtrA-like serine protease PepD interacts with and modulates the Mycobacterium tuberculosis 35-kDa antigen outer envelope protein. PLoS One *6*, e18175.

WHO (2010). In Treatment of Tuberculosis: Guidelines (Geneva).

WHO (2015). Global Tuberculosis Report 2015.

Wilson, L.G. (2005). Commentary: Medicine, population, and tuberculosis. Int J Epidemiol *34*, 521-524.

Wolf, A.J., Linas, B., Trevejo-Nunez, G.J., Kincaid, E., Tamura, T., Takatsu, K., and Ernst, J.D. (2007). Mycobacterium tuberculosis infects dendritic cells with high frequency and impairs their function in vivo. Journal of Immunology *179*, 2509-2519.

Wolff, K.A., Nguyen, H.T., Cartabuke, R.H., Singh, A., Ogwang, S., and Nguyen, L. (2009). Protein kinase G is required for intrinsic antibiotic resistance in mycobacteria. Antimicrob Agents Chemother *53*, 3515-3519.

Wolff, K.A., and Nguyen, L. (2012). Strategies for potentiation of ethionamide and folate antagonists against Mycobacterium tuberculosis. Expert Rev Anti Infect Ther *10*, 971-981.

Wolschendorf, F., Ackart, D., Shrestha, T.B., Hascall-Dove, L., Nolan, S., Lamichhane, G., Wang, Y., Bossmann, S.H., Basaraba, R.J., and Niederweis, M. (2011). Copper resistance is essential for virulence of Mycobacterium tuberculosis. P Natl Acad Sci USA *108*, 1621-1626.

Xu, X., Vilcheze, C., Av-Gay, Y., Gomez-Velasco, A., and Jacobs, W.R., Jr. (2011). Precise null deletion mutations of the mycothiol synthesis genes reveal their role in isoniazid and ethionamide resistance in Mycobacterium smegmatis. Antimicrob Agents Chemother *55*, 3133-3139.

Zahrt, T.C., and Deretic, V. (2001). Mycobacterium tuberculosis signal transduction system required for persistent infections. P Natl Acad Sci USA *98*, 12706-12711.

Zhang, Y., Bai, L., and Deng, Z. (2009). Functional characterization of the first two actinomycete 4-amino-4-deoxychorismate lyase genes. Microbiology *155*, 2450-2459.

Zhang, Y.J., Ioerger, T.R., Huttenhower, C., Long, J.E., Sassetti, C.M., Sacchettini, J.C., and Rubin, E.J. (2012). Global assessment of genomic regions required for growth in Mycobacterium tuberculosis. PLoS Pathog *8*, e1002946.

Zhang, Y.J., Reddy, M.C., Ioerger, T.R., Rothchild, A.C., Dartois, V., Schuster, B.M., Trauner, A., Wallis, D., Galaviz, S., Huttenhower, C.*, et al.* (2013). Tryptophan

biosynthesis protects mycobacteria from CD4 T-cell-mediated killing. Cell *155*, 1296-1308.

Zheng, J., Rubin, E.J., Bifani, P., Mathys, V., Lim, V., Au, M., Jang, J., Nam, J., Dick, T., Walker, J.R.*, et al.* (2013). para-Aminosalicylic Acid Is a Prodrug Targeting Dihydrofolate Reductase in Mycobacterium tuberculosis. Journal of Biological Chemistry *288*, 23447-23456.